

N71-15601
NASA CR-187288
1,70'

FINAL REPORT

STUDY OF INTERFACIAL CONDUCTIVITY

Contract No. NAS8-30171

Principal Investigators

R. Sexl
H. Sexl

D. G. Burkhard

Prepared By

P.E.C. RESEARCH ASSOCIATES, INC.

(Physics, Engineering & Chemistry)

P. O. Box 128

Louisville, Colorado 80027

(303-442-6015)

Athens, Georgia Office

115 Clifton Drive

Athens, Georgia 30601

(404-542-1810)

(404-549-1458)

Prepared For

NATIONAL AERONAUTICS AND SPACE ADMINISTRATION

GEORGE C. MARSHALL SPACE FLIGHT CENTER

Huntsville, Alabama

CASE FILE
COPY

INTRODUCTION

This report contains an expanded and improved version of our statistical theory of interfacial thermal conductivity and several applications of this theory, including numerical tables (users tables) predicting the values and fluctuations of the heat flow for various surface profiles.

The main progress which has been achieved this year is a comparison of our theory with the experimental data. This comparison (chapters 1+2) shows that the theory tends to over-predict the value of the interfacial conductivity by about a factor of 2. This is due to the simplified assumptions made about the surface. This deficiency of our theory has been corrected, meanwhile, in the recent experimental work done by N. Bhandari under the guidance of N. Veziroglu. The experiment performed by Bhandari was specifically designed to test the predictions of our theory, especially as far as the fluctuations of the heat flow are concerned. The existence of large fluctuations (50% r.m.s.) of the heat flow has been the main prediction of our theory. This prediction has been confirmed exactly by Bhandari's experiment. This shows, that previous measurements of the interface are completely unreliable, since a remeasurement under apparently identical conditions can lead to results which differ as much as 100% from those obtained the first time.

Bhandari has also suggested various improvements of our theory in order to achieve numerical agreement not only of the fluctuations but also of the heat flux itself with his measurements. This changes the predictions of the theory by a factor 2, as mentioned above. Bhandari's results have been made available to us, unfortunately, only in March 1970, so that the changes suggested there could not be incorporated fully into this final report. The users tables (chapter 2) therefore tend to overpredict the heat flow somewhat. Bhandari's results show furthermore that the experimental measurements of the surface characteristics which are necessary for a successful prediction of the interfacial heat flow is a very complex and tedious task. Surfaces are very complex objects, which can be characterized in a large number of ways. This implies that a determination of the interface resistance with the help of surface parameter measurements will always be a highly specialized and complex task. With the help of routine measurements alone (e.g. surface roughness) no successful predictions can be made, as has been amply demonstrated by the past history of the theory of interfacial conductivity.

There is one additional difficulty: All experimental determinations of interface resistance are performed using cylinders of about equal height and diameter as samples. In

actual applications surfaces are used, however, which are mostly of the form of thin plates. These plates have an elastic behaviour completely different from cylinders; by large scale elastic deformations some of the effects of surface waviness can be compensated, leading to an increase in the thermal conductance of the interface. A first theory of such effects has been attempted and is contained in chapter 3. We consider this direction of research to be the most promising one as far as practical applications are concerned.

Our work has shown that quantitative predictions of interfacial thermal conductivity are possible. The effort which is necessary for a successful prediction is, however, extremely high. The determination of the interface resistance from surface parameters is, therefore, not very convenient as far as practical applications are concerned. Only rough estimates of the order of magnitude of the heat flow are possible with the help of devices which are usually accessible to an engineer in a standard laboratory or by using the standard descriptions of the surfaces of commercially available products. Even if all the surface analyzers which are needed for quantitative predictions are available, the surface measurements required would be tedious and very time consuming.

Therefore a different approach to interfacial thermal conductivity is suggested:

A reliable device for the measurement of interfacial thermal conductivity should be developed which can be operated under standard engineering (and not highly sophisticated laboratory) conditions. Measurements of the heat flow can then be made using samples of the surface one is interested in for the actual application. These measurements would take only a fraction of the time necessary for the determination of all the surface parameters needed for a reliable theoretical calculation of the heat flow.

The role of the theory is then restricted to two very important tasks: Firstly, it has to predict the heat flow through the large surfaces used in actual applications (because of elastic deformations it is not permissible to multiply with the ratio of the surfaces, see chapter 3). Secondly, the fluctuations of the heat flow through these surfaces have to be calculated and the temperature variations in the system due to these fluctuations have to be evaluated.

We recommend therefore that additional experimental research is directed towards the construction of the engineering device for measuring interfacial thermal conductivity mentioned above and that, furthermore, the work started by Bhandari is to be continued. Theoretical work should concentrate to a large extent on the completely new theoretical development sketched in chapter 3, dealing with the large interface employed in actual applications.

A second part of this report contains our work on the theory of crystal growth under zero gravity conditions. This report contains only a survey of the literature, no theory exists yet of the effects which are to be expected under these conditions.

I. A STATISTICAL THEORY OF INTERFACIAL THERMAL CONDUCTIVITY

1. Introduction

One of the most complicated tasks in any calculation of the interfacial thermal conductivity (ITC) is the description of a rough surface. Various statistical [1-3] and semiempirical [4] approaches have been proposed to describe the properties of a surface and the contact between two such surfaces.

In this report we shall first investigate a special model of a surface. This model can best be applied to milled surfaces, since their characteristics resemble most closely the assumptions made here. This restriction to a special class of surfaces enables us to find rather explicit expressions for the heat flow, surface area in contact, etc. Furthermore, inelastic and elastic contacts can be taken into account simultaneously. Various other generalizations of the model, i.e. inclusion of void phase conduction, effects of surface films, etc. are discussed in chapter 10.

A slightly more complicated treatment of the contact between two surfaces is contained in chapter 11. This treatment enables one, however, to calculate the fluctuations of the heat flow. They turn out to be proportional to $n^{-1/2}$, where n is the number of contact points. Since n is rather small at low pressures, large fluctuations of the heat flow result.

Correlations between the heights of the asperities are taken into account next. There are two types of such correlations: Systematic features, like grooves, etc. tend to reduce the fluctuations of the heat flow. Irregular correlations, caused by surface waviness greatly increase the fluctuations and are the main source of experimental "irreproducibilities".

2. The Model

The surface of the metal will be represented by a series of equidistant spherical asperities of varying height, but equal curvature. Fig. 1 shows a cross section through our surface model.

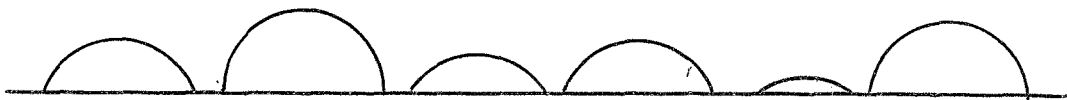


Fig. 1

Each spherical asperity is thus contained in a square of area B^2 . The distribution of the heights of the hills will be described in a statistical sense by a function $\rho(h)$ such

that

$$\rho(h) dh \quad (1)$$

= probability that an asperity has a height between h and $h + dh$.

ρ has to be normalized such that

$$\int \rho(h) dh = 1 \quad (2)$$

We shall always assume that there is an upper limit to the height of the hills, i.e. $\rho(h) = 0 \quad h > H$.

If we place two such surfaces above one another as shown in Fig. 2, they will begin to touch as soon as their distance of approach L reaches $2H$.

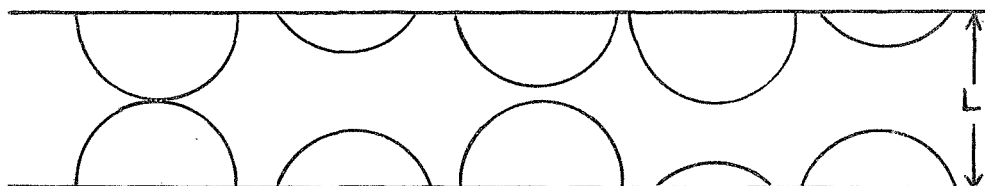


Fig. 2

However, only very few contact points will touch in this case. With rising pressure L decreases and the number of contact points increases accordingly. At the same time the

contact points will be deformed elastically or inelastically and ITC sets in.

An essential drawback of our model is, of course, that we assume the asperities to be distributed regularly. Furthermore, we assume that the hills on the two surfaces oppose one another exactly and no contacts such as the one in Fig. 3 are considered.

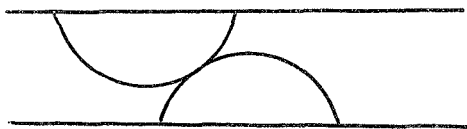


Fig. 3

This limits the applicability of our theory essentially to the contact of two milled surfaces. However, many of the results represented here are probably true also for other types of surface finish.

In the sequel we shall call opposing squares (containing one asperity each) a contact square, irrespective of the fact whether the two spheres actually touch or not.

3. Review of the Results for a Single Contact Point

The elastical deformation of two spheres that touch one another has been calculated by H. Hertz [5]. The basic results (generalizations of which have been given in [6] are the following). See Fig. 4

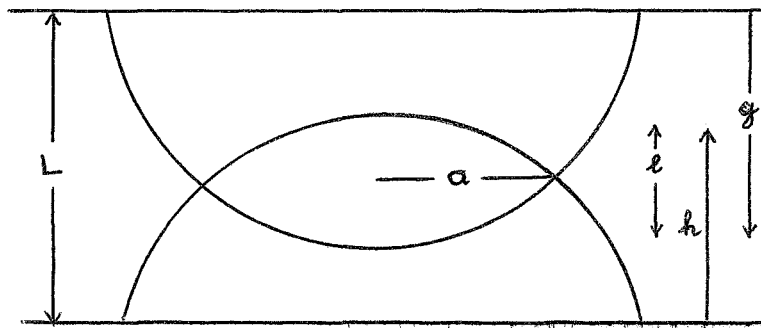


Fig. 4

If the two spheres are pressed together with a total force F they will be deformed elastically such that their apparent penetration depth l is given by

$$l = (2F^2 D^2 / R)^{1/3} \quad (3)$$

where

$$D = \frac{3}{4} \frac{1 - \sigma^2}{E} \quad (4)$$

(we assume that both spheres consist of the same material).

The radius of the contact circle is given by

$$a = \left(\frac{FRD}{2}\right)^{1/3} \quad (5)$$

The standard treatment of the heat flow through such a contact point is due to Cetinkale (Veziroglu) [7].

The contact is replaced by an idealized contact element as shown in Fig. 5.

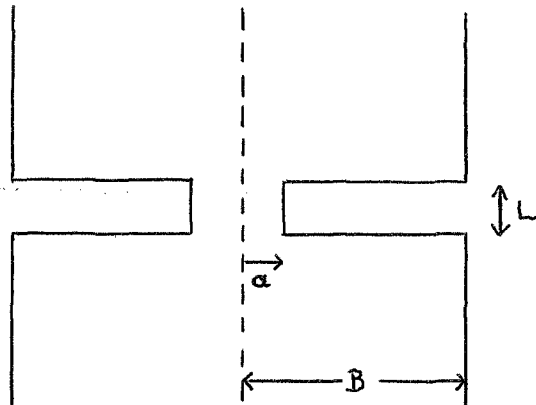


Fig. 5

The solution of the boundary value problem for the heat flow is rather complicated, due to the presence of liquid (lubricant) or gas in the gap between the two surfaces.

Since we are interested here mainly in the statistical features of the theory we shall consider the simplest case first, i.e. contact in vacuum. In this case the heat flow Q becomes

$$Q = 2 a k \Delta T \quad (6)$$

where ΔT is the temperature step at the interface and k is the thermal conductivity of the material. It is perhaps somewhat surprising that the heat flow is proportional to a rather than a^2 and independent of the height of the contact element (Equation (6) is valid for $L \ll a, B \gg a$).

The behaviour of Q is, however, due to the fact that the heat flow converges at the interface and is concentrated at the edges of the circle of radius a . This "skin effect" causes the dependence on a rather than a^2 , in complete analogy to the usual electromagnetic skin effect.

Equations (3-6) are the starting point of our theory.

4. Statistical Treatment of a Contact Element: Elastic Deformations

Consider the situation shown in Fig. 4, where two humps of heights h and g , respectively, have penetrated a distance ℓ given by

$$h + g = L + \ell \quad (7)$$

Eliminating F from equations (3) and (5) we obtain for the radius of the contact point

$$a = \sqrt{\frac{\ell R}{2}} \quad (8)$$

and the heat flow through this contact point becomes

$$Q = 2 k \Delta T \sqrt{\frac{R}{2}} \sqrt{\ell} \equiv \alpha B^2 \sqrt{\ell} \quad (9)$$

The penetration depth ℓ will, of course, differ for various contacts, because of the statistical distribution of their heights. We shall calculate now the average heat flux through one of the contact elements (keeping the distance L between the two surfaces fixed).

Consider first a sphere of fixed height g above the lower surface (see Fig. 4). Then the heat flow through the contact element will depend on the height of the upper sphere, i.e.

$$Q = B^2 \alpha \sqrt{\ell} = B^2 \alpha \sqrt{h + g - L} \quad (10)$$

Since these heights h have a statistical distribution $\rho(h)$, the average heat flow (averaged over many contacts with varying h) will be

$$Q(\text{averaged over } h) = \alpha B^2 \int_{L-g}^H (h + g - L)^{1/2} \rho(h) dh$$

$$\bar{Q} = \alpha B^2 \int_0^H dg \rho(g) \int_{L-g}^H dh \rho(h) (h + g - L)^{1/2} \quad (11)$$

This gives the average heat flow \bar{Q} through one contact element as a function of L . To obtain the total heat flux q through a unit surface area we have to multiply with the number N of contact square, i.e. with $N = 1/B^2$, i.e. $q = \bar{Q}/B^2$.

Similarly we calculate now the average force on the two interfaces as a function of L . From (3) we have

$$F = B^2 \gamma \ell^{3/2} \quad \gamma = \frac{1}{DB^2} \sqrt{\frac{R}{2}} \quad (12)$$

The average force due to one contact point becomes

$$\bar{F} = \gamma B^2 \int (h + g - L)^{3/2} \rho(h) \rho(g) dh dg \quad (13)$$

which together with

$$\bar{Q} = \alpha B^2 \int (h + g - L)^{1/2} \rho(h) \rho(g) dh dg \quad (14)$$

determines the heat flow as a function of the applied pressure $p = \bar{F}/B^2$.

The integrals (13) and (14) can be extended over a region in the (g,h) plane, such that $h + g > L$, i.e. we have to average only over such contact squares that actually touch one another.

This region of integration is shown in Fig. 6.

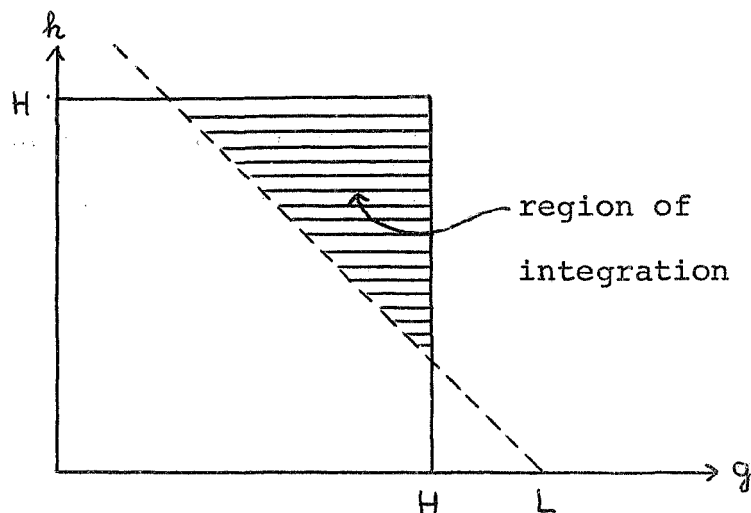


Fig. 6

5. Statistical Treatment of a Contact Element: Inelastic Deformations

If a critical pressure P (equal to the hardness of the material) is exceeded the material begins to flow plastically. While it is hardly possible to treat these phenomena exactly we shall take them into account in the phenomenological manner described below.

In this treatment we shall assume that in the case of plastic flow the basic relations (6) and (8) remain valid, while the relation (5) between the radius of the contact point and the force has to be changed. The simplest modification of (5) is

$$F = P \pi a^2 \quad (15)$$

i.e. the material flows until the pressure is equal to the critical pressure all over the contact surface. Inserting (8) this becomes

$$F = P \pi \frac{\ell R}{2} \quad (16)$$

This relation replaces (12) in the case of inelastic contacts, while the expression for the heat flow Q remains unchanged.

Next we have to determine when the critical pressure will be exceeded at a contact point. The pressure distribution at the contact is (see e.g. [6])

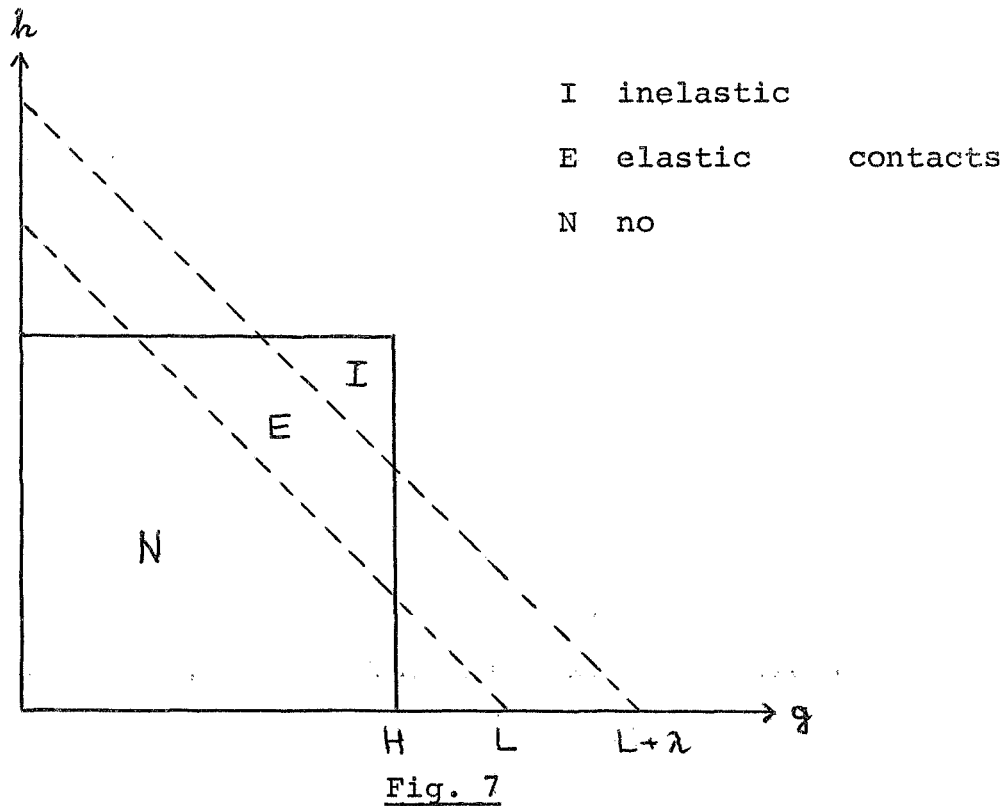
$$p(r) = \frac{3F}{2\pi a^2} \sqrt{1 - r^2/a^2} \quad (17)$$

The pressure is thus largest in the center

$$p_0 = \frac{3F}{2\pi a^2} \quad (18)$$

Plastic flow sets in if $p_0 > P$. Since both F and a are functions of $\ell = h + g - L$, this means that there is a critical value of ℓ , $\ell = \lambda$, above which the contact begins to flow.

Therefore, the situation is as shown in Fig. 7.



Thus the relation between the pressure p and the surface distance L is modified to

$$\begin{aligned}
 p = & \gamma \int_E (h + g - L)^{3/2} \rho(h) \rho(g) dh dg + \\
 & + \frac{P\pi}{2B^2} R \int_I (h + g - L) \rho(h) \rho(g) dh dg
 \end{aligned} \tag{19}$$

where the integrals are to be extended over the elastic (E) and inelastic (I) regions, respectively.

The relation between P and λ is given by

$$P = \frac{3}{\pi} \frac{1}{D} \sqrt{\frac{\lambda}{R}} \quad (20)$$

This follows from (18), (12) and (8).

Equations (14) and (19) are our basic results; they determine heat flow and force as functions of the distance of approach.

6. The Interface Correlation Function

The two-dimensional integrals that appear in (14) and (19) can be re-written by a transformation of variables into a considerably simpler form.

The integrals that appear in (14) and (19) are of the general type (the factor H^{-n} is introduced to make $A_n(L)$ dimensionless)

$$A_n(L) = H^{-n} \int (h + g - L)^{-n} \rho(h) \rho(g) dh dg \quad (21)$$

integrated over some suitable domain. We introduce new variables by

$$\begin{aligned} h &= x + y & h + g &= 2x \\ g &= x - y & h - g &= 2y \end{aligned} \quad (22)$$

$A_n(L)$ then becomes

$$\begin{aligned} A_n(L) &= 2 \int \int \left(\frac{2x-L}{H}\right)^n \rho(x+y) \rho(x-y) dx dy = \\ &= 2 \int \left(\frac{2x-L}{H}\right)^n K(x) dx / H \end{aligned} \quad (23)$$

where

$$K(x) = H \int dy \rho(x+y) \rho(x-y) \quad (24)$$

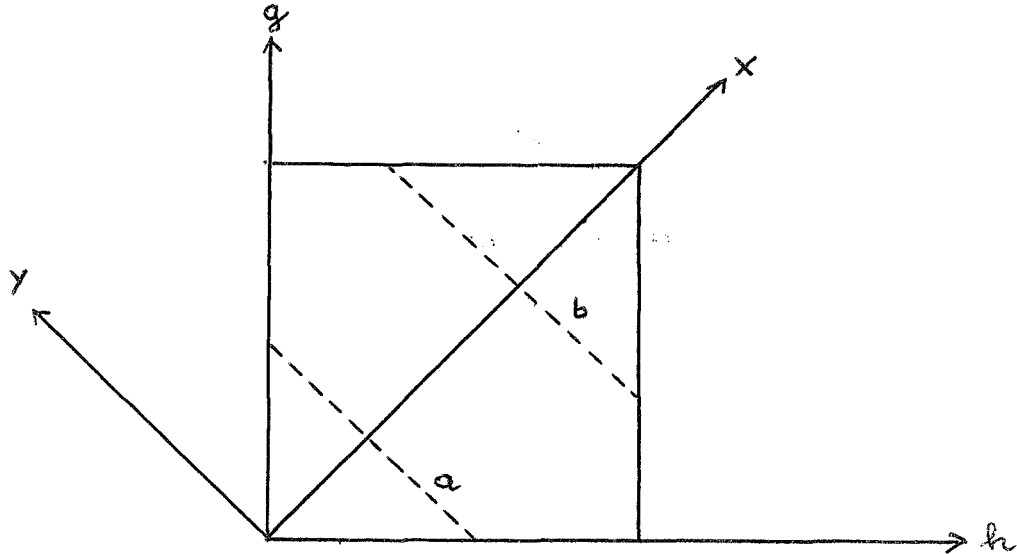


Fig. 8

The integral (24) is to be taken along the dotted lines (fig. 8) in the (x,y) plane. Therefore the limits of integration are

$$K(x) = H \int_{-x}^x dy \rho(x+y) \rho(x-y) \quad (25)$$

if the path is analogous to (a) in Fig. 8 or

$$K(x) = 2H \int_0^{H-x} dy \rho(x+y) \rho(x-y) \quad (26)$$

for paths like (b). In the last step we used the obvious symmetry of the integrand of (26).

For simplicity we shall restrict ourselves here to case (b), i.e. we do not consider distance of approach $L < H$. This can, however, easily be done if necessary.

$K(x)$ will be called the interface correlation function. It plays the dominant role in the theory of the contact between two surfaces. To bring our result into its final form we introduce a new variable

$$z = 2x - L = h + g - L \quad (27)$$

in (24) whereupon the integrals A_n become

$$A_n(L) = H^{-n-1} \int z^n K\left(\frac{z+L}{2}\right) dz \quad (28)$$

The limits of integration over z still have to be determined.

Let us first study the case of elastic contacts only.

Then the limits of the integration are given by $z = 0$ and $z = 2H - L = d$ respectively, as can easily be seen from Fig. 9.

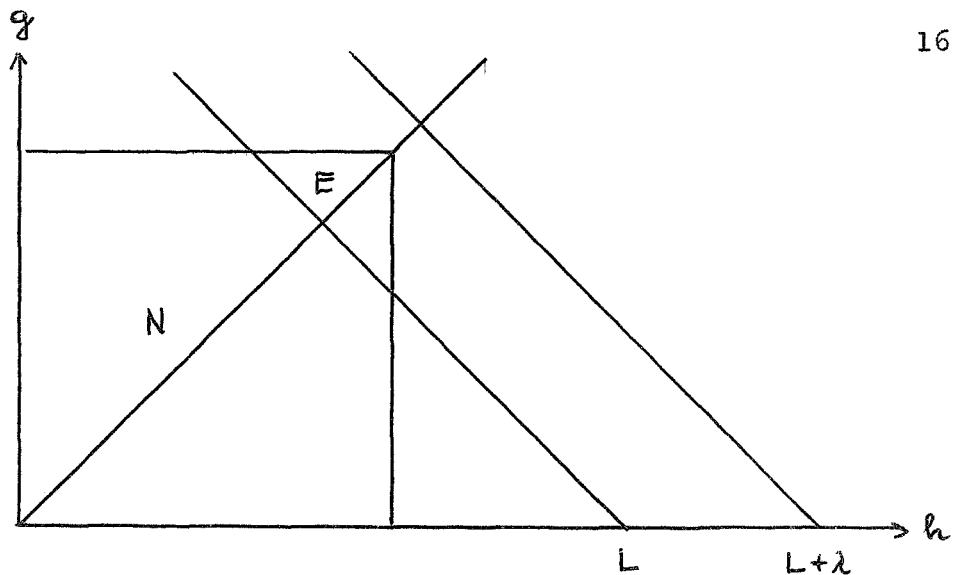


Fig. 9

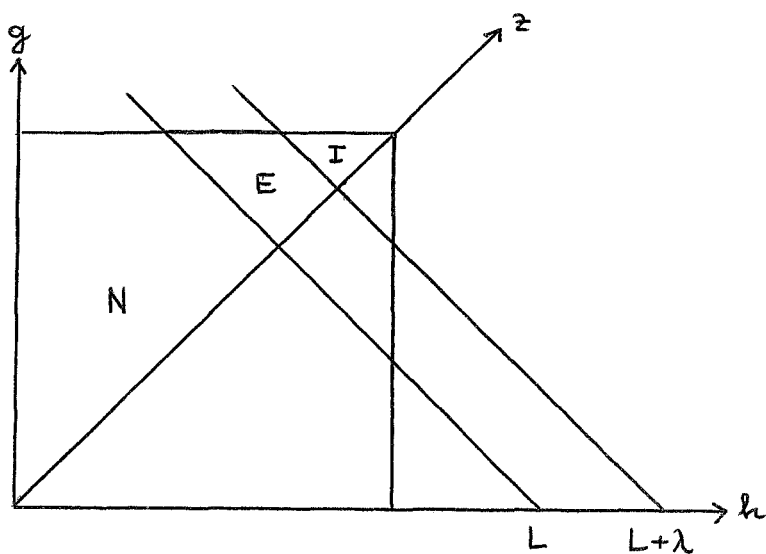


Fig. 10

In the presence of elastic and inelastic contact points the situation is as shown in Fig. 10. There the elastic integrals go from 0 to λ , the inelastic ones from λ to d . Therefore, the expression for heat flux q and the pressure p become finally

$$\frac{q_B}{k\Delta T} = \sqrt{\frac{zRH}{B}} A_{1/2}(L) \quad (29)$$

$$p = \begin{aligned} & \frac{\gamma}{H} \int_0^d z^{3/2} K\left(\frac{z+L}{2}\right) dz && \text{Elastic contacts only} \\ & \frac{\gamma}{H} \int_0^\lambda z^{3/2} K\left(\frac{z+L}{2}\right) dz + \frac{P\pi R}{2HB^2} \int_\lambda^d z K\left(\frac{z+L}{2}\right) dz && \text{Elastic and inelastic contacts} \end{aligned} \quad (30)$$

where

$$\gamma = \frac{1}{B^2 D} \sqrt{\frac{R}{2}} \quad D = \frac{3}{4} \left(\frac{1-\sigma^2}{E} \right)$$

$$d = 2H - L \quad P = \frac{3}{\pi} \frac{1}{D} \sqrt{\frac{\lambda}{R}} \quad (31)$$

$$K(x) = 2H \int_0^{H-x} dy \rho(x+y) \rho(x-y)$$

Equations (29-31) are our final results. The form in which Equation (29) is written has the advantage that both sides are dimensionless and the square root is a factor of order unity.

7. Examples

We shall calculate how the expectation values for the heat flux and the force F for some simple distribution functions.

The first step is the calculation of the interface correlation function.

The following height distribution functions will be considered

$$\begin{aligned} \text{a) } \rho_\delta(x) &= \delta(H - x) \\ \text{b) } \rho_\theta(x) &= \frac{1}{H} \theta(H - x) \\ \text{c) } \rho_m(x) &= (H - x)^m v_m \end{aligned} \tag{32}$$

(v_m is a normalization factor)

The corresponding interface correlation functions are

$$\begin{aligned} \text{a) } K(x) &= H \delta(H - x) \\ \text{b) } K(x) &= \frac{2}{H} (H - x) \quad 0 \leq x \leq H, \\ \text{c) } K(x) &= w_m (H - x)^{2m+1} \quad 0 \leq x \leq H, \end{aligned} \tag{33}$$

(w_m = normalization factor)

Inserting these correlation functions into the integrals (29) and (30) respectively, we obtain the following expressions for the heat flux and force (we restrict ourselves at the moment to elastic contacts)

$$\text{a) } q \approx d^{1/2} \quad p \approx d^{3/2}$$

$$b) q = \frac{4\alpha}{15} \frac{d^{5/2}}{H^2} \quad p = \frac{4\gamma}{35H^2} d^{7/2} \quad (34)$$

$$c) q \approx d^{5/2 + 2m} \quad p \approx d^{7/2 + 2m}$$

Therefore, simple power laws result

$$a) q \approx p^{1/3} \quad b) q \approx p^{5/7} \quad (35)$$

$$c) q \approx p^{(5+4m)/(7+4m)}$$

(35a) is just the well known relation between heat flow and force that results from the assumption that all asperities have the same height H.

As an example for the transition from elastic to inelastic deformations we calculate the heat flow in case b, the result is

$$q = \frac{4\alpha}{15} \frac{d^{5/2}}{H^2}$$

$$\frac{4\gamma}{35H^2} d^{7/2} \quad d < \lambda \quad p = \quad (36)$$

$$\frac{2\gamma}{35H^2} \lambda^{5/2} (7d - 5\lambda) + \frac{\pi PR}{12H^2B^2} (d - \lambda)^2 (d + 2\lambda) \quad d > \lambda$$

Here the power law changes slowly from

$$q \approx p^{5/7} \quad \text{to} \quad q \approx p^{5/6} \quad (37)$$

when inelastic effects set in.

The remarkable common feature of all the examples given above is that they result in power laws with exponents smaller than one. In this respect our results are similar to those of Held [4].

For more complicated height distribution functions the heat flow can be calculated numerically only.

The strong dependence of the functional form of $q(p)$ on the height distribution indicates why attempts to calculate the heat flow from simple models are generally unsuccessful.

The results obtained hitherto are in agreement with the experimental data in the low and medium pressure region ($p < 10^{-3}$ P) where power laws with exponents < 1 are generally observed. At higher pressures, however, a much stronger increase of the heat flow is sometimes observed, suggesting power laws $q \approx p^2$. The standard explanation of this is that in this pressure region a strong increase in the number of contact points takes place. A quantitative formulation of this argument can be given in our theory, by assuming a height distribution of the form

$$\rho(h) = \frac{s}{H} \theta(H - x) + (1 - s) \delta(G - x) \quad (38)$$

$$G < H \quad s < 1$$

A typical curve $q(p)$ that results from (38) is shown in Fig. 11 (assuming inelastic contacts only).

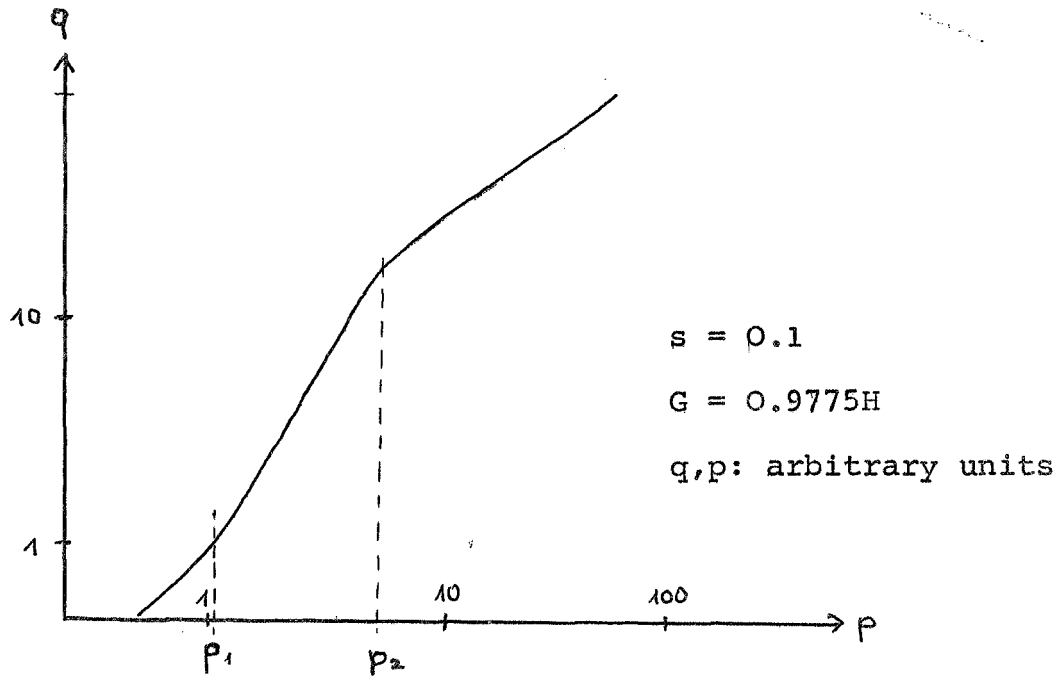


Fig. 11

The onset of the change in slope at p_1 depends, of course, on the values of the parameters used in (38), as does p_2 . With typical parameters s and G one obtains $p_2/p_1 \approx 2 - 4$, i.e. the steep slope can be maintained only over a relatively small pressure range. Since this is not in agreement with the experiment, the slopes >1 will have to be interpreted in a different way. This will be done in chapter 10.

8. Comparison with Experiment

In this section we shall compare our theory with some recent experimental measurements of thermal contact conductance. For this purpose we choose a height distribution function

$$\rho(x) = \begin{cases} \frac{6}{H^3} x (H - x) & 0 \leq x \leq H \\ 0 & x > H \end{cases} \quad (39)$$

The reason for this choice of $\rho(x)$ is that (39) is a good approximation to a Gaussian distribution of asperities, which is to be expected because of the statistical distribution of the asperities on the interface. The advantage of the choice (39) over a Gaussian-ansatz for $\rho(x)$ is that the integrals required for the calculation of q and F can be carried out analytically when the distribution (39) is used.

Inserting (39) into (31) we obtain for the interface correlation function

$$K(x) = \frac{48}{H^5} [x^2 - \frac{1}{5}(x-H)^2] (H-x)^3 \quad (40)$$

This result is valid in the region $H/2 < x < H$.

Since most experiments are performed at pressures for which inelastic contacts dominate we shall neglect the elastic contribution to the total pressure in (30b). For the calculation

of q and p resp. we need the integrals ($\xi = d/H$)

$$A_{1/2}(\xi) = \frac{64}{15015} \xi^{9/2} (143 - 104\xi + 16\xi^2) \quad (41)$$

$$A_1(\xi) = \frac{1}{70} \xi^5 (21 - 14\xi + 2\xi^2) \quad (42)$$

Pressure and heat flow can be expressed in terms of these integrals as

$$\frac{qB}{k\Delta T} = \sqrt{\frac{2RH}{B^2}} A_{1/2}(\xi) \quad (43)$$

$$p/P = \frac{\pi RH}{2B^2} A_1(\xi) \quad (44)$$

For $\xi \ll 1$ an approximate power law

$$q \approx p^{0.9} \quad (45)$$

results. It is interesting to note that Tien [10] has suggested a phenomenological relation

$$q \approx p^{0.85} \quad (46)$$

in order to explain a large number of experimental data. The relation suggested by Tien is (in our notation)

$$\frac{qB}{k\Delta T} = 0.55 \left(\frac{p}{P}\right)^{0.85} m \quad (47)$$

surface
where m is the RMS slope. In this theory B is the autocorrelation length of the surface.

The relation (45) derived here can be rewritten in a form similar to (47)

$$\frac{qB}{k\Delta T} = \left(\frac{B^2}{RH}\right)^{0.4} 2.8 \left(\frac{p}{P}\right)^{0.9} \quad (48)$$

It differs from (47) by the numerical factor 2.8 instead of 0.55 and by the factor $(B^2/RH)^{0.4}$, which is related to the slope of the surface as shown in Fig. 11

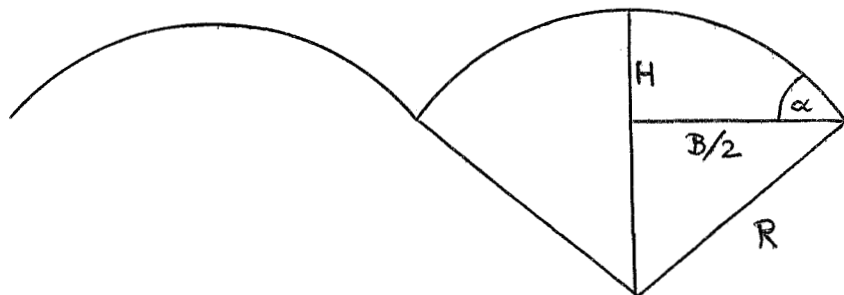


Fig. 11

In this figure an asperity of maximum height H is shown. The relation between H , B and R is

$$\sin\alpha = B/2R \quad \cos\alpha = \frac{R-H}{R} \quad (49)$$

or

$$H = R(1-\cos\alpha) \quad B = 2R \sin\alpha \quad (50)$$

and thus

$$\frac{B^2}{RH} = \frac{4R^2 \sin^2 \alpha}{R^2(1-\cos \alpha)} = \frac{16 \sin^2 \alpha / 2 \cos^2 \alpha / 2}{2 \sin^2 \alpha / 2} = 8 \cos^2 \alpha / 2 \quad (51)$$

For $0 \leq \alpha \leq 90^\circ$ we have

$$2.27 \geq \left(\frac{B^2}{RH}\right)^{0.4} \geq 1.75 \quad (52)$$

We can therefore replace this factor within an accuracy of 12% by

$$\left(\frac{B^2}{RH}\right)^{0.4} \approx 2 \quad (53)$$

and (48) simplifies them to

$$\frac{qB}{k\Delta T} = 5.5 \left(\frac{p}{P}\right)^{0.9} \quad (54)$$

Here we have made the assumption that the asperities of maximal height touch one another, as shown in Fig. 11.

For surfaces for which this is not fulfilled (Fig. 12)

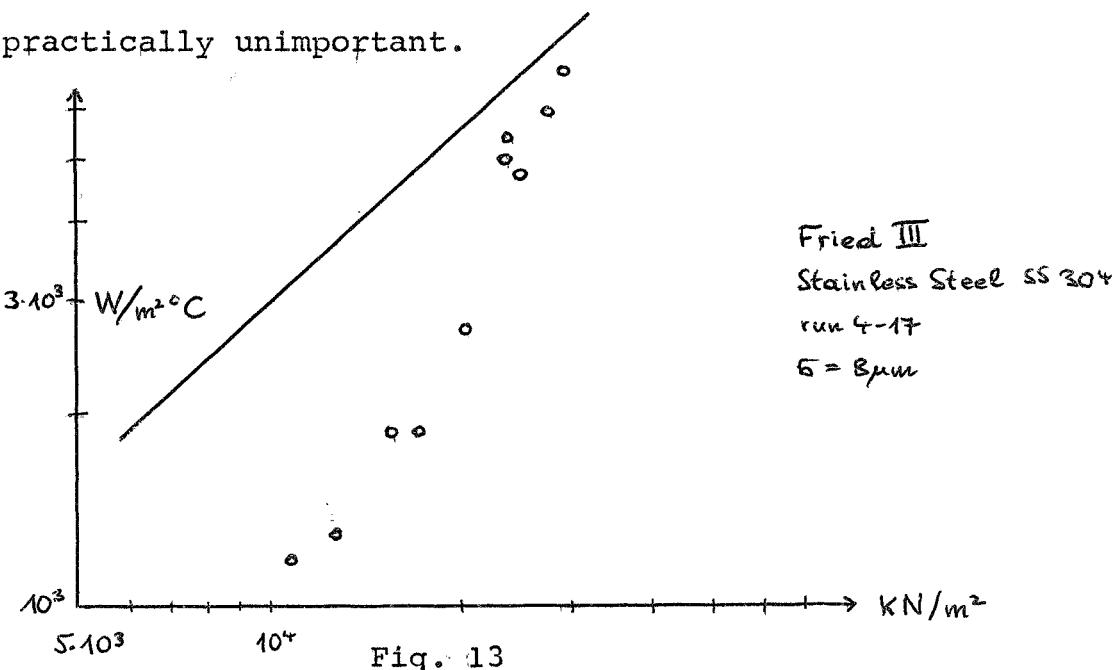


Fig. 12

B has to be defined as shown in the figure.

The main difference between (54) and Tien's relation (47) is thus the lack of the factor m in our relation (54). The reason for this is, that the results derived here are valid for very rough surfaces, while Tien has concentrated on nominally flat surfaces ($m \ll 1$). Formal agreement between (47) and (54) can be achieved if we put $m = 10$. We shall compare our theory here with the experiments of Fried [8], since in this case all the relevant surface parameters are known. The agreement between theory and experiment is shown in Fig. 13.

The figure shows that the theory tends to overestimate the heat flux by about a factor of 2 and predicts, furthermore, a linear relation between $\ln q$ and $\ln p$, while the actual curve seems to be nonlinear. We shall show, however, in chapter 3 that the disagreement of theory and experiment is about of the order of the fluctuations of the heat flow which are to be expected on purely statistical reasons. This disagreement is, thus, practically unimportant.



9. Surface Films and Electrical Conductivity

It has often been suggested that the mechanism for interfacial thermal and electrical conductivity are rather similar. Recent measurements by Fried [8] have shown that this is only partially correct. A typical plot of the ratio electrical/thermal resistance vs. pressure is shown in Fig. 14.

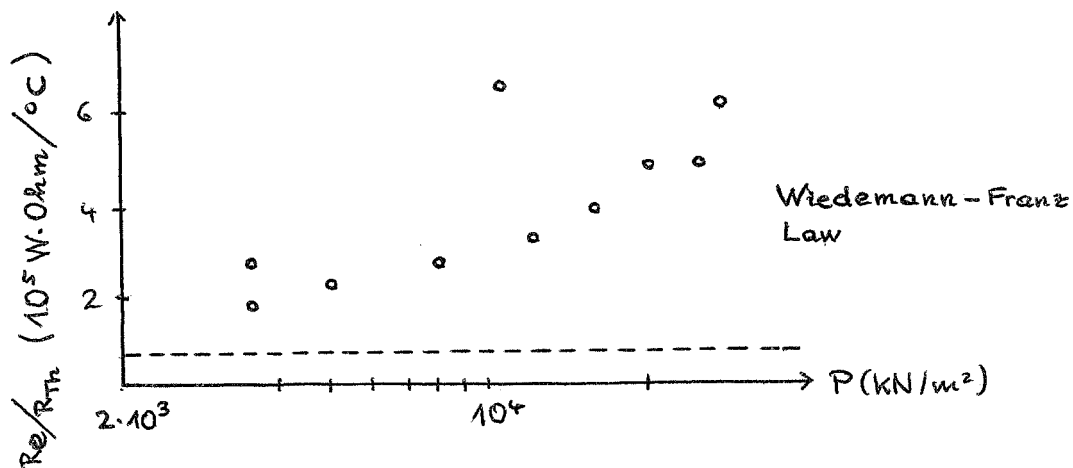


Fig. 14

If the mechanisms for both electrical and thermal conductivity were the same, one would expect the ratio R_E/R_{Th} to be equal to a constant

$$R_E/R_{Th} = 7.35 \cdot 10^{-6} \frac{\text{Ohm Watt}}{\text{°C}} \quad (55)$$

(at a temperature $T = 27^\circ\text{C}$).

Actually the ratios are always higher than the one given by the Wiedemann-Franz law (55). This indicates that the resistance stemming from the surface film is the dominant one as

far as electrical conductivity is concerned, while it can probably be neglected for thermal conductivity. (There is, however, no clear proof of this).

If both constriction resistance and surface film resistance are important, the basic equation (6) for the heat flow has to be changed to

$$q = \frac{\Delta T / B^2}{1/2ka + b/\pi a^2 k_s} \quad (56)$$

since the constriction resistance ($1/2ka$) and the surface film resistance ($b/k_s a^2$) have to be added to one another. In (56) k_s is the thermal conductivity, b the thickness of the surface film,

Similarly the electrical current through one contact element becomes

$$J = \frac{V}{1/2\sigma a + b/\pi a^2 \sigma_s} \quad (57)$$

where V is the voltage across the interface; σ and σ_s are the electrical conductivities of metal and surface film, resp.

If the effects of the surface film were small the ratio of electrical/thermal resistance

$$\frac{R_E}{R_{Th}} = \frac{1/2\sigma a + b/\pi a^2 \sigma_s}{1/2ka + b/\pi a^2 k_s} \approx k/\sigma \quad (58)$$

would be given by the Wiedemann-Franz law. The experimental evidence is, however, that $R_E/R_{Th} \gg k/\sigma$ and a function of pressure. This indicates that surface films are dominant as far as the electrical conductivity is concerned, while the constriction resistance is the important one for heat transfer. Neglecting the appropriate terms in (56), (57), (58) we have

$$q = \frac{2ka}{B^2} \Delta T \quad (59)$$

$$J = \frac{\pi a^2 \sigma_s V}{b} \quad (60)$$

$$R_E/R_{Th} = \frac{2}{\pi} \left(\frac{b}{a}\right) \frac{k}{\sigma_s} \quad (61)$$

Since the pressure p and the electrical current J are both proportional to a^2 (for inelastic contacts), we obtain

$$J = \text{const. } p \quad (62)$$

which agrees well with experiment [8].

10. The High Pressure Region

In the high pressure region ($p \geq 10^{-3}$ P) the approximation (6) for the constriction resistance is not applicable anymore and a more accurate expression has to be used. A particularly

simple relation is the one given by Cetinkale and Fishenden [9]

$$q = \frac{\pi k a \Delta T / B^2}{\tan^{-1}(\frac{B}{a} - 1)} \quad (63)$$

For $B \gg a$ this agrees with the expression discussed before (6). If, however, $B \approx a$, i.e. if the contact points become large then

$$q = \frac{\pi k a^2 \Delta T}{(B-a) B^2} \quad (64)$$

Equation (61) has to be changed accordingly. It becomes

$$\frac{R_E}{R_{Th}} = \frac{k}{\sigma_s} \frac{1}{B-a} \quad (65)$$

The strong dependence of (64) on a is the probable reason for the striking increase of the heat flow at high pressures. However, more work has to be done before quantitative predictions about the behaviour of the heat flow in the high pressure region can be made.

11. Alternative Calculation of q

In this chapter we shall repeat our calculation of the heat flow as a function of pressure with a different method. This method, which takes into account the whole interface simultaneously will enable us to take into account the whole

interface at once and permit, furthermore, a calculation of the fluctuations of the heat flow. These fluctuations result when the two surfaces which form the interface are separated and put together again in a slightly different position.

For this purpose it is insufficient to deal with one contact only and we have to take the whole interface into account at once. The interface shall consist of N contact squares, the height of the asperities being h_i and g_i resp., $i = 1, 2, \dots, N$. The total heat flow Q_I through the interface is given by

$$Q_I = \alpha B^2 \sum_{i=1}^N (h_i + g_i - L)^{1/2} \quad (66)$$

The total force pressing the interface together is given by

$$F = \gamma B^2 \sum_{i=1}^N (h_i + g_i - L)^{3/2} \quad (67)$$

(We shall consider elastic contacts only). Here we have to average the heat flow not only over all possible values of h_i and g_i , but also over all values of L that are compatible with the value of F given by (67). This can be accomplished by including an integral

$$\langle J(L) \rangle = \int dL \delta[F - \gamma B^2 \sum_{i=1}^N (h_i + g_i - L)^{3/2}] w(L) \quad (68)$$

into the averaging procedure. $w(L)$ has to be chosen such as to normalize the integral to one. The integral (68) is of the form

$$\int dL \delta(f(L)) w(L) = \int \frac{dL}{|f'(L_0)|} \delta(L-L_0) w(L_0) \quad (69)$$

where $f(L_0) = 0$, $f'(L_0) = \left(\frac{df}{dL}\right)_{L=L_0}$. The normalization $J = 1$ requires

$$w(L_0) = |f'(L_0)| = 2\gamma B^2 \sum_{i=1}^N (h_i + g_i - L)^{1/2} \quad (70)$$

The average of \bar{Q}_I over all possible values of h_i , g_i and L is thus obtained in the same manner as before by integrating over the height distribution functions.

$$\begin{aligned} \bar{Q}_I &= \gamma B^2 \int d^N h_i \int d^N g_i \int dL Q_I(h_i, g_k, L) \frac{3}{2} \sum_i^N (h_i + g_i - L)^{1/2} \cdot \\ &\cdot \prod_{k=1}^N \rho(h_k) \prod_{\ell=1}^N \rho(g_\ell) \delta[F - \gamma B^2 \sum_{m=1}^N (h_m + g_m - L)^{3/2}] \end{aligned} \quad (71)$$

where $\bar{Q}_I(h_i, g_k, L)$ is given by (66). We introduce new variables by

$$h_i + g_i - L = z_i \quad , \quad h_i - g_i = 2y_i \quad (72)$$

and obtain inserting (66)

$$\bar{Q}_I = \frac{3\alpha\gamma B^4}{2H^N} \int d^N z_i \prod_{i=1}^N \int dL \left(\sum_{\ell=1}^N z_\ell^{1/2} \right)^2 \delta(F-B^2\gamma \sum_k z_k^{3/2}) K\left(\frac{z_i+L}{2}\right) \quad (73)$$

where

$$K(x) = H \int dz \rho(x-z) \rho(x+z) \quad (74)$$

is the interface correlation function. The sum $(\sum_i z_i^{1/2})^2$ contains N terms of type $z_i^{1/2}$ and $N(N-1)$ terms $z_i^{1/2} z_k^{1/2}$, $i \neq k$.

Because of the obvious symmetry of the integrand all values of i, k contribute equally to \bar{Q}_I and thus (73) becomes

$$\bar{Q}_I = \frac{3N\alpha\gamma B^4}{2H^N} \int d^N z_i \int dL \prod_{i=1}^N K\left(\frac{z_i+L}{2}\right) \delta(F-B^2\gamma \sum_\ell z_\ell^{3/2}) (z_1 + (N-1)\sqrt{z_1 z_2}) \quad (75)$$

To proceed further we use the well-known integral representation of the δ -function

$$\delta(y) = \int \frac{dx}{2\pi} e^{ixy} \quad (76)$$

With the help of (76) the expression for \bar{Q}_I factorizes into a product of N integrals of the form

$$J_n(L, x) = dz z^n e^{-i\gamma B^2 x z^{3/2}} K\left(\frac{z+L}{2}\right)/H^{n+1} \quad (77)$$

$$\begin{aligned} \bar{Q}_I = & \frac{3N\alpha\gamma B^4 H}{2} \int \frac{dx}{2\pi} e^{iFx} \int dL [J_1(L, x) J_0^{N-1}(L, x) + (N-1) J_{1/2}^2(L, x) \\ & \cdot J_0^{N-2}(L, x)] \end{aligned} \quad (78)$$

This is the general expression for the heat flow through N contact squares. To simplify this further we consider the limit $N \gg 1$ (in actual experiments $N \approx 10^4$). Putting $F = NpB^2$ and $y = Nx$ (78) becomes

$$\bar{Q}_I = \frac{3\gamma\alpha B^4}{2} \int \frac{dy}{2\pi} e^{ipB^2y} \int dL [J_1(L, \frac{y}{N}) J_o^{N-1}(L, \frac{y}{N}) + (N-1) J_{1/2}^2(L, \frac{y}{N}) J_o^{N-2}(L, \frac{y}{N})] \quad (79)$$

To evaluate this we expand $J_n(L, x)$ into a power series

$$J_n(L, x) = A_n(L) - ix\gamma H A_{n+3/2}(L) - \frac{x^2\gamma^2 H^2}{2} A_{n+3}(L) + \dots \quad (80)$$

where $A_n(L)$ are the integrals

$$A_n(L) = \int dz z^n K(\frac{z+L}{2}) / H^{n+1} \quad (81)$$

The following limits are needed in (79)

$$\lim_{N \rightarrow \infty} J_1(L, \frac{y}{N}) = A_1(L) \quad \lim_{N \rightarrow \infty} J_{1/2}^2(L, \frac{y}{N}) = A_{1/2}^2(L) \quad (82)$$

$$\lim_{N \rightarrow \infty} J_o^N(L, \frac{y}{N}) = \lim_{N \rightarrow \infty} [1 - i\gamma \frac{y}{N} A_{3/2}(L)]^N = \exp[-i\gamma y A_{3/2}(L)] \quad (83)$$

(Observe here and in the next step that $A_0(L) = 1$), Thus \bar{Q}_I becomes for $N \gg 1$

$$\bar{Q}_I = \frac{3\alpha\gamma B^4}{2} \int \frac{dy}{2\pi} e^{iFy} \int dL [A_1(L) + (N-1)A_{1/2}^2(L)] \\ \exp[-iy A_{3/2}(L)] \quad (84)$$

The integral over y can be carried out, the result is

$$\bar{Q}_I = \frac{3\alpha\gamma B^4}{2} \int dL \delta[F - \gamma A_{3/2}(L)] \{A_1(L) + (N-1)A_{1/2}^2(L)\} \quad (85)$$

The δ -function shows that in the limit of infinite N only one value of L contributes to the integral, i.e.

$$F = \gamma A_{3/2}(L_o) \quad (86)$$

This shows that in the limit of infinitely large interfaces the fluctuations vanish and a fixed value of F corresponds to a fixed value of L . To evaluate (85) we use (67) and note that (see (24))

$$\frac{d}{dL} A_n(L) = -n A_{n-1}(L)/H \quad (87)$$

Thus \bar{Q}_I becomes

$$\bar{Q}_I = \alpha(N-1) A_{1/2}(L_o) + \alpha A_1(L_o)/A_{1/2}(L_o) \quad (88)$$

and the average flow through one contact square becomes

$$\bar{Q} = \lim_{N \rightarrow \infty} \frac{\bar{Q}_I}{N} = \alpha A_{1/2}(L_o) \quad (89)$$

where L_o is determined by (86). This is identical with (29). Therefore the simple analysis described in chapters 3-7 becomes exact in the limit of infinite N.

12. Finite Interfaces and Fluctuations

All experiments on interfacial conductivity suffer from a lack of reproducibility. Whenever the 2 surfaces are slightly shifted, a measurement of the heat flux will give results that differ appreciably from those obtained before. We shall show here that this is but a natural consequence of the finiteness of the interface.

A calculation of the fluctuations of the heat current turns out to be a rather complicated task, since \bar{Q} and \bar{Q}^2 have to be calculated to order $1/N$. We neglected numerous such terms in the manipulations leading from (79) to (89). The terms included in (88) that contribute in order 1 to \bar{Q}_I and thus in order $1/N$ to \bar{Q} are only 2 out of 6 terms of this type. However, the following observation simplifies our task considerably. The two terms that are of order 1 in (88) are $A_{1/2}$ and $A_1/A_{1/2}$. Evaluation of these quantities for model (32 b) leads to

$$A_n(L) = \frac{(2H - L)^{n+2}}{H^{2+n} (n+1)(n+2)} \quad n > 0 \quad (90)$$

Therefore we have

$$A_{1/2} = \frac{4}{15H^{5/2}} (2H - L)^{5/2}, \quad A_1/A_{1/2} = \frac{5}{8} \sqrt{\frac{2H-L}{H}} \quad (91)$$

For low pressures - where fluctuations are largest and thus of practical interest - $2H-L \ll H$, Hence the term $A_1/A_{1/2}$ is the leading one in the low pressure region on which we shall concentrate in the sequel. In this case (88) can be approximated by

$$\bar{Q}_I = \alpha N A_{1/2}(L) + \alpha A_1(L)/A_{1/2}(L) \quad (92)$$

An inspection of the terms neglected in the steps leading from (78) to (92) are that they are all of the type $A_{1/2}$ rather than $A_1/A_{1/2}$ and can thus be neglected. The reasons why some terms in the expression for the fluctuations are more important than others will become clear below.

To calculate the fluctuation

$$\frac{\Delta \bar{Q}}{\bar{Q}} = \left(\frac{\bar{Q}^2 - \bar{Q}^2}{\bar{Q}^2} \right)^{1/2} \quad (93)$$

we need \bar{Q}^2 . This is given by

$$\bar{Q}_I^{(2)} = \frac{3}{2} \alpha^2 \gamma \int d^N h \int d^N g \int dL \pi_p(h) \pi_p(g) \delta[K - \gamma \sum_k (h_k + g_k - L)]^{3/2} \cdot \sum_\lambda (h_\lambda + g_\lambda - L)^{1/2})^3 \quad (94)$$

Repeating the steps that lead from (70) to (80) we arrive at

$$\begin{aligned} \bar{Q}^{(2)} = & \frac{3\alpha^2 \gamma}{2} \int \frac{dx}{2\pi} e^{ikx} \int dL [N J_{3/2}(L, x) J_0^{N-1}(L, x) + \\ & + 3N(N-1) J_{1/2}(L, x) J_1(L, x) J_0^{N-2}(L, x) + \\ & + N(N-1)(N-2) J_{1/2}^3(L, x) J_0^{N-3}(L, x)] \end{aligned} \quad (95)$$

The first term in (95) can be neglected in the limit of large N , while the second one has to be taken into account in a calculation of the fluctuations. The last term is, of course, the leading one. After manipulations analogous to those discussed before the expression for $\bar{Q}^{(2)}$ becomes

$$\bar{Q}^{(2)} = \alpha N^2 A_{1/2}^2(L) + 2\alpha N A(L) + \dots \quad (96)$$

All terms that can be neglected in the region $2H-L \ll H$ have been omitted in (96). Inserting our results into (93) we obtain for the fluctuations

$$\frac{\Delta \bar{Q}}{\bar{Q}} = \frac{1}{\sqrt{N}} \frac{\sqrt{A_{1/2}}}{A_{1/2}} \quad (97)$$

The fluctuation is proportional to $N^{-1/2}$, as one expects, but is multiplied by the factor $\sqrt{A_1}/A_{1/2} \gg 1$. The meaning of this factor becomes transparent when we calculate the number of contact squares that touch one another, i.e., the number of contact elements. This number is given by

$$n = N \int dz \theta(z) K\left(\frac{z+L}{2}\right) \quad (98)$$

Using the same model as before this becomes

$$\frac{n}{N} = \frac{(2H-L)^2}{2H^2} \ll 1 \quad (99)$$

while

$$A_1/A_{1/2}^2 = \frac{225}{54} \frac{H^2}{(2H-L)^2} \quad (100)$$

Using (99) and (100) the fluctuation (96) becomes

$$\frac{\Delta \bar{Q}}{\bar{Q}} = \sqrt{\frac{225}{108}} \frac{1}{\sqrt{N}} \sqrt{\frac{N}{n}} \approx \frac{1.5}{\sqrt{n}} \quad (101)$$

Thus we obtain the intuitively very satisfactory result that the fluctuations are proportional to the inverse square root of the number of actual rather than possible contacts.

At the same time the approximations made above become clear; The terms neglected above contribute in order $N^{-1/2}$ rather than $n^{-1/2}$ to the fluctuations. Since $N \approx 10^4$ these

fluctuations are only about 1% and can be neglected at the present experimental accuracy.

The result (101) was derived in a special model. However, it is of such a simple nature that one expects it to hold generally. Of course, the numerical factor in (101) will depend on the form of the height distribution function.

13. Line-like Correlations

Here we shall deal with the situation actually encountered in measurements using milled saw tooth profiles. The different ridges (lines) have a height distribution

$$\sigma(h)dh = \text{probability that a line has a height between } h, h+dh \quad (102)$$

The variations of the height of the ridges along their length can be taken into account by a distribution $\tau(\kappa)$ such that

$$\tau(\kappa)d\kappa = \text{probability that a point on a ridge has a height between } \kappa \text{ and } \kappa+d\kappa \text{ above (or below) the average height of the ridge.} \quad (103)$$

This implies

$$\int \tau(\kappa) d\kappa = 0 \quad (104)$$

The formalism given before can easily be generalized to this situation. The average heat flow through one contact square becomes

$$\bar{Q} = Q(x_1 + x_2 + x_3 + x_4 - L) \quad (105)$$

$$\tau(x_1) \tau(x_2) \sigma(x_3) \sigma(x_4) dx_1 dx_2 dx_3 dx_4$$

where $Q(x)$ is given by (10).

Introducing new coordinates

$$\begin{aligned} x_1 + x_3 &= y_1 & x_2 + x_4 &= y_2 \\ x_1 - x_3 &= 2z_1 & x_2 - x_4 &= 2z_2 \end{aligned} \quad (106)$$

(105) becomes

$$\bar{Q} = \int_Q(y_1 + y_2 - L) \omega(y_1) \omega(y_2) dy_1 dy_2 \quad (107)$$

where $\omega(y)$ is defined by

$$\omega(y) = H \int \tau(z+y) \sigma(z-y) dz \quad (108)$$

(107) shows that $\omega(x)$ is the probability that an asperity has a height between x and $x+dx$. From here on the formalism works in exactly the same way as before, with the exception of the fluctuations. These have to be treated differently, since there is now a correlation between the heights of the contact point. This is best seen for $\tau(x) = \delta(x)$, i.e. the height varies from ridge to ridge but not along the ridges. Then there are no fluctuations of the heat flow at all. Therefore, the distribution $\sigma(x)$ does not give rise to fluctuations, while $\tau(x)$ does. Therefore, the square of the heat flow becomes

$$\bar{Q}^2 = \int [Q(x_1+x_2+x_3+x_4-L) \sigma(x_1) \sigma(x_2) dx_1 dx_2]^2 (109)$$

$$\tau(x_3) \tau(x_4) dx_3 dx_4$$

rather than

$$\int Q^2(x_1+x_2+x_3+x_4-L) \sigma(x_1) \sigma(x_2) \tau(x_3) \tau(x_4) dx_1 dx_2 dx_3 dx_4$$

(110)

(110) would be correct if the asperities were distributed at random.

That (109) rather than (110) is the correct expression for \bar{Q}^2 reduces the fluctuations.

This is the main reason for the better reproducibility of the measurements for saw tooth milled surfaces, as compared to polished surfaces. Because of the lack of experimental data on $\tau(x)$ and $\sigma(x)$ we cannot compare the theory with experiment at the moment. Both distributions can be obtained easily by measuring several closely spaced profiles of the test sample orthogonal to the ridges.

14. Surface Waviness

In this section we shall consider the correlations of the asperities that are due to surface waviness. This can be treated in our formalism by studying the simplified model of waviness shown in Fig. 15.

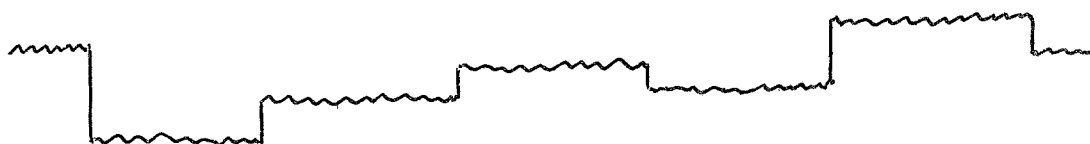


Fig. 15

The surface is approximated by s patches of contact points, each patch containing M contact squares. A height distribution (waviness) is defined by

$$\mu(x)dx = \text{probability that a patch has a height between } x \text{ and } x+dx. \quad (111)$$

The average heat flux through one contact square becomes

$$\langle \bar{Q} \rangle = \int \bar{Q}(L-x_1-x_2) \mu(x_1) \mu(x_2) dx_1 dx_2 \quad (112)$$

where \bar{Q} is given by (107). Inserting (107) into (112) we obtain

$$\langle \bar{Q} \rangle = \int Q(x_1+x_2+x_3+x_4+x_5+x_6-L) \tau(x_1) \tau(x_2) \sigma(x_3) \sigma(x_4) \mu(x_5) \mu(x_6) \cdot d^6x \quad (113)$$

Introducing new variables by

$$\begin{aligned} x_1+x_3+x_5 &= 3y_1 & x_1-x_3 &= 3z_1 & x_2-x_4 &= 3u_1 \\ &&&&& \end{aligned} \quad (114)$$

$$x_2+x_4+x_6 = 3y_2 \quad x_1-x_5 = 3z_2 \quad x_2-x_6 = 3u_2$$

$\langle \bar{Q} \rangle$ becomes

$$\langle \bar{Q} \rangle = \int Q(y_1+y_2-L) \phi(y_1) \phi(y_2) dy_1 dy_2 \quad (115)$$

where

$$\phi(y_1) = H^2 \int dz_1 dz_2 \tau(y_1 + z_1 + z_2) \sigma(y_1 + z_2 - 2z_1) \mu(y_1 + z_1 - 2z_2)$$
(116)

(115) is again the standard formula (14) where the height distribution function is given now by (116). The manner in which τ and σ can be measured has been indicated before; $\mu(x)$ can be determined by a flatness measurement with the help of a dial indicator and a surface plate. Therefore, all the distributions entering (116) can be determined experimentally.

Next we shall calculate the fluctuations of the heat flow. For this purpose we write the total heat flow through the interface in the form

$$G = \sum_{\alpha=1}^S G_{1\alpha} \quad (117)$$

where $G_{1\alpha}$ is the heat flow through patch α :

$$G_{1\alpha} = \sum_{i=1}^M Q_{i\alpha} \quad (118)$$

The average heat flow through one patch is

$$\bar{G}_{1\alpha} = M \bar{Q}_\alpha \quad (119a)$$

$$\bar{G} = \sum_{\alpha} \bar{G}_{1\alpha} = M \sum_{\alpha} \bar{Q}_\alpha \quad (119b)$$

$$\left\langle \sum_{\alpha} \bar{Q}_{\alpha} \right\rangle = s \left\langle \bar{\bar{Q}} \right\rangle \quad (120)$$

The bar denotes averaging over σ and τ as before. The total average heat flow thus becomes if we also average over the patch distribution μ

$$\left\langle \bar{G} \right\rangle = M s \left\langle \bar{\bar{Q}} \right\rangle \quad (121)$$

Next we have to calculate

$$\begin{aligned} G^2 &= (\sum_{\alpha} G_{1\alpha})^2 = \sum_{\alpha=1}^M G_{1\alpha}^2 + \sum_{\alpha \neq \rho} G_{1\alpha} G_{1\rho} = \sum_{\alpha} (\sum_i Q_{ik})^2 + \\ &+ \sum_{\alpha \neq \rho} (\sum_i Q_{ik}) (\sum_k Q_{k\rho}) \end{aligned} \quad (122)$$

Averaging first over σ and τ we have

$$\bar{G}^2 = M \sum_{\alpha} \bar{Q}^2 + \sum_{\alpha} M(M-1) \bar{Q}_{\alpha}^2 + M^2 \sum_{\alpha \neq \rho} \bar{Q}_{\alpha} \bar{Q}_{\rho} \quad (123)$$

Next we average over μ and obtain

$$\left\langle \bar{G}^2 \right\rangle = \left\langle \bar{G} \right\rangle^2 + s M \{ \left\langle \bar{Q}^2 \right\rangle - \left\langle \bar{\bar{Q}}^2 \right\rangle \} + s M^2 \{ \left\langle \bar{Q}^2 \right\rangle - \left\langle \bar{\bar{Q}}^2 \right\rangle \} \quad (124)$$

Therefore the fluctuations become

$$\frac{\Delta G}{G} = \frac{1}{s} \left\{ \frac{\left[\left\langle \bar{Q}^2 \right\rangle - \left\langle \bar{\bar{Q}}^2 \right\rangle \right] / M + \left[\left\langle \bar{Q}^2 \right\rangle - \left\langle \bar{\bar{Q}}^2 \right\rangle \right]}{\left\langle \bar{\bar{Q}} \right\rangle^2} \right\} \quad (125)$$

References

1. Ling, F.F. J. Appl. Phys. 24, 981-88 (1958)
2. Myers, N.O. Wear 5, 182-189 (1962)
3. Henry, J.J. AEC Reprint MIT-2029-2, Massachusetts Institute of Technology, 1964
4. Held, W. Allgemeine Wärmetechnik 8, 1-8 (1957)
5. See e.g. Lamb, H. Treatise on the Mathematical Theory of Elasticity, Dover 1957
6. Abbe, W., Ashby, N., Bartel, L., Ross, J.R., Sexl, R. and Thirring, W., NAS-1-6-28-00008
7. Cetinkale (Veziroglu) T.N., Thesis, University of London, 1951
8. Fried, E. Technical Report, NASA 66 SD 4471
9. Cetinkale, T.N. and Fishenden, M., General Discussions of Heat Transfer, Proc. Inst. of Mechanical Engineers and ASME, p.271-275, 1951
10. Tien, C.L. Proc 7th Conference on Thermal Conductivity, 755-760, 1967

II. USER'S TABLES

Abstract:

The formulae relating heat flux and applied pressure between two surfaces in contact to parameters of the surfaces given in the preceding part are rewritten in a form which facilitates evaluation. We further present the results of a computation of the integrals $A_n(L)$ for several height distribution functions in a series of tables. Also, the factor which multiplies the $N^{-1/2}$ (N the number of possible contact points) in the expression for the statistical fluctuation of the heat flux is given for spherical and ridgelike asperities.

1. Introduction

In part I the heat flow through one contact square and the applied force have been calculated from the height distribution function ρ and the surface parameters B , R and H . They are given as certain integrals and are therefore related to each other in a parametric form. Only for the very simplest height distributions (e.g. if all asperities have the same height) a simple algebraic relation between heat flow and force may be written down. For this reason we give in the tables below the values of the integrals $A_n(L)$ which have been obtained by numerical integration (for several different distribution functions).

In chapter 2 we recast the relevant formulae in a form which is better suited for evaluation. In chapter 3 we present the tables, and chapter 4 contains simple examples of how to use the tables as well as a discussion of several experiments.

2. Useful Form of the Equations

In terms of the previously defined integral

$$A_n(L) = H^{-n-1} \int_0^{2H-L} z^n K\left(\frac{z+L}{2}\right) dz \quad (1)$$

the expressions for heat flux q and pressure p may be written as

$$q = \alpha A_{1/2}(L) \quad (2)$$

$$\gamma A_{3/2}(L) \quad \text{for elastic contacts only} \quad (3a)$$

$$p =$$

$$\gamma A_{3/2}(2H-\lambda) + \beta [A_1(L) - A_1(2H-\lambda)] \quad (3b)$$

where

$$\alpha = \frac{2k\Delta T}{B^2} \sqrt{\frac{RH}{2}} , \quad \beta = \frac{P\pi RH}{2B^2} , \quad \gamma = \frac{H}{DB^2} \sqrt{\frac{RH}{2}} , \quad P = \frac{3}{\pi D} \sqrt{\frac{\lambda}{R}}$$

$$K(x) = 2H \int_0^{H-x} dy \rho(x+y) \rho(x-y) \quad \text{for } x \leq H \quad (4a)$$

$$= H \int_{-x}^x dy \rho(x+y) \rho(x-y) \quad \text{for } x > H \quad (4b)$$

and L is the distance of approach between the two surfaces. Instead of L we will use $d = 2H-L$. Furthermore $\rho(x)$ is normalized

$$\int_0^H \rho(x) dx = 1 \quad (5)$$

$\rho(x)$ has the dimension of an inverse length while $K(x)$ and $A_n(L)$ are dimensionless. It is therefore convenient to introduce, instead of $\rho(x)$, a dimensionless function $\bar{\rho}(\xi)$ and dimensionless variable ξ , where the relation to $\rho(x)$, $K(x)$, $A_n(L)$ is given by

$$\xi = x/H, \quad \delta = d/H = (2H-L)/H, \quad \rho(x) = \frac{1}{H} \bar{\rho}(\xi)$$

$$K(x) = \bar{K}(\xi), \quad A_n(L) = \bar{A}_n(\delta)$$

We have, therefore,

$$\int_0^1 \bar{\rho}(\xi) d\xi = 1, \quad \bar{\rho}(\xi) = 0 \quad \text{for } \xi < 0 \text{ and } \xi > 1$$

$$\begin{aligned} \bar{K}(\xi) &= 2 \int_0^{1-\xi} d\eta \bar{\rho}(\xi+\eta) \bar{\rho}(\xi-\eta) & \xi \leq 1 \\ &\int_{-\xi}^{\xi} d\eta \bar{\rho}(\xi+\eta) \bar{\rho}(\xi-\eta) & \xi > 1 \end{aligned}$$

$$\bar{A}_n(\delta) = \int_0^\delta \xi^n \bar{K}(1 + \frac{\xi-\delta}{2}) d\xi.$$

q and p are now given by

$$q = \alpha \bar{A}_{1/2}(\delta) \quad (6)$$

$$\gamma \bar{A}_{3/2}(\delta) \quad (7a)$$

$p =$

$$\gamma \bar{A}_{3/2}(\lambda/H) + \beta [\bar{A}_1(\delta) - \bar{A}_1(\lambda/H)] \quad (7b)$$

Except for inelastic contacts all dependence on parameters of the material are contained in the factors α and γ . But in the usual case of inelastic contacts λ/H is a very small number and one may therefore put λ/H to zero to get

$$p = \gamma \bar{A}_1(\delta) .$$

3. Evaluation of $\bar{A}_n(\delta)$ and Tables

For simple distribution $\bar{\rho}(\xi)$ the integrals $\bar{A}_n(\delta)$ are easily evaluated. For instance take

$$a) \bar{\rho}(\xi) = \theta(1-\xi) \qquad b) \bar{\rho}(\xi) = 6\xi(1-\xi) .$$

Then we get

$$\bar{K}(\xi) = 2(1-\xi) \qquad \bar{K}(\xi) = 48(1-\xi)^3(\xi^2 - \frac{1}{5}(1-\xi)^2) \qquad 0 < \xi < 1$$

$$a) \bar{A}_n(\delta) = \frac{1}{(n+1)(n+2)} \delta^{n+2}$$

$$\text{b) } \bar{A}_{1/2}(\delta) = 64 \delta^{9/2} (16\delta^2 - 104\delta + 143)/15015$$

$$\bar{A}_1(\delta) = \delta^5 (2\delta^2 - 14\delta + 21)/70 \quad (0 < \delta < 1)$$

For more complicated distribution functions numerical evaluation is preferable. This has been done, and the results are listed in the tables for the following height distribution functions

$$\bar{\rho}_1(\xi) = 1$$

$$\bar{\rho}_2(\xi) = 6\xi(1-\xi)$$

$$\bar{\rho}_3(\xi) = N_3 (\xi+0.1)^{-1}$$

$$\bar{\rho}_4(\xi) = N_4 \sin \pi \xi$$

$$\bar{\rho}_5(\xi) = N_5 \exp(-(2\xi-1)^2) \quad 0 \leq \xi \leq 1$$

$$\bar{\rho}_5(\xi) = \begin{cases} N_6 \exp[-(12\xi-4)^2] & \xi < 1/3 \\ N_6 \exp[-(\xi-1/3)] & \xi \geq 1/3 \end{cases}$$

(The $N_3 \dots N_6$ are normalization factors, $N_i^{-1} = \int_0^1 \bar{\rho}_i(\xi) d\xi$).

In Tables I - VI one finds in columns 1 - 5 δ , $\bar{A}_{1/2}(\delta)$, $\bar{A}_1(\delta)$, $\bar{A}_{3/2}(\delta)$ and $\bar{A}_2(\delta)$, in columns 6 and 7 the fluctuation enhancement factors $F_{1/2}(\delta)$ and $F_1(\delta)$ which are defined by

$$F_n(\delta) = \sqrt{\bar{A}_{2n}(\delta)} / \bar{A}_n(\delta) \quad (8)$$

These factors enter in the expressions for the statistical fluctuations of the heat flow

$$\frac{\Delta Q}{Q} = \frac{1}{\sqrt{N}} \frac{\sqrt{\bar{A}_1(\delta)}}{\bar{A}_{1/2}(\delta)} = \frac{1}{\sqrt{N}} F_{1/2}(\delta) \quad (9)$$

$F_1(\delta)$ is given in the tables because in a recent work [1] with accordingly machined surfaces (ridgelike asperities) of the test probes a slightly different connection for \bar{q} and \bar{F} was assumed, namely with $\bar{q} \propto \bar{A}_1(\delta)$ and $\bar{F} \propto \bar{A}_2(\delta)$ and therefore with a fluctuation enhancement factor $F_1(\delta)$ instead of $F_{1/2}(\delta)$. In Table VII we compare $\bar{A}_1(\delta)$ with $\tilde{A}_1(\delta)$, where $\tilde{A}_1(\delta)$ is defined by

$$\tilde{A}_1(\delta) = \int_0^\delta \xi \bar{K}(1 + \frac{\xi - \delta}{2}) [\tan^{-1}(\frac{B}{H\xi}) - 1] \quad .$$

This function replaces $\bar{A}_1(\delta)$ in a refined expression for the heat flow which will be discussed below in connection with Bhandari's experiment. (In Table VII the ratio B/H has been fixed at a value of 2.1). One can see very easily that $\tilde{A}_1(\delta)$ increases faster than $\bar{A}_1(\delta)$.

4. Comparison with Experiment

In this chapter we will compare our theory with several of the large number of experiments. We will begin with the only experiment which has been done following our proposed experimental procedure and which shows that the statistical fluctuations, esp. at low pressure, are extremely important.

a) Bhandari's experiment

Measurements with stainless steel SS 303 have been done at the University of Miami by Bhandari [1] using 15 pairs of test probes with the same surface finish. As may be seen from Fig. 1, the data scatter appreciably, e.g. at a pressure of about 3000 psi the fluctuation around the mean value is 50%. The three curves in Fig. 2 were calculated by Bhandari under the following assumptions:

a) the asperities are ridgelike and of triangular shape with opening angle 2θ and the lay directions of two opposing test probes are 90° apart. Then the modified formulae for contact conductance h_c and applied pressure p are

$$h_c = \frac{k \tan\theta}{B^2} \overline{A}_1(\delta)$$

$$p = \frac{\pi P}{4B^2} \tan^2\theta \overline{A}_2(\delta) .$$

b) from an analysis of the surfaces a height distribution function was deduced which resembled a Gaussian curve with

maximum at about 2000 μ -inches and a width of about 250 μ -inches (Fig. 3).

Under these assumptions curve A in Fig. 2 has been calculated. In curve B a different connection between contact conductance of a single contact which has already been discussed in section , (viz. $Q \propto z/\tan^{-1}(B/z - 1)$ (see Eq. (63) of Part I) instead of $h \propto z$, has been used.

A major change is obtained by folding surface waviness into the height distribution (curve B in Fig. 2) which results in an effective distribution function which reaches out much longer (Fig. 3). It is an absolute prediction. The result is curve C. The agreement is excellent. Let us note another feature of the data: the ratio of the fluctuations of the contact conductance increases with decreasing pressure. We have

$$\text{at } p = 12000 \text{ psi} \quad h_C = (3 \pm 0.5) 10^3 \text{ BTU/(hr)(ft}^2\text{)} (\text{°F})$$

$$\text{and at } p = 3500 \text{ psi} \quad h_C = (5 \pm 2) 10^2 \text{ BTU/(hr)(ft}^2\text{)} (\text{°F})$$

This increase in the percentage error by a factor of nearly 3 is in good accordance with our predictions. (Compare f.i. in Table II the values of F_1 for $\delta = 0.5$ (lower pressure) and $\delta = 1!$)

b) Cassidy and Mark

Cassidy and Mark [2] measured contact conductance of stain-less steel SS 414 in a pressure range between 300 and 1400 psi.

Their results are very well described by a behaviour

$$h \propto p^n \quad n \approx 0.93$$

in accordance with our theory. (Fig. 4a). Unfortunately their determination of surface parameters cannot be used, because the test probes were preloaded by arbitrary loads prior to actual heat conductance measurement and after determination of surface parameters.

The surface used, therefore, was different from the one analyzed before, since the whole surface was deformed inelastically by the preloading procedure.

As a check of our equations we use the simplified form

$$\frac{qB}{k\Delta T} = \frac{h_c B}{k} = 5.5 \left(\frac{P}{P}\right)^{0.9} \quad (10)$$

(h_c = contact conductance).

From this a value $B \approx 10^{-2}$ inch may be deduced from one experimental point. A look at the surface analyzer waviness trace (Fig. 4 of [2]) shows that this is a very reasonable result.

c) Fried's experiments

A careful determination of surface parameters, but not of a height distribution function, has been made in the many contact conductance experiments of Fried.

We will discuss here several measurements, one with stainless steel SS 304 (sample 1,2 of Fried [3]), another with

aluminium T6 (sample 9,10) and two with aluminium T4 (Fried II [4]).

Fried has measured the following surface parameters:

- a) rms roughness: this corresponds to $H/2$
- b) peak-to-peak ridge distance: B
- c) flatness deviation, i.e. the amplitude of the waviness.

Neither the wavelength of the waviness nor R have been determined. In view of the lack of a height distribution function, no absolute calculation is possible. Nevertheless, we can use our tables to get information about the fluctuations which are to be expected.

To this purpose we eliminate the unknown parameter R from the equations to get

$$\frac{h_c B}{2k} \frac{\sqrt{A_1(\delta)}}{\bar{A}_{1/2}(\delta)} = \sqrt{\frac{p}{p_0}} \quad (11)$$

Let us first consider stainless steel SS 304. By choosing as our point of reference $h_c \approx 10^3 \text{W/m}^2\text{C}$, $p \approx 10^4 \text{kN/m}^2$ and using $B = 10^{-4} \text{ m}$ (as determined by Fried) we find

$$\sqrt{\bar{A}_1(\delta)/\bar{A}_{1/2}(\delta)} = 10 \quad ,$$

corresponding to $\delta = 1/3$ in Table II. As the measurements cover a range of pressure between 1600 kN/m^2 (corresponding

to $\delta=0.2$) and 30000kN/m^2 (corresponding approximately to $\delta = 0.4$), the fluctuation enhancement factors are big. (Fig. 4b).

Similar considerations apply to aluminium T6. Now taking for reference $h_c = 3 \cdot 10^4 \text{W/m}^2\text{C}$, $p_s = 10^4 \text{kN/m}^2$ and $B = 6 \cdot 10^{-5} \text{m}$ we find $\delta = 0.32$. The arguments about fluctuations above remain valid (Fig. 5).

The expected scatter of the data points cannot be seen in the figures as the points are the results of one single experiment. Repetition of the measurements with other test probes with identical surface finish would bring them into the picture.

We conclude this section with two examples of measurements with aluminium T4.

Test probes 19 and 20 of Fried II [4] have a very fine surface with a rms roughness of only $0.2 \mu\text{m}$. The data from two different series of measurements with the same probes are shown in Fig. 6. At low pressures (100 - 200 psi), the values of contact conductance obtained differ by a factor of 4. The curve is a prediction of our simplified theory and was calculated by (10) and deducing the unknown parameter B from fitting the curve through one of the data points. As always happens, B turns out to be of the right magnitude, namely $B = 1,3 \cdot 10^{-4} \text{m}$.

Fig. 7 shows results with test probes 21 and 22, also aluminium T4, but with a much coarser surface (roughness about $1.2 \mu\text{m}$). Here only one series of measurements exists and the

data points fit quite well to our curve. Here again B is about $2,5 \cdot 10^{-4}$ m.

Our results show that it is exceedingly important to take into account surface waviness in any determination of the interface characteristics. If this is omitted the theoretical curves will fit the data not too well but only a rough agreement between theory and experiment will result. As Bhandari has shown one can get excellent numerical predictions of the heat flow if the statistical theory and the tables presented here are used correctly.

References

1. Bhandari, N., M.Sc.Thesis, University Miami 1969
2. Cassidy, J.F. and Mark,H., paper presented at 4th Thermophysics Conference, 1969
3. Fried, E. GE Document No. 66-SD 4471 (1966)
4. Fried, E. GE Document No. 65-SD 4395 (1965)

Tab. I/1 $\bar{\rho}(\xi) = 1$

δ	$\bar{A}_{\nu_2}(\delta)$	$\bar{A}_1(\delta)$	$\bar{A}_{3/2}(\delta)$	$\bar{A}_2(\delta)$	$F_{\nu_2}(\delta)$	$F_1(\delta)$
0.01	0.266E-05	0.166E-06	0.113E-07	0.824E-09	153.1	173.2
0.02	0.151E-04	0.133E-05	0.129E-06	0.133E-07	76.50	86.60
0.03	0.416E-04	0.45CE-05	0.534E-06	0.675E-07	51.00	57.73
0.04	0.854E-04	0.107E-04	0.146E-05	0.213E-06	38.25	43.30
0.05	0.149E-03	0.208E-04	0.319E-05	0.521E-06	30.60	34.64
0.06	0.235E-03	0.36CE-04	0.605E-05	0.108E-05	25.50	28.87
0.07	0.346E-03	0.572E-04	0.104E-04	0.200E-05	21.86	24.74
0.08	0.483E-03	0.853E-04	0.166E-04	0.341E-05	19.12	21.65
0.09	0.648E-03	0.122E-03	0.25CE-04	0.547E-05	17.00	19.24
0.10	0.844E-03	0.167E-03	0.361E-04	0.833E-05	15.30	17.32
0.11	0.107E-02	0.222E-03	0.504E-04	0.122E-04	13.91	15.75
0.12	0.133E-02	0.288E-03	0.684E-04	0.173E-04	12.75	14.43
0.13	0.163E-02	0.366E-03	0.905E-04	0.238E-04	11.77	13.32
0.14	0.196E-02	0.457E-03	0.117E-03	0.320E-04	10.93	12.37
0.15	0.233E-02	0.562E-03	0.149E-03	0.422E-04	10.20	11.55
0.16	0.273E-02	0.683E-03	0.187E-03	0.546E-04	9.562	10.83
0.17	0.318E-02	0.819E-03	0.232E-03	0.696E-04	9.000	10.19
0.18	0.367E-02	0.972E-03	0.283E-03	0.875E-04	8.500	9.623
0.19	0.420E-02	0.114E-02	0.342E-03	0.109E-03	8.052	9.116
0.20	0.477E-02	0.133E-02	0.409E-03	0.133E-03	7.650	8.660
0.21	0.539E-02	0.154E-02	0.485E-03	0.162E-03	7.285	8.248
0.22	0.606E-02	0.177E-02	0.571E-03	0.195E-03	6.954	7.873
0.23	0.677E-02	0.203E-02	0.667E-03	0.233E-03	6.652	7.531
0.24	0.753E-02	0.23CE-02	0.774E-03	0.276E-03	6.375	7.217
0.25	0.834E-02	0.26CE-02	0.893E-03	0.326E-03	6.120	6.928
0.26	0.920E-02	0.293E-02	0.102E-02	0.381E-03	5.884	6.662
0.27	0.101E-01	0.328E-02	0.117E-02	0.443E-03	5.666	5.415
0.28	0.111E-01	0.366E-02	0.133E-02	0.512E-03	5.464	5.186
0.29	0.121E-01	0.406E-02	0.150E-02	0.589E-03	5.276	5.973
0.30	0.132E-01	0.450E-02	0.169E-02	0.675E-03	5.100	5.774

*

Tab.I/2

δ	$\bar{A}_{1/2}(\delta)$	$\bar{A}_1(\delta)$	$\bar{A}_{3/2}(\delta)$	$\bar{A}_2(\delta)$	$F_{1/2}(\delta)$	$F_1(\delta)$
0.31	0.143E-01	0.497E-02	0.190E-02	0.770E-03	4.935	5.587
0.32	0.155E-01	0.546E-02	0.212E-02	0.874E-03	4.781	5.413
0.33	0.167E-01	0.599E-02	0.236E-02	0.988E-03	4.636	5.249
0.34	0.180E-01	0.655E-02	0.262E-02	0.111E-02	4.500	5.094
0.35	0.193E-01	0.715E-02	0.290E-02	0.125E-02	4.371	4.949
0.36	0.207E-01	0.778E-02	0.320E-02	0.140E-02	4.250	4.811
0.37	0.222E-01	0.844E-02	0.352E-02	0.156E-02	4.135	4.681
0.38	0.238E-01	0.915E-02	0.387E-02	0.174E-02	4.026	4.558
0.39	0.253E-01	0.985E-02	0.423E-02	0.193E-02	3.923	4.441
0.40	0.270E-01	0.107E-01	0.463E-02	0.213E-02	3.825	4.330
0.41	0.287E-01	0.115E-01	0.504E-02	0.235E-02	3.732	4.225
0.42	0.305E-01	0.123E-01	0.549E-02	0.259E-02	3.643	4.124
0.43	0.324E-01	0.133E-01	0.596E-02	0.285E-02	3.558	4.028
0.44	0.343E-01	0.142E-01	0.646E-02	0.312E-02	3.477	3.936
0.45	0.362E-01	0.152E-01	0.699E-02	0.342E-02	3.400	3.849
0.46	0.383E-01	0.162E-01	0.754E-02	0.373E-02	3.326	3.765
0.47	0.404E-01	0.173E-01	0.813E-02	0.407E-02	3.255	3.685
0.48	0.426E-01	0.184E-01	0.876E-02	0.442E-02	3.187	3.608
0.49	0.448E-01	0.196E-01	0.941E-02	0.480E-02	3.122	3.535
0.50	0.472E-01	0.208E-01	0.101E-01	0.521E-02	3.060	3.464
0.51	0.496E-01	0.221E-01	0.108E-01	0.564E-02	3.000	3.396
0.52	0.520E-01	0.234E-01	0.116E-01	0.609E-02	2.942	3.331
0.53	0.546E-01	0.248E-01	0.124E-01	0.658E-02	2.887	3.268
0.54	0.572E-01	0.262E-01	0.132E-01	0.709E-02	2.833	3.207
0.55	0.599E-01	0.277E-01	0.141E-01	0.763E-02	2.782	3.149
0.56	0.626E-01	0.293E-01	0.150E-01	0.820E-02	2.732	3.093
0.57	0.655E-01	0.309E-01	0.160E-01	0.880E-02	2.684	3.039
0.58	0.684E-01	0.325E-01	0.170E-01	0.943E-02	2.638	2.986
0.59	0.713E-01	0.342E-01	0.180E-01	0.101E-01	2.593	2.936
0.60	0.744E-01	0.360E-01	0.191E-01	0.108E-01	2.550	2.887

Tab. I/3

δ	$\bar{A}_{1/2}(\delta)$	$\bar{A}_1(\delta)$	$\bar{A}_{3/2}(\delta)$	$\bar{A}_2(\delta)$	$F_{1/2}(\delta)$	$F_1(\delta)$
0.61	0.775E-01	0.378E-01	0.203E-01	0.115E-01	2.508	2.839
0.62	0.808E-01	0.397E-01	0.214E-01	0.123E-01	2.468	2.794
0.63	0.841E-01	0.417E-01	0.227E-01	0.131E-01	2.428	2.749
0.64	0.874E-01	0.437E-01	0.240E-01	0.140E-01	2.391	2.706
0.65	0.905E-01	0.456E-01	0.253E-01	0.149E-01	2.354	2.665
0.66	0.944E-01	0.475E-01	0.267E-01	0.158E-01	2.318	2.624
0.67	0.980E-01	0.501E-01	0.281E-01	0.168E-01	2.284	2.585
0.68	0.102E 00	0.524E-01	0.296E-01	0.178E-01	2.250	2.547
0.69	0.106E 00	0.548E-01	0.312E-01	0.189E-01	2.217	2.510
0.70	0.109E 00	0.572E-01	0.328E-01	0.200E-01	2.186	2.474
0.71	0.113E 00	0.597E-01	0.345E-01	0.212E-01	2.155	2.440
0.72	0.117E 00	0.622E-01	0.362E-01	0.224E-01	2.125	2.406
0.73	0.121E 00	0.648E-01	0.380E-01	0.237E-01	2.096	2.373
0.74	0.126E 00	0.675E-01	0.398E-01	0.250E-01	2.067	2.341
0.75	0.130E 00	0.703E-01	0.418E-01	0.264E-01	2.040	2.309
0.76	0.134E 00	0.732E-01	0.437E-01	0.278E-01	2.013	2.279
0.77	0.139E 00	0.761E-01	0.458E-01	0.293E-01	1.987	2.249
0.78	0.143E 00	0.791E-01	0.479E-01	0.308E-01	1.961	2.221
0.79	0.148E 00	0.822E-01	0.501E-01	0.325E-01	1.937	2.192
0.80	0.153E 00	0.853E-01	0.523E-01	0.341E-01	1.912	2.165
0.81	0.158E 00	0.886E-01	0.547E-01	0.359E-01	1.889	2.138
0.82	0.162E 00	0.919E-01	0.571E-01	0.377E-01	1.866	2.112
0.83	0.167E 00	0.953E-01	0.595E-01	0.395E-01	1.843	2.087
0.84	0.173E 00	0.988E-01	0.621E-01	0.415E-01	1.821	2.062
0.85	0.178E 00	0.102E 00	0.647E-01	0.435E-01	1.800	2.038
0.86	0.183E 00	0.106E 00	0.674E-01	0.456E-01	1.779	2.014
0.87	0.188E 00	0.110E 00	0.702E-01	0.477E-01	1.759	1.991
0.88	0.194E 00	0.114E 00	0.731E-01	0.500E-01	1.739	1.968
0.89	0.199E 00	0.117E 00	0.760E-01	0.523E-01	1.719	1.946
0.90	0.205E 00	0.121E 00	0.790E-01	0.547E-01	1.700	1.924

Tab. I/4

δ	$\bar{A}_{1/2}(\delta)$	$\bar{A}_1(\delta)$	$\bar{A}_{3/2}(\delta)$	$\bar{A}_2(\delta)$	$F_{1/2}(\delta)$	$F_1(\delta)$
0.91	C.211E CC	C.126E CC	C.822E-C1	C.571E-C1	1.681	1.903
0.92	C.217E CC	C.130E CC	C.854E-C1	C.597E-C1	1.663	1.883
0.93	C.223E CC	C.134E CC	C.886E-C1	C.623E-C1	1.645	1.862
0.94	C.229E CC	C.138E CC	C.920E-C1	C.651E-C1	1.628	1.843
0.95	C.235E CC	C.143E CC	C.955E-C1	C.679E-C1	1.610	1.823
0.96	C.241E CC	C.147E CC	C.991E-C1	C.708E-01	1.594	1.804
0.97	C.247E CC	C.152E CC	C.103E CC	C.738E-01	1.577	1.786
0.98	C.254E CC	C.157E CC	C.106E CC	C.769E-01	1.561	1.767
0.99	C.260E CC	C.162E CC	C.110E CC	C.800E-C1	1.545	1.750
1.00	C.267E CC	C.167E CC	C.114E CC	C.833E-C1	1.530	1.732

Tab. II $\bar{\xi}(\xi) = 6\xi(1-\xi)$

δ	$\bar{A}_{y_2}(\delta)$	$\bar{A}_1(\delta)$	$\bar{A}_{3/2}(\delta)$	$\bar{A}_2(\delta)$	$F_{y_2}(\delta)$	$F_1(\delta)$
0.01	0.600E-09	0.298E-10	0.165E-11	0.594E-13	9006.	0.1058E 05
0.02	0.136E-07	0.947E-09	0.743E-10	0.633E-11	2261.	2655.
0.03	0.838E-07	0.714E-08	0.687E-09	0.717E-10	1009.	1185.
0.04	0.304E-06	0.299E-07	0.332E-08	0.400E-09	569.7	669.0
0.05	0.822E-06	0.506E-07	0.113E-07	0.152E-08	366.1	429.8
0.06	0.185E-05	0.224E-06	0.305E-07	0.451E-08	255.2	299.7
0.07	0.368E-05	0.481E-06	0.708E-07	0.113E-07	188.3	221.0
0.08	0.667E-05	0.931E-06	0.147E-06	0.250E-07	144.7	169.9
0.09	0.112E-04	0.167E-05	0.278E-06	0.504E-07	114.8	134.8
0.10	0.179E-04	0.280E-05	0.494E-06	0.944E-07	93.40	109.6
0.11	0.273E-04	0.448E-05	0.829E-06	0.166E-06	77.51	90.94
0.12	0.401E-04	0.688E-05	0.133E-05	0.278E-06	65.40	76.72
0.13	0.570E-04	0.102E-04	0.205E-05	0.447E-06	55.96	65.63
0.14	0.790E-04	0.147E-04	0.306E-05	0.694E-06	48.46	56.82
0.15	0.107E-03	0.200E-04	0.445E-05	0.104E-05	42.39	49.70
0.16	0.142E-03	0.282E-04	0.630E-05	0.153E-05	37.41	43.86
0.17	0.185E-03	0.379E-04	0.874E-05	0.218E-05	33.28	39.01
0.18	0.237E-03	0.501E-04	0.119E-04	0.306E-05	29.82	34.94
0.19	0.300E-03	0.651E-04	0.159E-04	0.421E-05	26.88	31.49
0.20	0.375E-03	0.836E-04	0.209E-04	0.569E-05	24.36	28.54
0.21	0.464E-03	0.106E-03	0.272E-04	0.757E-05	22.19	25.99
0.22	0.567E-03	0.133E-03	0.349E-04	0.995E-05	20.31	23.78
0.23	0.687E-03	0.164E-03	0.443E-04	0.129E-04	18.66	21.85
0.24	0.825E-03	0.202E-03	0.556E-04	0.166E-04	17.22	20.15
0.25	0.984E-03	0.246E-03	0.691E-04	0.210E-04	15.94	18.65
0.26	0.116E-02	0.297E-03	0.851E-04	0.265E-04	14.80	17.32
0.27	0.137E-02	0.356E-03	0.104E-03	0.330E-04	13.79	16.13
0.28	0.160E-02	0.424E-03	0.126E-03	0.407E-04	12.88	15.06
0.29	0.186E-02	0.501E-03	0.152E-03	0.500E-04	12.06	14.10
0.30	0.214E-02	0.589E-03	0.182E-03	0.609E-04	11.32	13.24

Tab. II/2

δ	$\bar{A}_{V_2}(\delta)$	$\bar{A}_1(\delta)$	$\bar{A}_{3/2}(\delta)$	$\bar{A}_2(\delta)$	$F_{V_2}(\delta)$	$F_1(\delta)$
0.31	0.247E-02	0.689E-03	0.217E-03	0.736E-04	10.65	12.45
0.32	0.282E-02	0.802E-03	0.256E-03	0.885E-04	10.04	11.74
0.33	0.321E-02	0.928E-03	0.301E-03	0.106E-03	9.486	11.08
0.34	0.364E-02	0.107E-02	0.352E-03	0.126E-03	8.978	10.49
0.35	0.411E-02	0.123E-02	0.41CE-03	0.149E-03	8.512	9.942
0.36	0.463E-02	0.14CE-02	0.476E-03	0.175E-03	8.084	9.440
0.37	0.519E-02	0.159E-02	0.549E-03	0.205E-03	7.689	8.977
0.38	0.580E-02	0.181E-02	0.632E-03	0.235E-03	7.324	8.550
0.39	0.647E-02	0.204E-02	0.723E-03	0.277E-03	6.987	8.154
0.40	0.719E-02	0.23CE-02	0.826E-03	0.321E-03	6.674	7.787
0.41	0.796E-02	0.258E-02	0.939E-03	0.369E-03	6.383	7.446
0.42	0.879E-02	0.289E-02	0.106E-02	0.424E-03	6.113	7.129
0.43	0.969E-02	0.322E-02	0.12CE-02	0.485E-03	5.860	6.833
0.44	0.106E-01	0.359E-02	0.135E-02	0.553E-03	5.625	6.556
0.45	0.117E-01	0.398E-02	0.152E-02	0.629E-03	5.404	6.298
0.46	0.128E-01	0.441E-02	0.171E-02	0.713E-03	5.198	6.056
0.47	0.139E-01	0.487E-02	0.191E-02	0.805E-03	5.004	5.828
0.48	0.152E-01	0.537E-02	0.212E-02	0.898E-03	4.822	5.615
0.49	0.165E-01	0.59CE-02	0.236E-02	0.102E-02	4.651	5.414
0.50	0.179E-01	0.647E-02	0.262E-02	0.114E-02	4.490	5.225
0.51	0.194E-01	0.709E-02	0.290E-02	0.128E-02	4.338	5.047
0.52	0.210E-01	0.775E-02	0.320E-02	0.143E-02	4.194	4.878
0.53	0.226E-01	0.845E-02	0.353E-02	0.159E-02	4.058	4.719
0.54	0.244E-01	0.92CE-02	0.388E-02	0.177E-02	3.930	4.569
0.55	0.263E-01	0.100CE-01	0.426E-02	0.196E-02	3.808	4.426
0.56	0.282E-01	0.108E-01	0.467E-02	0.217E-02	3.693	4.291
0.57	0.302E-01	0.117E-01	0.510E-02	0.239E-02	3.584	4.163
0.58	0.324E-01	0.127E-01	0.557E-02	0.264E-02	3.480	4.041
0.59	0.346E-01	0.137E-01	0.607E-02	0.290E-02	3.381	3.925
0.60	0.37CE-01	0.148E-01	0.661E-02	0.319E-02	3.287	3.815

Tab. II/3

δ	$\bar{A}_{1/2}(\delta)$	$\bar{A}_1(\delta)$	$\bar{A}_{3/2}(\delta)$	$\bar{A}_2(\delta)$	$F_{1/2}(\delta)$	$F_1(\delta)$
0.61	0.355E-01	0.159E-01	0.718E-02	0.349E-02	3.198	3.710
0.62	0.420E-01	0.171E-01	0.779E-02	0.382E-02	3.113	3.610
0.63	0.447E-01	0.184E-01	0.844E-02	0.418E-02	3.032	3.514
0.64	0.475E-01	0.197E-01	0.913E-02	0.456E-02	2.954	3.423
0.65	0.505E-01	0.211E-01	0.987E-02	0.497E-02	2.880	3.337
0.66	0.535E-01	0.226E-01	0.106E-01	0.541E-02	2.809	3.253
0.67	0.567E-01	0.241E-01	0.115E-01	0.587E-02	2.742	3.174
0.68	0.600E-01	0.258E-01	0.123E-01	0.637E-02	2.677	3.098
0.69	0.634E-01	0.275E-01	0.133E-01	0.690E-02	2.615	3.025
0.70	0.669E-01	0.292E-01	0.142E-01	0.747E-02	2.556	2.956
0.71	0.706E-01	0.311E-01	0.153E-01	0.807E-02	2.499	2.889
0.72	0.744E-01	0.331E-01	0.164E-01	0.872E-02	2.445	2.825
0.73	0.782E-01	0.351E-01	0.175E-01	0.940E-02	2.392	2.763
0.74	0.823E-01	0.372E-01	0.187E-01	0.101E-01	2.342	2.704
0.75	0.865E-01	0.394E-01	0.200E-01	0.109E-01	2.294	2.647
0.76	0.908E-01	0.417E-01	0.213E-01	0.117E-01	2.248	2.593
0.77	0.953E-01	0.441E-01	0.227E-01	0.126E-01	2.203	2.540
0.78	0.999E-01	0.466E-01	0.242E-01	0.135E-01	2.161	2.490
0.79	0.105E CC	0.492E-01	0.257E-01	0.144E-01	2.120	2.442
0.80	0.109E CC	0.519E-01	0.273E-01	0.154E-01	2.080	2.395
0.81	0.114E CC	0.547E-01	0.290E-01	0.165E-01	2.042	2.350
0.82	0.120E CC	0.575E-01	0.307E-01	0.176E-01	2.005	2.307
0.83	0.125E CC	0.605E-01	0.326E-01	0.188E-01	1.970	2.265
0.84	0.130E CC	0.636E-01	0.345E-01	0.200E-01	1.936	2.224
0.85	0.136E CC	0.668E-01	0.365E-01	0.213E-01	1.903	2.186
0.86	0.142E CC	0.702E-01	0.385E-01	0.227E-01	1.871	2.148
0.87	0.147E CC	0.736E-01	0.407E-01	0.241E-01	1.841	2.112
0.88	0.153E CC	0.771E-01	0.430E-01	0.257E-01	1.811	2.077
0.89	0.159E CC	0.808E-01	0.453E-01	0.272E-01	1.783	2.043
0.90	0.166E CC	0.845E-01	0.477E-01	0.289E-01	1.756	2.011

Tab. II/4

δ	$\bar{A}_{1/2}(\delta)$	$\bar{A}_1(\delta)$	$\bar{A}_{3/2}(\delta)$	$\bar{A}_2(\delta)$	$F_{1/2}(\delta)$	$F_1(\delta)$
0.91	0.172E CC	0.884E-C1	0.503E-C1	0.306E-C1	1.729	1.979
0.92	0.178E CC	0.924E-C1	0.529E-C1	0.324E-C1	1.704	1.949
0.93	0.185E CC	0.965E-C1	0.556E-C1	0.343E-C1	1.679	1.920
0.94	0.192E CC	0.101E CO	0.584E-C1	0.363E-C1	1.655	1.891
0.95	0.199E CC	0.105E CC	0.614E-C1	0.383E-C1	1.632	1.864
0.96	0.206E CC	0.110E CC	0.644E-C1	0.405E-C1	1.610	1.837
0.97	0.213E CC	0.114E CC	0.675E-C1	0.427E-C1	1.588	1.811
0.98	0.220E CC	0.119E CC	0.708E-C1	0.451E-C1	1.568	1.787
0.99	0.227E CC	0.124E CC	0.741E-C1	0.475E-C1	1.548	1.762
1.00	0.235E CC	0.129E CO	0.776E-C1	0.500E-C1	1.528	1.739

Tab. III/1

$$\bar{\rho}_3(\xi) = N_3 \cdot (\xi + 0.1)^{-1}$$

$$\bar{A}_{3/2}(\delta)$$

$$\bar{A}_2(\delta)$$

$$F_{1/2}(\delta)$$

$$F_i(\delta)$$

 δ

$$\bar{A}_{1/2}(\delta)$$

$$\bar{A}_1(\delta)$$

δ	$\bar{A}_{1/2}(\delta)$	$\bar{A}_1(\delta)$	$\bar{A}_{3/2}(\delta)$	$\bar{A}_2(\delta)$	$F_{1/2}(\delta)$	$F_i(\delta)$
0.0100	0.384E-06	0.239E-07	0.164E-08	0.119E-09	402.7	455.7
0.0200	0.219E-05	0.193E-06	0.187E-07	0.193E-08	200.6	227.2
0.0300	0.607E-05	0.656E-06	0.778E-07	0.981E-08	133.3	151.0
0.0400	0.125E-04	0.156E-05	0.214E-06	0.311E-07	99.70	113.0
0.0500	0.220E-04	0.306E-05	0.469E-06	0.762E-07	79.52	90.12
0.0600	0.349E-04	0.532E-05	0.891E-06	0.159E-06	66.07	74.89
0.0700	0.516E-04	0.849E-05	0.153E-05	0.295E-06	56.46	64.01
0.0800	0.724E-04	0.127E-04	0.246E-05	0.505E-06	49.25	55.85
0.0900	0.978E-04	0.182E-04	0.373E-05	0.812E-06	43.65	49.50
0.1000	0.128E-03	0.251E-04	0.541E-05	0.124E-05	39.16	44.43
0.1100	0.163E-03	0.336E-04	0.759E-05	0.183E-05	35.49	40.27
0.1200	0.204E-03	0.438E-04	0.103E-04	0.260E-05	32.43	36.81
0.1300	0.251E-03	0.559E-04	0.137E-04	0.359E-05	29.84	33.88
0.1400	0.303E-03	0.702E-04	0.179E-04	0.485E-05	27.63	31.37
0.1500	0.362E-03	0.868E-04	0.229E-04	0.641E-05	25.70	29.19
0.1600	0.428E-03	0.106E-03	0.288E-04	0.834E-05	24.02	27.28
0.1700	0.501E-03	0.128E-03	0.357E-04	0.107E-04	22.53	25.60
0.1800	0.581E-03	0.152E-03	0.438E-04	0.135E-04	21.21	24.11
0.1900	0.669E-03	0.180E-03	0.532E-04	0.168E-04	20.03	22.77
0.2000	0.765E-03	0.211E-03	0.639E-04	0.207E-04	18.97	21.57
0.2100	0.870E-03	0.245E-03	0.762E-04	0.252E-04	18.01	20.48
0.2200	0.983E-03	0.283E-03	0.901E-04	0.305E-04	17.13	19.49
0.2300	0.110E-02	0.326E-03	0.106E-03	0.366E-04	16.33	18.58
0.2400	0.124E-02	0.372E-03	0.123E-03	0.436E-04	15.60	17.75
0.2500	0.138E-02	0.422E-03	0.143E-03	0.515E-04	14.92	16.99
0.2600	0.153E-02	0.478E-03	0.165E-03	0.605E-04	14.30	16.29
0.2700	0.169E-02	0.538E-03	0.189E-03	0.706E-04	13.73	15.63
0.2800	0.186E-02	0.603E-03	0.215E-03	0.820E-04	13.19	15.03
0.2900	0.204E-02	0.673E-03	0.245E-03	0.948E-04	12.69	14.46
0.3000	0.224E-02	0.749E-03	0.277E-03	0.109E-03	12.23	13.94

Tab. III/2

δ	$\bar{A}_{1/2}(\delta)$	$\bar{A}_1(\delta)$	$\bar{A}_{3/2}(\delta)$	$\bar{A}_2(\delta)$	$F_{1/2}(\delta)$	$F_1(\delta)$
0.3100	0.244E-02	0.831E-03	0.312E-03	0.125E-03	11.79	13.44
0.3200	0.266E-02	0.919E-03	0.350E-03	0.142E-03	11.38	12.98
0.3300	0.289E-02	0.101E-02	0.392E-03	0.162E-03	11.00	12.55
0.3400	0.314E-02	0.111E-02	0.437E-03	0.183E-03	10.64	12.14
0.3500	0.340E-02	0.122E-02	0.486E-03	0.206E-03	10.30	11.75
0.3600	0.367E-02	0.134E-02	0.539E-03	0.232E-03	9.973	11.39
0.3700	0.395E-02	0.146E-02	0.596E-03	0.260E-03	9.669	11.04
0.3800	0.425E-02	0.159E-02	0.657E-03	0.290E-03	9.380	10.72
0.3900	0.457E-02	0.173E-02	0.723E-03	0.323E-03	9.105	10.40
0.4000	0.490E-02	0.188E-02	0.794E-03	0.359E-03	8.845	10.11
0.4100	0.524E-02	0.203E-02	0.870E-03	0.398E-03	8.597	9.830
0.4200	0.560E-02	0.220E-02	0.951E-03	0.441E-03	8.361	9.562
0.4300	0.598E-02	0.237E-02	0.104E-02	0.486E-03	8.135	9.307
0.4400	0.638E-02	0.255E-02	0.113E-02	0.535E-03	7.920	9.064
0.4500	0.679E-02	0.275E-02	0.123E-02	0.588E-03	7.714	8.831
0.4600	0.723E-02	0.295E-02	0.133E-02	0.645E-03	7.517	8.608
0.4700	0.768E-02	0.317E-02	0.145E-02	0.707E-03	7.328	8.395
0.4800	0.815E-02	0.339E-02	0.156E-02	0.772E-03	7.147	8.190
0.4900	0.864E-02	0.363E-02	0.169E-02	0.842E-03	6.974	7.994
0.5000	0.915E-02	0.388E-02	0.182E-02	0.917E-03	6.807	7.805
0.5100	0.968E-02	0.414E-02	0.196E-02	0.998E-03	6.646	7.624
0.5200	0.102E-01	0.442E-02	0.211E-02	0.108E-02	6.492	7.449
0.5300	0.108E-01	0.471E-02	0.227E-02	0.117E-02	6.343	7.281
0.5400	0.114E-01	0.501E-02	0.244E-02	0.127E-02	6.200	7.119
0.5500	0.120E-01	0.533E-02	0.261E-02	0.137E-02	6.062	6.963
0.5600	0.127E-01	0.566E-02	0.280E-02	0.148E-02	5.928	6.813
0.5700	0.134E-01	0.600E-02	0.299E-02	0.160E-02	5.800	6.667
0.5800	0.141E-01	0.636E-02	0.320E-02	0.172E-02	5.675	6.527
0.5900	0.148E-01	0.674E-02	0.342E-02	0.186E-02	5.555	6.391
0.6000	0.155E-01	0.714E-02	0.364E-02	0.199E-02	5.438	6.259

Tab. III / 3

δ	$\bar{A}_{1/2}(\delta)$	$\bar{A}_1(\delta)$	$\bar{A}_{3/2}(\delta)$	$\bar{A}_2(\delta)$	$F_{1/2}(\delta)$	$F_1(\delta)$
0.6100	0.163E-01	0.755E-02	0.388E-02	0.214E-02	5.326	6.132
0.6200	0.171E-01	0.798E-02	0.413E-02	0.230E-02	5.216	6.009
0.6300	0.180E-01	0.842E-02	0.439E-02	0.246E-02	5.111	5.889
0.6400	0.188E-01	0.889E-02	0.467E-02	0.263E-02	5.008	5.773
0.6500	0.197E-01	0.938E-02	0.496E-02	0.282E-02	4.908	5.661
0.6600	0.207E-01	0.988E-02	0.526E-02	0.301E-02	4.811	5.552
0.6700	0.216E-01	0.104E-01	0.558E-02	0.321E-02	4.717	5.445
0.6800	0.226E-01	0.110E-01	0.591E-02	0.343E-02	4.626	5.342
0.6900	0.237E-01	0.115E-01	0.626E-02	0.365E-02	4.537	5.242
0.7000	0.247E-01	0.121E-01	0.662E-02	0.389E-02	4.451	5.145
0.7100	0.258E-01	0.127E-01	0.700E-02	0.413E-02	4.367	5.050
0.7200	0.270E-01	0.134E-01	0.739E-02	0.440E-02	4.285	4.958
0.7300	0.282E-01	0.140E-01	0.781E-02	0.467E-02	4.205	4.868
0.7400	0.294E-01	0.147E-01	0.824E-02	0.496E-02	4.127	4.780
0.7500	0.307E-01	0.154E-01	0.869E-02	0.526E-02	4.051	4.695
0.7600	0.320E-01	0.162E-01	0.916E-02	0.558E-02	3.977	4.612
0.7700	0.334E-01	0.170E-01	0.965E-02	0.591E-02	3.905	4.530
0.7800	0.348E-01	0.178E-01	0.102E-01	0.625E-02	3.834	4.451
0.7900	0.362E-01	0.186E-01	0.107E-01	0.662E-02	3.766	4.374
0.8000	0.377E-01	0.195E-01	0.112E-01	0.700E-02	3.698	4.298
0.8100	0.393E-01	0.204E-01	0.118E-01	0.740E-02	3.632	4.224
0.8200	0.409E-01	0.213E-01	0.124E-01	0.781E-02	3.563	4.152
0.8300	0.426E-01	0.223E-01	0.130E-01	0.825E-02	3.505	4.081
0.8400	0.443E-01	0.233E-01	0.137E-01	0.870E-02	3.443	4.012
0.8500	0.461E-01	0.243E-01	0.144E-01	0.918E-02	3.383	3.944
0.8600	0.479E-01	0.254E-01	0.151E-01	0.968E-02	3.323	3.878
0.8700	0.498E-01	0.265E-01	0.158E-01	0.102E-01	3.265	3.813
0.8800	0.518E-01	0.276E-01	0.166E-01	0.107E-01	3.208	3.749
0.8900	0.539E-01	0.288E-01	0.174E-01	0.113E-01	3.152	3.686
0.9000	0.560E-01	0.301E-01	0.182E-01	0.119E-01	3.098	3.625

Tab. III/4

δ	$\bar{A}_{1/2}(\delta)$	$\bar{A}_1(\delta)$	$\bar{A}_{3/2}(\delta)$	$\bar{A}_2(\delta)$	$F_{1/2}(\delta)$	$F_1(\delta)$
0.9100	0.582E-01	0.314E-01	0.190E-01	0.125E-01	3.044	3.565
0.9200	0.605E-01	0.327E-01	0.199E-01	0.131E-01	2.991	3.506
0.9300	0.628E-01	0.341E-01	0.209E-01	0.138E-01	2.938	3.448
0.9400	0.653E-01	0.355E-01	0.218E-01	0.145E-01	2.887	3.391
0.9500	0.678E-01	0.370E-01	0.228E-01	0.152E-01	2.837	3.335
0.9600	0.705E-01	0.386E-01	0.238E-01	0.160E-01	2.787	3.280
0.9700	0.732E-01	0.402E-01	0.249E-01	0.168E-01	2.738	3.226
0.9800	0.760E-01	0.418E-01	0.260E-01	0.176E-01	2.689	3.172
0.9900	0.790E-01	0.435E-01	0.272E-01	0.184E-01	2.641	3.119
1.0000	0.821E-01	0.453E-01	0.284E-01	0.193E-01	2.594	3.067

Tab. IV/1 $\bar{S}_4(\xi) = N_4 \cdot \sin(\pi\xi)$

δ	$\bar{A}_{1/2}(\delta)$	$\bar{A}_1(\delta)$	$\bar{A}_{3/2}(\delta)$	$\bar{A}_2(\delta)$	$F_{1/2}(\delta)$	$F_i(\delta)$
0.0100	0.413E-09	0.203E-10	0.113E-11	0.677E-13	0.1090E 05	0.1281E 07
0.0200	0.935E-08	0.650E-09	0.509E-10	0.433E-11	2726.	3204.
0.0300	0.579E-07	0.493E-08	0.473E-09	0.493E-10	1212.	1424.
0.0400	0.211E-06	0.208E-07	0.230E-08	0.277E-09	681.9	801.3
0.0500	0.577E-06	0.634E-07	0.785E-08	0.106E-08	436.6	513.0
0.0600	0.131E-05	0.158E-06	0.214E-07	0.315E-08	303.3	356.4
0.0700	0.262E-05	0.340E-06	0.499E-07	0.795E-08	222.9	261.9
0.0800	0.477E-05	0.663E-06	0.104E-06	0.177E-07	170.8	200.6
0.0900	0.809E-05	0.119E-05	0.199E-06	0.359E-07	135.0	158.6
0.1000	0.130E-04	0.202E-05	0.354E-06	0.674E-07	109.4	128.5
0.1100	0.199E-04	0.325E-05	0.598E-06	0.119E-06	90.48	106.3
0.1200	0.294E-04	0.502E-05	0.964E-06	0.201E-06	76.09	89.38
0.1300	0.421E-04	0.748E-05	0.150E-05	0.325E-06	64.88	76.21
0.1400	0.587E-04	0.108E-04	0.225E-05	0.506E-06	55.99	65.76
0.1500	0.800E-04	0.152E-04	0.328E-05	0.765E-06	48.82	57.34
0.1600	0.107E-03	0.210E-04	0.467E-05	0.112E-05	42.95	50.44
0.1700	0.140E-03	0.284E-04	0.651E-05	0.162E-05	38.09	44.72
0.1800	0.181E-03	0.378E-04	0.890E-05	0.227E-05	34.01	39.93
0.1900	0.230E-03	0.494E-04	0.120E-04	0.314E-05	30.56	35.88
0.2000	0.289E-03	0.637E-04	0.158E-04	0.427E-05	27.62	32.42
0.2100	0.359E-03	0.812E-04	0.207E-04	0.571E-05	25.08	29.44
0.2200	0.442E-03	0.102E-03	0.267E-04	0.754E-05	22.89	26.86
0.2300	0.538E-03	0.127E-03	0.340E-04	0.983E-05	20.97	24.61
0.2400	0.650E-03	0.157E-03	0.429E-04	0.127E-04	19.29	22.63
0.2500	0.779E-03	0.192E-03	0.535E-04	0.162E-04	17.80	20.89
0.2600	0.927E-03	0.234E-03	0.663E-04	0.204E-04	16.49	19.34
0.2700	0.110E-02	0.281E-03	0.814E-04	0.255E-04	15.31	17.96
0.2800	0.129E-02	0.337E-03	0.992E-04	0.317E-04	14.26	16.73
0.2900	0.150E-02	0.400E-03	0.120E-03	0.391E-04	13.32	15.62
0.3000	0.174E-02	0.473E-03	0.144E-03	0.478E-04	12.47	14.62

Tab. IV/2

δ	$\bar{A}_{1/2}(\delta)$	$\bar{A}_1(\delta)$	$\bar{A}_{3/2}(\delta)$	$\bar{A}_2(\delta)$	$F_{1/2}(\delta)$	$F_1(\delta)$
0.3100	0.201E-02	0.555E-03	0.172E-03	0.580E-04	11.70	13.72
0.3200	0.231E-02	0.649E-03	0.205E-03	0.701E-04	11.01	12.90
0.3300	0.265E-02	0.754E-03	0.242E-03	0.841E-04	10.37	12.15
0.3400	0.302E-02	0.873E-03	0.284E-03	0.100E-03	9.791	11.47
0.3500	0.343E-02	0.101E-02	0.332E-03	0.119E-03	9.260	10.85
0.3600	0.387E-02	0.115E-02	0.387E-03	0.141E-03	8.772	10.27
0.3700	0.436E-02	0.132E-02	0.449E-03	0.165E-03	8.324	9.748
0.3800	0.490E-02	0.150E-02	0.518E-03	0.194E-03	7.911	9.262
0.3900	0.548E-02	0.170E-02	0.596E-03	0.226E-03	7.529	8.814
0.4000	0.612E-02	0.193E-02	0.682E-03	0.262E-03	7.176	8.398
0.4100	0.681E-02	0.217E-02	0.779E-03	0.303E-03	6.848	8.013
0.4200	0.755E-02	0.244E-02	0.887E-03	0.349E-03	6.543	7.655
0.4300	0.835E-02	0.273E-02	0.101E-02	0.401E-03	6.260	7.321
0.4400	0.922E-02	0.305E-02	0.114E-02	0.458E-03	5.995	7.010
0.4500	0.101E-01	0.340E-02	0.128E-02	0.523E-03	5.748	6.720
0.4600	0.111E-01	0.378E-02	0.144E-02	0.595E-03	5.518	6.449
0.4700	0.122E-01	0.419E-02	0.162E-02	0.674E-03	5.301	6.194
0.4800	0.134E-01	0.464E-02	0.181E-02	0.763E-03	5.099	5.956
0.4900	0.146E-01	0.512E-02	0.202E-02	0.860E-03	4.908	5.732
0.5000	0.159E-01	0.563E-02	0.224E-02	0.968E-03	4.729	5.521
0.5100	0.173E-01	0.619E-02	0.249E-02	0.109E-02	4.560	5.323
0.5200	0.187E-01	0.679E-02	0.276E-02	0.122E-02	4.401	5.136
0.5300	0.203E-01	0.743E-02	0.305E-02	0.136E-02	4.252	4.960
0.5400	0.219E-01	0.812E-02	0.337E-02	0.151E-02	4.110	4.793
0.5500	0.237E-01	0.885E-02	0.371E-02	0.168E-02	3.976	4.636
0.5600	0.255E-01	0.963E-02	0.408E-02	0.187E-02	3.849	4.486
0.5700	0.274E-01	0.105E-01	0.447E-02	0.207E-02	3.729	4.345
0.5800	0.295E-01	0.114E-01	0.490E-02	0.229E-02	3.616	4.211
0.5900	0.316E-01	0.123E-01	0.536E-02	0.252E-02	3.508	4.084
0.6000	0.339E-01	0.133E-01	0.585E-02	0.278E-02	3.405	3.963

Tab. IV/3

δ	$\bar{A}_{1/2}(\delta)$	$\bar{A}_1(\delta)$	$\bar{A}_{3/2}(\delta)$	$\bar{A}_2(\delta)$	$F_{1/2}(\delta)$	$F_1(\delta)$
0.6100	0.362E-01	0.144E-01	0.637E-02	0.306E-02	3.308	3.848
0.6200	0.387E-01	0.155E-01	0.693E-02	0.335E-02	3.215	3.739
0.6300	0.413E-01	0.167E-01	0.753E-02	0.367E-02	3.127	3.635
0.6400	0.440E-01	0.179E-01	0.817E-02	0.402E-02	3.042	3.536
0.6500	0.468E-01	0.193E-01	0.885E-02	0.439E-02	2.962	3.442
0.6600	0.498E-01	0.207E-01	0.958E-02	0.479E-02	2.886	3.351
0.6700	0.529E-01	0.221E-01	0.103E-01	0.522E-02	2.813	3.265
0.6800	0.561E-01	0.237E-01	0.112E-01	0.568E-02	2.743	3.183
0.6900	0.594E-01	0.253E-01	0.120E-01	0.617E-02	2.676	3.104
0.7000	0.629E-01	0.270E-01	0.129E-01	0.669E-02	2.613	3.029
0.7100	0.665E-01	0.288E-01	0.139E-01	0.725E-02	2.552	2.957
0.7200	0.702E-01	0.307E-01	0.149E-01	0.784E-02	2.493	2.888
0.7300	0.741E-01	0.326E-01	0.160E-01	0.847E-02	2.437	2.822
0.7400	0.781E-01	0.347E-01	0.172E-01	0.915E-02	2.384	2.759
0.7500	0.823E-01	0.368E-01	0.184E-01	0.986E-02	2.332	2.698
0.7600	0.865E-01	0.390E-01	0.196E-01	0.106E-01	2.283	2.640
0.7700	0.910E-01	0.414E-01	0.209E-01	0.114E-01	2.236	2.584
0.7800	0.955E-01	0.438E-01	0.223E-01	0.123E-01	2.190	2.530
0.7900	0.100E 00	0.463E-01	0.238E-01	0.132E-01	2.147	2.479
0.8000	0.105E 00	0.489E-01	0.254E-01	0.141E-01	2.105	2.429
0.8100	0.110E 00	0.517E-01	0.270E-01	0.151E-01	2.065	2.381
0.8200	0.115E 00	0.545E-01	0.287E-01	0.162E-01	2.026	2.335
0.8300	0.121E 00	0.574E-01	0.304E-01	0.173E-01	1.989	2.291
0.8400	0.126E 00	0.605E-01	0.323E-01	0.185E-01	1.953	2.248
0.8500	0.132E 00	0.636E-01	0.342E-01	0.197E-01	1.918	2.207
0.8600	0.137E 00	0.669E-01	0.362E-01	0.210E-01	1.885	2.168
0.8700	0.143E 00	0.703E-01	0.383E-01	0.224E-01	1.853	2.130
0.8800	0.149E 00	0.738E-01	0.405E-01	0.239E-01	1.822	2.093
0.8900	0.155E 00	0.774E-01	0.428E-01	0.254E-01	1.793	2.058
0.9000	0.161E 00	0.811E-01	0.451E-01	0.269E-01	1.764	2.024

Tab. IV/4

δ	$\bar{A}_{1/2}(\delta)$	$\bar{A}_1(\delta)$	$\bar{A}_{3/2}(\delta)$	$\bar{A}_2(\delta)$	$F_{1/2}(\delta)$	$F_1(\delta)$
0.9100	0.168E 00	0.850E-01	0.476E-01	0.286E-01	1.736	1.991
0.9200	0.174E 00	0.889E-01	0.502E-01	0.303E-01	1.710	1.959
0.9300	0.181E 00	0.930E-01	0.528E-01	0.322E-01	1.684	1.928
0.9400	0.188E 00	0.972E-01	0.556E-01	0.341E-01	1.659	1.899
0.9500	0.195E 00	0.102E 00	0.585E-01	0.361E-01	1.636	1.870
0.9600	0.202E 00	0.106E 00	0.614E-01	0.381E-01	1.613	1.842
0.9700	0.209E 00	0.111E 00	0.645E-01	0.403E-01	1.590	1.816
0.9800	0.216E 00	0.115E 00	0.677E-01	0.426E-01	1.569	1.790
0.9900	0.224E 00	0.120E 00	0.710E-01	0.449E-01	1.548	1.765
1.0000	0.231E 00	0.125E 00	0.744E-01	0.474E-01	1.528	1.741

$$\text{Tab. V/1} \quad \bar{\rho}_5(\xi) = N_5 \exp(-(2\xi - 1)^2)$$

δ	$\bar{A}_{1/2}(\delta)$	$\bar{A}_1(\delta)$	$\bar{A}_{3/2}(\delta)$	$\bar{A}_2(\delta)$	$F_{1/2}(\delta)$	$F_1(\delta)$
0.0100	0.660E-06	0.410E-07	0.280E-08	0.203E-09	306.9	347.5
0.0200	0.383E-05	0.337E-06	0.325E-07	0.334E-08	151.4	171.7
0.0300	0.108E-04	0.116E-05	0.137E-06	0.172E-07	99.65	113.1
0.0400	0.227E-04	0.280E-05	0.381E-06	0.552E-07	73.80	83.83
0.0500	0.405E-04	0.558E-05	0.846E-06	0.137E-06	58.31	66.28
0.0600	0.653E-04	0.983E-05	0.163E-05	0.288E-06	47.99	54.59
0.0700	0.982E-04	0.159E-04	0.285E-05	0.542E-06	40.63	46.26
0.0800	0.140E-03	0.242E-04	0.462E-05	0.940E-06	35.12	40.01
0.0900	0.192E-03	0.352E-04	0.710E-05	0.153E-05	30.84	35.16
0.1000	0.256E-03	0.492E-04	0.104E-04	0.237E-05	27.42	31.29
0.1100	0.332E-03	0.667E-04	0.148E-04	0.352E-05	24.63	28.13
0.1200	0.421E-03	0.882E-04	0.204E-04	0.506E-05	22.32	25.49
0.1300	0.525E-03	0.114E-03	0.275E-04	0.708E-05	20.36	23.27
0.1400	0.645E-03	0.145E-03	0.363E-04	0.967E-05	18.69	21.37
0.1500	0.783E-03	0.182E-03	0.470E-04	0.129E-04	17.24	19.73
0.1600	0.939E-03	0.225E-03	0.598E-04	0.170E-04	15.98	18.30
0.1700	0.112E-02	0.275E-03	0.752E-04	0.220E-04	14.87	17.04
0.1800	0.131E-02	0.333E-03	0.934E-04	0.281E-04	13.89	15.92
0.1900	0.153E-02	0.398E-03	0.115E-03	0.354E-04	13.01	14.92
0.2000	0.178E-02	0.473E-03	0.139E-03	0.441E-04	12.22	14.03
0.2100	0.205E-02	0.557E-03	0.168E-03	0.543E-04	11.52	13.22
0.2200	0.235E-02	0.652E-03	0.201E-03	0.664E-04	10.88	12.49
0.2300	0.268E-02	0.759E-03	0.239E-03	0.805E-04	10.29	11.83
0.2400	0.303E-02	0.877E-03	0.281E-03	0.968E-04	9.761	11.22
0.2500	0.342E-02	0.101E-02	0.330E-03	0.116E-03	9.273	10.67
0.2600	0.385E-02	0.115E-02	0.384E-03	0.137E-03	8.825	10.16
0.2700	0.431E-02	0.131E-02	0.445E-03	0.162E-03	8.413	9.684
0.2800	0.481E-02	0.149E-02	0.514E-03	0.190E-03	8.031	9.248
0.2900	0.534E-02	0.168E-02	0.590E-03	0.222E-03	7.678	8.844
0.3000	0.592E-02	0.189E-02	0.674E-03	0.257E-03	7.349	8.469

Tab. V/2

δ	$\bar{A}_{1/2}(\delta)$	$\bar{A}_1(\delta)$	$\bar{A}_{3/2}(\delta)$	$\bar{A}_2(\delta)$	$F_{1/2}(\delta)$	$F_1(\delta)$
0.3100	0.654E-02	0.212E-02	0.767E-03	0.298E-03	7.044	8.119
0.3200	0.721E-02	0.237E-02	0.870E-03	0.343E-03	6.759	7.793
0.3300	0.792E-02	0.265E-02	0.984E-03	0.393E-03	6.493	7.488
0.3400	0.869E-02	0.294E-02	0.111E-02	0.449E-03	6.243	7.202
0.3500	0.95CE-02	0.326E-02	0.124E-02	0.510E-03	6.010	6.934
0.3600	0.104E-01	0.360E-02	0.139E-02	0.579E-03	5.790	6.683
0.3700	0.113E-01	0.397E-02	0.156E-02	0.655E-03	5.584	6.446
0.3800	0.123E-01	0.437E-02	0.173E-02	0.738E-03	5.389	6.222
0.3900	0.133E-01	0.479E-02	0.192E-02	0.829E-03	5.206	6.012
0.4000	0.144E-01	0.525E-02	0.213E-02	0.930E-03	5.033	5.812
0.4100	0.156E-01	0.573E-02	0.235E-02	0.104E-02	4.869	5.624
0.4200	0.168E-01	0.625E-02	0.260E-02	0.116E-02	4.714	5.446
0.4300	0.181E-01	0.681E-02	0.286E-02	0.129E-02	4.567	5.277
0.4400	0.194E-01	0.740E-02	0.314E-02	0.143E-02	4.428	5.116
0.4500	0.209E-01	0.802E-02	0.344E-02	0.159E-02	4.296	4.964
0.4600	0.224E-01	0.869E-02	0.376E-02	0.175E-02	4.170	4.819
0.4700	0.239E-01	0.940E-02	0.411E-02	0.193E-02	4.050	4.681
0.4800	0.256E-01	0.101E-01	0.448E-02	0.213E-02	3.937	4.549
0.4900	0.273E-01	0.109E-01	0.488E-02	0.234E-02	3.828	4.424
0.5000	0.291E-01	0.118E-01	0.530E-02	0.257E-02	3.725	4.304
0.5100	0.310E-01	0.127E-01	0.575E-02	0.281E-02	3.626	4.190
0.5200	0.330E-01	0.136E-01	0.623E-02	0.307E-02	3.532	4.081
0.5300	0.351E-01	0.146E-01	0.674E-02	0.335E-02	3.442	3.977
0.5400	0.372E-01	0.156E-01	0.728E-02	0.366E-02	3.356	3.877
0.5500	0.395E-01	0.167E-01	0.786E-02	0.398E-02	3.273	3.781
0.5600	0.418E-01	0.178E-01	0.846E-02	0.432E-02	3.194	3.690
0.5700	0.442E-01	0.190E-01	0.911E-02	0.469E-02	3.119	3.602
0.5800	0.467E-01	0.203E-01	0.979E-02	0.508E-02	3.046	3.518
0.5900	0.494E-01	0.216E-01	0.105E-01	0.550E-02	2.977	3.437
0.6000	0.521E-01	0.230E-01	0.113E-01	0.595E-02	2.910	3.359

Tab. V13

δ	$\bar{A}_{V_2}(\delta)$	$\bar{A}_1(\delta)$	$\bar{A}_{3V_2}(\delta)$	$\bar{A}_2(\delta)$	$F_{V_2}(\delta)$	$F_1(\delta)$
0.6100	0.549E-01	0.244E-01	0.121E-01	0.642E-02	2.846	3.285
0.6200	0.578E-01	0.259E-01	0.129E-01	0.693E-02	2.784	3.213
0.6300	0.608E-01	0.275E-01	0.138E-01	0.746E-02	2.725	3.144
0.6400	0.639E-01	0.291E-01	0.147E-01	0.802E-02	2.668	3.078
0.6500	0.672E-01	0.308E-01	0.157E-01	0.862E-02	2.614	3.014
0.6600	0.705E-01	0.326E-01	0.168E-01	0.926E-02	2.561	2.953
0.6700	0.739E-01	0.344E-01	0.178E-01	0.993E-02	2.510	2.894
0.6800	0.775E-01	0.364E-01	0.190E-01	0.106E-01	2.461	2.837
0.6900	0.811E-01	0.383E-01	0.202E-01	0.114E-01	2.414	2.782
0.7000	0.849E-01	0.404E-01	0.214E-01	0.122E-01	2.369	2.729
0.7100	0.887E-01	0.426E-01	0.227E-01	0.130E-01	2.325	2.678
0.7200	0.927E-01	0.448E-01	0.241E-01	0.139E-01	2.283	2.628
0.7300	0.968E-01	0.471E-01	0.255E-01	0.148E-01	2.242	2.581
0.7400	0.101E 00	0.495E-01	0.270E-01	0.158E-01	2.203	2.535
0.7500	0.105E 00	0.520E-01	0.285E-01	0.168E-01	2.165	2.490
0.7600	0.110E 00	0.546E-01	0.301E-01	0.178E-01	2.129	2.447
0.7700	0.114E 00	0.572E-01	0.318E-01	0.190E-01	2.093	2.406
0.7800	0.119E 00	0.600E-01	0.335E-01	0.201E-01	2.059	2.365
0.7900	0.124E 00	0.628E-01	0.354E-01	0.214E-01	2.026	2.327
0.8000	0.129E 00	0.657E-01	0.373E-01	0.226E-01	1.994	2.289
0.8100	0.134E 00	0.688E-01	0.392E-01	0.240E-01	1.963	2.252
0.8200	0.139E 00	0.719E-01	0.413E-01	0.254E-01	1.933	2.217
0.8300	0.144E 00	0.751E-01	0.434E-01	0.269E-01	1.904	2.183
0.8400	0.149E 00	0.784E-01	0.456E-01	0.284E-01	1.876	2.150
0.8500	0.155E 00	0.818E-01	0.478E-01	0.300E-01	1.849	2.118
0.8600	0.160E 00	0.853E-01	0.502E-01	0.317E-01	1.823	2.087
0.8700	0.166E 00	0.889E-01	0.527E-01	0.334E-01	1.797	2.057
0.8800	0.172E 00	0.926E-01	0.552E-01	0.352E-01	1.772	2.028
0.8900	0.178E 00	0.964E-01	0.578E-01	0.371E-01	1.748	1.999
0.9000	0.184E 00	0.100E 00	0.605E-01	0.391E-01	1.725	1.972

Tab. V/4

δ	$\bar{A}_{1/2}(\delta)$	$\bar{A}_1(\delta)$	$\bar{A}_{3/2}(\delta)$	$\bar{A}_2(\delta)$	$F_{1/2}(\delta)$	$F_1(\delta)$
0.9100	0.190E 00	0.104E 00	0.633E-01	0.411E-01	1.703	1.945
0.9200	0.196E 00	0.108E 00	0.662E-01	0.433E-01	1.681	1.919
0.9300	0.202E 00	0.113E 00	0.692E-01	0.455E-01	1.660	1.894
0.9400	0.209E 00	0.117E 00	0.723E-01	0.478E-01	1.639	1.870
0.9500	0.215E 00	0.121E 00	0.754E-01	0.501E-01	1.619	1.846
0.9600	0.222E 00	0.126E 00	0.787E-01	0.526E-01	1.600	1.823
0.9700	0.228E 00	0.130E 00	0.821E-01	0.552E-01	1.581	1.801
0.9800	0.235E 00	0.135E 00	0.855E-01	0.578E-01	1.563	1.779
0.9900	0.242E 00	0.140E 00	0.891E-01	0.606E-01	1.545	1.758
1.0000	0.249E 00	0.145E 00	0.928E-01	0.634E-01	1.528	1.737

Tab. VI/1. $\bar{\rho}_6(\xi)$ (as given in the main text)

δ	$\bar{A}_{1/2}(\delta)$	$\bar{A}_1(\delta)$	$\bar{A}_{3/2}(\delta)$	$\bar{A}_2(\delta)$	$F_{Y_2}(\delta)$	$F_i(\delta)$
0.01	0.224E-05	0.140E-06	0.955E-08	0.694E-09	166.6	188.5
0.02	0.128E-04	0.113E-05	0.109E-06	0.113E-07	82.97	93.97
0.03	0.355E-04	0.383E-05	0.455E-06	0.573E-07	55.14	62.46
0.04	0.733E-04	0.913E-05	0.125E-05	0.182E-06	41.22	46.70
0.05	0.129E-03	0.179E-04	0.274E-05	0.446E-06	32.87	37.25
0.06	0.204E-03	0.311E-04	0.521E-05	0.928E-06	27.30	30.95
0.07	0.302E-03	0.497E-04	0.898E-05	0.173E-05	23.33	26.45
0.08	0.424E-03	0.745E-04	0.144E-04	0.296E-05	20.34	23.07
0.09	0.572E-03	0.107E-03	0.218E-04	0.476E-05	18.03	20.45
0.10	0.750E-03	0.147E-03	0.317E-04	0.728E-05	16.17	18.35
0.11	0.957E-03	0.197E-03	0.445E-04	0.107E-04	14.65	16.63
0.12	0.120E-02	0.257E-03	0.606E-04	0.152E-04	13.39	15.20
0.13	0.147E-02	0.328E-03	0.805E-04	0.210E-04	12.32	13.98
0.14	0.178E-02	0.412E-03	0.105E-03	0.284E-04	11.40	12.95
0.15	0.213E-02	0.509E-03	0.134E-03	0.376E-04	10.61	12.05
0.16	0.251E-02	0.621E-03	0.169E-03	0.489E-04	9.911	11.26
0.17	0.294E-02	0.749E-03	0.210E-03	0.626E-04	9.298	10.56
0.18	0.341E-02	0.893E-03	0.257E-03	0.789E-04	8.752	9.947
0.19	0.393E-02	0.106E-02	0.312E-03	0.984E-04	8.265	9.395
0.20	0.450E-02	0.124E-02	0.375E-03	0.121E-03	7.826	8.898
0.21	0.511E-02	0.144E-02	0.447E-03	0.148E-03	7.429	8.448
0.22	0.577E-02	0.166E-02	0.529E-03	0.179E-03	7.068	8.040
0.23	0.649E-02	0.191E-02	0.621E-03	0.215E-03	6.738	7.666
0.24	0.726E-02	0.218E-02	0.724E-03	0.256E-03	6.436	7.325
0.25	0.809E-02	0.248E-02	0.838E-03	0.302E-03	6.159	7.010
0.26	0.897E-02	0.280E-02	0.966E-03	0.355E-03	5.902	6.720
0.27	0.992E-02	0.316E-02	0.111E-02	0.415E-03	5.665	6.451
0.28	0.109E-01	0.354E-02	0.126E-02	0.482E-03	5.445	6.201
0.29	0.120E-01	0.395E-02	0.144E-02	0.556E-03	5.240	5.969
0.30	0.131E-01	0.440E-02	0.162E-02	0.640E-03	5.048	5.752

Tab. VI/2

δ	$\bar{A}_{1/2}(\delta)$	$\bar{A}_1(\delta)$	$\bar{A}_{3/2}(\delta)$	$\bar{A}_2(\delta)$	$F_{1/2}(\delta)$	$F_1(\delta)$
0.31	0.143E-01	0.488E-02	0.183E-02	0.733E-03	4.869	5.550
0.32	0.156E-01	0.536E-02	0.205E-02	0.835E-03	4.702	5.360
0.33	0.170E-01	0.594E-02	0.230E-02	0.948E-03	4.544	5.181
0.34	0.184E-01	0.653E-02	0.256E-02	0.107E-02	4.396	5.013
0.35	0.199E-01	0.717E-02	0.285E-02	0.121E-02	4.256	4.855
0.36	0.215E-01	0.784E-02	0.316E-02	0.136E-02	4.124	4.705
0.37	0.231E-01	0.855E-02	0.349E-02	0.152E-02	3.999	4.564
0.38	0.249E-01	0.931E-02	0.385E-02	0.170E-02	3.881	4.430
0.39	0.267E-01	0.1011E-01	0.424E-02	0.190E-02	3.769	4.303
0.40	0.286E-01	0.110E-01	0.465E-02	0.211E-02	3.663	4.182
0.41	0.306E-01	0.119E-01	0.510E-02	0.234E-02	3.561	4.068
0.42	0.327E-01	0.128E-01	0.557E-02	0.258E-02	3.465	3.958
0.43	0.349E-01	0.139E-01	0.608E-02	0.285E-02	3.373	3.854
0.44	0.372E-01	0.149E-01	0.662E-02	0.314E-02	3.285	3.755
0.45	0.396E-01	0.160E-01	0.719E-02	0.345E-02	3.202	3.660
0.46	0.420E-01	0.172E-01	0.780E-02	0.378E-02	3.122	3.569
0.47	0.446E-01	0.185E-01	0.845E-02	0.414E-02	3.045	3.482
0.48	0.473E-01	0.198E-01	0.914E-02	0.452E-02	2.972	3.399
0.49	0.501E-01	0.211E-01	0.987E-02	0.493E-02	2.901	3.319
0.50	0.530E-01	0.226E-01	0.106E-01	0.537E-02	2.834	3.243
0.51	0.561E-01	0.241E-01	0.115E-01	0.583E-02	2.769	3.169
0.52	0.592E-01	0.257E-01	0.123E-01	0.633E-02	2.706	3.098
0.53	0.625E-01	0.273E-01	0.132E-01	0.686E-02	2.646	3.030
0.54	0.659E-01	0.291E-01	0.142E-01	0.742E-02	2.589	2.965
0.55	0.694E-01	0.309E-01	0.152E-01	0.802E-02	2.533	2.902
0.56	0.730E-01	0.328E-01	0.163E-01	0.866E-02	2.479	2.841
0.57	0.768E-01	0.347E-01	0.174E-01	0.933E-02	2.428	2.782
0.58	0.807E-01	0.368E-01	0.186E-01	0.100E-01	2.378	2.726
0.59	0.847E-01	0.389E-01	0.198E-01	0.108E-01	2.330	2.671
0.60	0.889E-01	0.411E-01	0.211E-01	0.116E-01	2.283	2.618

Tab. VI/3

δ	$\bar{A}_{12}(\delta)$	$\bar{A}_1(\delta)$	$\bar{A}_{3/2}(\delta)$	$\bar{A}_2(\delta)$	$F_{1/2}(\delta)$	$F_1(\delta)$
0.61	0.932E-01	0.435E-01	0.225E-01	0.125E-01	2.238	2.567
0.62	0.976E-01	0.459E-01	0.239E-01	0.133E-01	2.194	2.518
0.63	0.102E 00	0.484E-01	0.254E-01	0.143E-01	2.152	2.470
0.64	0.107E 00	0.510E-01	0.270E-01	0.153E-01	2.111	2.423
0.65	0.112E 00	0.537E-01	0.286E-01	0.163E-01	2.072	2.379
0.66	0.117E 00	0.565E-01	0.303E-01	0.174E-01	2.034	2.335
0.67	0.122E 00	0.595E-01	0.321E-01	0.186E-01	1.996	2.293
0.68	0.128E 00	0.625E-01	0.340E-01	0.198E-01	1.960	2.252
0.69	0.133E 00	0.657E-01	0.359E-01	0.211E-01	1.925	2.212
0.70	0.139E 00	0.689E-01	0.380E-01	0.224E-01	1.892	2.174
0.71	0.145E 00	0.723E-01	0.401E-01	0.238E-01	1.859	2.136
0.72	0.151E 00	0.758E-01	0.423E-01	0.253E-01	1.827	2.100
0.73	0.157E 00	0.794E-01	0.446E-01	0.269E-01	1.796	2.065
0.74	0.163E 00	0.832E-01	0.470E-01	0.285E-01	1.766	2.030
0.75	0.170E 00	0.870E-01	0.495E-01	0.302E-01	1.737	1.997
0.76	0.176E 00	0.910E-01	0.521E-01	0.320E-01	1.710	1.965
0.77	0.183E 00	0.952E-01	0.548E-01	0.339E-01	1.683	1.934
0.78	0.190E 00	0.994E-01	0.576E-01	0.358E-01	1.657	1.903
0.79	0.197E 00	0.104E 00	0.605E-01	0.378E-01	1.633	1.874
0.80	0.204E 00	0.108E 00	0.635E-01	0.399E-01	1.609	1.846
0.81	0.212E 00	0.113E 00	0.666E-01	0.422E-01	1.587	1.819
0.82	0.219E 00	0.118E 00	0.699E-01	0.445E-01	1.565	1.793
0.83	0.227E 00	0.122E 00	0.732E-01	0.469E-01	1.544	1.768
0.84	0.234E 00	0.127E 00	0.766E-01	0.494E-01	1.524	1.744
0.85	0.242E 00	0.133E 00	0.802E-01	0.520E-01	1.505	1.720
0.86	0.250E 00	0.138E 00	0.839E-01	0.547E-01	1.487	1.697
0.87	0.258E 00	0.143E 00	0.877E-01	0.575E-01	1.469	1.675
0.88	0.266E 00	0.149E 00	0.917E-01	0.604E-01	1.451	1.653
0.89	0.274E 00	0.154E 00	0.957E-01	0.634E-01	1.434	1.632
0.90	0.282E 00	0.160E 00	0.999E-01	0.666E-01	1.418	1.612

Tab. VI / 4

δ	$\bar{A}_{1/2}(\delta)$	$\bar{A}_1(\delta)$	$\bar{A}_{3/2}(\delta)$	$\bar{A}_2(\delta)$	$F_{1/2}(\delta)$	$F_1(\delta)$
0.91	0.291E 00	0.166E 00	0.104E 00	0.699E-01	1.402	1.592
0.92	0.299E 00	0.172E 00	0.109E 00	0.733E-01	1.387	1.573
0.93	0.308E 00	0.178E 00	0.113E 00	0.768E-01	1.373	1.555
0.94	0.316E 00	0.184E 00	0.118E 00	0.804E-01	1.359	1.538
0.95	0.325E 00	0.191E 00	0.123E 00	0.841E-01	1.346	1.521
0.96	0.333E 00	0.197E 00	0.128E 00	0.880E-01	1.333	1.505
0.97	0.342E 00	0.204E 00	0.133E 00	0.920E-01	1.321	1.490
0.98	0.350E 00	0.210E 00	0.138E 00	0.961E-01	1.309	1.475
0.99	0.359E 00	0.217E 00	0.143E 00	0.100E 00	1.298	1.461
1.00	0.367E 00	0.223E 00	0.148E 00	0.105E 00	1.288	1.448
1.01	0.376E 00	0.230E 00	0.154E 00	0.109E 00	1.277	1.434
1.02	0.384E 00	0.237E 00	0.159E 00	0.114E 00	1.267	1.422
1.03	0.393E 00	0.244E 00	0.165E 00	0.119E 00	1.258	1.410
1.04	0.402E 00	0.251E 00	0.171E 00	0.124E 00	1.248	1.398
1.05	0.410E 00	0.259E 00	0.177E 00	0.129E 00	1.239	1.386
1.06	0.419E 00	0.266E 00	0.183E 00	0.134E 00	1.231	1.375
1.07	0.428E 00	0.274E 00	0.190E 00	0.139E 00	1.222	1.363
1.08	0.437E 00	0.281E 00	0.196E 00	0.145E 00	1.214	1.353
1.09	0.446E 00	0.289E 00	0.203E 00	0.151E 00	1.205	1.342
1.10	0.455E 00	0.297E 00	0.210E 00	0.157E 00	1.197	1.331
1.11	0.465E 00	0.305E 00	0.217E 00	0.163E 00	1.189	1.321
1.12	0.474E 00	0.314E 00	0.224E 00	0.169E 00	1.181	1.311
1.13	0.484E 00	0.322E 00	0.231E 00	0.175E 00	1.174	1.301
1.14	0.493E 00	0.331E 00	0.239E 00	0.182E 00	1.166	1.291
1.15	0.503E 00	0.339E 00	0.247E 00	0.189E 00	1.159	1.281
1.16	0.512E 00	0.348E 00	0.254E 00	0.196E 00	1.151	1.272
1.17	0.522E 00	0.357E 00	0.262E 00	0.203E 00	1.144	1.263
1.18	0.532E 00	0.366E 00	0.271E 00	0.211E 00	1.138	1.254
1.19	0.541E 00	0.375E 00	0.279E 00	0.218E 00	1.131	1.246
1.20	0.551E 00	0.384E 00	0.287E 00	0.226E 00	1.125	1.237

Tab. VI/15

δ	$\bar{A}_{1/2}(\delta)$	$\bar{A}_1(\delta)$	$\bar{A}_{3/2}(\delta)$	$\bar{A}_2(\delta)$	$F_{k_2}(\delta)$	$F(\delta)$
1.21	0.560E 00	0.393E 00	0.296E 00	0.234E 00	1.119	1.229
1.22	0.570E 00	0.402E 00	0.304E 00	0.242E 00	1.114	1.222
1.23	0.579E 00	0.411E 00	0.313E 00	0.250E 00	1.108	1.215
1.24	0.588E 00	0.420E 00	0.321E 00	0.258E 00	1.103	1.208
1.25	0.597E 00	0.429E 00	0.330E 00	0.266E 00	1.098	1.202
1.26	0.605E 00	0.438E 00	0.339E 00	0.275E 00	1.094	1.196
1.27	0.614E 00	0.447E 00	0.348E 00	0.283E 00	1.090	1.190
1.28	0.622E 00	0.457E 00	0.357E 00	0.292E 00	1.086	1.184
1.29	0.631E 00	0.466E 00	0.366E 00	0.301E 00	1.082	1.179
1.30	0.639E 00	0.475E 00	0.375E 00	0.310E 00	1.078	1.174
1.31	0.647E 00	0.484E 00	0.385E 00	0.320E 00	1.075	1.169
1.32	0.655E 00	0.493E 00	0.394E 00	0.329E 00	1.071	1.164
1.33	0.663E 00	0.502E 00	0.403E 00	0.339E 00	1.069	1.160
1.34	0.671E 00	0.511E 00	0.413E 00	0.349E 00	1.066	1.156
1.35	0.678E 00	0.520E 00	0.423E 00	0.358E 00	1.063	1.152
1.36	0.686E 00	0.529E 00	0.432E 00	0.369E 00	1.061	1.148
1.37	0.694E 00	0.538E 00	0.442E 00	0.379E 00	1.058	1.144
1.38	0.701E 00	0.548E 00	0.452E 00	0.390E 00	1.056	1.140
1.39	0.709E 00	0.557E 00	0.463E 00	0.400E 00	1.053	1.136
1.40	0.716E 00	0.566E 00	0.473E 00	0.411E 00	1.051	1.133
1.41	0.723E 00	0.576E 00	0.483E 00	0.422E 00	1.049	1.129
1.42	0.730E 00	0.585E 00	0.494E 00	0.434E 00	1.048	1.126
1.43	0.737E 00	0.594E 00	0.505E 00	0.445E 00	1.046	1.123
1.44	0.744E 00	0.604E 00	0.516E 00	0.457E 00	1.044	1.120
1.45	0.751E 00	0.614E 00	0.527E 00	0.469E 00	1.043	1.117
1.46	0.758E 00	0.623E 00	0.538E 00	0.482E 00	1.041	1.113
1.47	0.766E 00	0.633E 00	0.549E 00	0.494E 00	1.039	1.110
1.48	0.773E 00	0.643E 00	0.561E 00	0.507E 00	1.038	1.107
1.49	0.779E 00	0.653E 00	0.572E 00	0.520E 00	1.037	1.105
1.50	0.786E 00	0.663E 00	0.584E 00	0.533E 00	1.036	1.102

Tab. VI/6

δ	$\bar{A}_{1/2}(\delta)$	$\bar{A}_1(\delta)$	$\bar{A}_{3/2}(\delta)$	$\bar{A}_2(\delta)$	$F_{1/2}(\delta)$	$F_1(\delta)$
1.51	0.793E 00	0.673E 00	0.596E 00	0.547E 00	1.035	1.099
1.52	0.795E 00	0.683E 00	0.608E 00	0.561E 00	1.033	1.097
1.53	0.806E 00	0.693E 00	0.621E 00	0.575E 00	1.032	1.094
1.54	0.813E 00	0.703E 00	0.633E 00	0.589E 00	1.031	1.092
1.55	0.820E 00	0.714E 00	0.646E 00	0.604E 00	1.030	1.089
1.56	0.827E 00	0.724E 00	0.659E 00	0.619E 00	1.029	1.086
1.57	0.834E 00	0.734E 00	0.672E 00	0.634E 00	1.028	1.084
1.58	0.841E 00	0.745E 00	0.685E 00	0.649E 00	1.027	1.081
1.59	0.847E 00	0.755E 00	0.698E 00	0.665E 00	1.026	1.079
1.60	0.854E 00	0.766E 00	0.712E 00	0.681E 00	1.025	1.077
1.61	0.861E 00	0.777E 00	0.725E 00	0.697E 00	1.024	1.075
1.62	0.868E 00	0.788E 00	0.739E 00	0.713E 00	1.023	1.072
1.63	0.875E 00	0.799E 00	0.753E 00	0.730E 00	1.021	1.070
1.64	0.882E 00	0.810E 00	0.768E 00	0.747E 00	1.020	1.067
1.65	0.890E 00	0.822E 00	0.782E 00	0.765E 00	1.019	1.065
1.66	0.897E 00	0.833E 00	0.797E 00	0.783E 00	1.017	1.062
1.67	0.905E 00	0.845E 00	0.812E 00	0.801E 00	1.016	1.060
1.68	0.912E 00	0.856E 00	0.827E 00	0.819E 00	1.014	1.057
1.69	0.920E 00	0.867E 00	0.842E 00	0.837E 00	1.013	1.055
1.70	0.927E 00	0.879E 00	0.857E 00	0.856E 00	1.011	1.053
1.71	0.934E 00	0.890E 00	0.872E 00	0.875E 00	1.010	1.051
1.72	0.941E 00	0.901E 00	0.887E 00	0.893E 00	1.009	1.049
1.73	0.948E 00	0.912E 00	0.902E 00	0.912E 00	1.008	1.047
1.74	0.954E 00	0.924E 00	0.917E 00	0.932E 00	1.007	1.045
1.75	0.961E 00	0.934E 00	0.932E 00	0.951E 00	1.006	1.043
1.76	0.967E 00	0.945E 00	0.947E 00	0.970E 00	1.005	1.042
1.77	0.973E 00	0.956E 00	0.962E 00	0.990E 00	1.005	1.040
1.78	0.979E 00	0.967E 00	0.977E 00	0.101E 01	1.004	1.039
1.79	0.985E 00	0.977E 00	0.992E 00	0.103E 01	1.004	1.038
1.80	0.990E 00	0.987E 00	0.101E 01	0.105E 01	1.004	1.037

Tab. VI/7

δ	$\bar{A}_{1/2}(\delta)$	$\bar{A}_1(\delta)$	$\bar{A}_{3/2}(\delta)$	$\bar{A}_2(\delta)$	$F_{1/2}(\delta)$	$F_1(\delta)$
1.81	0.995E 00	0.997E 00	0.102E 01	0.107E 01	1.004	1.037
1.82	0.100E C1	0.101E C1	0.104E C1	0.109E 01	1.004	1.036
1.83	0.100E C1	0.102E C1	0.105E C1	0.111E 01	1.004	1.036
1.84	0.101E 01	0.103E C1	0.106E C1	0.113E 01	1.005	1.035
1.85	0.101E C1	0.103E C1	0.108E C1	0.115E 01	1.005	1.035
1.86	0.102E C1	0.104E C1	0.109E C1	0.117E 01	1.006	1.035
1.87	0.102E 01	0.105E C1	0.111E C1	0.119E 01	1.006	1.035
1.88	0.102E C1	0.106E C1	0.112E C1	0.121E 01	1.006	1.035
1.89	0.103E 01	0.107E C1	0.114E C1	0.123E 01	1.007	1.034
1.90	0.103E C1	0.108E C1	0.115E C1	0.125E 01	1.007	1.034
1.91	0.104E C1	0.109E C1	0.117E C1	0.127E 01	1.008	1.034
1.92	0.104E C1	0.110E C1	0.118E C1	0.129E 01	1.008	1.034
1.93	0.104E 01	0.111E C1	0.119E C1	0.131E C1	1.008	1.034
1.94	0.105E 01	0.112E C1	0.121E C1	0.133E 01	1.009	1.034
1.95	0.105E C1	0.112E C1	0.122E C1	0.135E 01	1.009	1.033
1.96	0.106E C1	0.113E C1	0.124E C1	0.137E 01	1.009	1.033
1.97	0.106E 01	0.114E C1	0.125E C1	0.139E 01	1.009	1.033
1.98	0.106E C1	0.115E C1	0.127E C1	0.141E 01	1.009	1.032
1.99	0.107E C1	0.116E C1	0.128E C1	0.144E 01	1.009	1.032
2.00	0.107E 01	0.117E C1	0.130E C1	0.146E 01	1.008	1.031

Tab. VII/1

δ	$\bar{A}_1(\delta)$	$\tilde{A}_1(\delta)$	δ	$\bar{A}_1(\delta)$	$\tilde{A}_1(\delta)$
0.01	0.140E-06	0.140E-06	0.31	0.488E-02	0.513E-02
0.02	0.113E-05	0.113E-05	0.32	0.539E-02	0.569E-02
0.03	0.383E-05	0.385E-05	0.33	0.594E-02	0.628E-02
0.04	0.913E-05	0.918E-05	0.34	0.653E-02	0.692E-02
0.05	0.179E-04	0.181E-04	0.35	0.717E-02	0.760E-02
0.06	0.311E-04	0.314E-04	0.36	0.784E-02	0.833E-02
0.07	0.497E-04	0.502E-04	0.37	0.855E-02	0.910E-02
0.08	0.745E-04	0.754E-04	0.38	0.931E-02	0.993E-02
0.09	0.107E-03	0.108E-03	0.39	0.101E-01	0.108E-01
0.10	0.147E-03	0.149E-03	0.40	0.110E-01	0.118E-01
0.11	0.197E-03	0.200E-03	0.41	0.119E-01	0.127E-01
0.12	0.257E-03	0.261E-03	0.42	0.128E-01	0.138E-01
0.13	0.328E-03	0.335E-03	0.43	0.139E-01	0.149E-01
0.14	0.412E-03	0.421E-03	0.44	0.149E-01	0.161E-01
0.15	0.509E-03	0.521E-03	0.45	0.160E-01	0.173E-01
0.16	0.621E-03	0.637E-03	0.46	0.172E-01	0.187E-01
0.17	0.749E-03	0.769E-03	0.47	0.185E-01	0.200E-01
0.18	0.893E-03	0.919E-03	0.48	0.198E-01	0.215E-01
0.19	0.106E-02	0.109E-02	0.49	0.211E-01	0.231E-01
0.20	0.124E-02	0.128E-02	0.50	0.226E-01	0.247E-01
0.21	0.144E-02	0.149E-02	0.51	0.241E-01	0.264E-01
0.22	0.166E-02	0.172E-02	0.52	0.257E-01	0.282E-01
0.23	0.191E-02	0.198E-02	0.53	0.273E-01	0.300E-01
0.24	0.218E-02	0.227E-02	0.54	0.291E-01	0.320E-01
0.25	0.248E-02	0.258E-02	0.55	0.309E-01	0.341E-01
0.26	0.280E-02	0.292E-02	0.56	0.328E-01	0.362E-01
0.27	0.316E-02	0.330E-02	0.57	0.347E-01	0.385E-01
0.28	0.354E-02	0.370E-02	0.58	0.368E-01	0.409E-01
0.29	0.395E-02	0.414E-02	0.59	0.389E-01	0.433E-01
0.30	0.440E-02	0.462E-02	0.60	0.411E-01	0.459E-01

Tab. VII / 2

δ	$\bar{A}_1(\delta)$	$\hat{A}_1(\delta)$	δ	$\bar{A}_1(\delta)$	$\hat{A}_1(\delta)$
0.61	0.435E-01	0.486E-01		0.91	0.166F 00
0.62	0.459E-01	0.514E-01		0.92	0.172E 00
0.63	0.484E-01	0.544E-01		0.93	0.178E 00
0.64	0.510E-01	0.574E-01		0.94	0.184E 00
0.65	0.537E-01	0.606E-01		0.95	0.191E 00
0.66	0.565E-01	0.640E-01		0.96	0.197E 00
0.67	0.595E-01	0.674E-01		0.97	0.204E 00
0.68	0.625E-01	0.710E-01		0.98	0.210E 00
0.69	0.657E-01	0.748E-01		0.99	0.217E 00
0.70	0.689E-01	0.787E-01		1.00	0.223E 00
0.71	0.723E-01	0.828E-01		1.01	0.230E 00
0.72	0.758E-01	0.870E-01		1.02	0.237E 00
0.73	0.794E-01	0.914E-01		1.03	0.244E 00
0.74	0.832E-01	0.959E-01		1.04	0.251E 00
0.75	0.870E-01	0.101E 00		1.05	0.259E 00
0.76	0.910E-01	0.106E 00		1.06	0.266E 00
0.77	0.952E-01	0.111E 00		1.07	0.274E 00
0.78	0.994E-01	0.116E 00		1.08	0.281E 00
0.79	0.104E 00	0.121E 00		1.09	0.289E 00
0.80	0.108E 00	0.127E 00		1.10	0.297E 00
0.81	0.113E 00	0.133E 00		1.11	0.305E 00
0.82	0.118E 00	0.138E 00		1.12	0.314E 00
0.83	0.122E 00	0.145E 00		1.13	0.322E 00
0.84	0.127E 00	0.151E 00		1.14	0.331E 00
0.85	0.133E 00	0.157E 00		1.15	0.339E 00
0.86	0.138E 00	0.164E 00		1.16	0.348E 00
0.87	0.143E 00	0.171E 00		1.17	0.357E 00
0.88	0.149E 00	0.178E 00		1.18	0.366E 00
0.89	0.154E 00	0.186E 00		1.19	0.375E 00
0.90	0.160E 00	0.193E 00		1.20	0.384E 00

Tab. VII/3

δ	$\bar{A}_i(\delta)$	$\tilde{A}_i(\delta)$	δ	$\bar{A}_i(\delta)$	$\tilde{A}_i(\delta)$
1.21	0.393E 00	0.540E 00	1.51	0.673E 00	0.114E 01
1.22	0.402E 00	0.555E 00	1.52	0.683E 00	0.117E 01
1.23	0.411E 00	0.571E 00	1.53	0.693E 00	0.120E 01
1.24	0.420E 00	0.587E 00	1.54	0.703E 00	0.123E 01
1.25	0.429E 00	0.603E 00	1.55	0.714E 00	0.126E 01
1.26	0.438E 00	0.619E 00	1.56	0.724E 00	0.129E 01
1.27	0.447E 00	0.636E 00	1.57	0.734E 00	0.132E 01
1.28	0.457E 00	0.653E 00	1.58	0.745E 00	0.135E 01
1.29	0.466E 00	0.670E 00	1.59	0.755E 00	0.139E 01
1.30	0.475E 00	0.687E 00	1.60	0.766E 00	0.142E 01
1.31	0.484E 00	0.705E 00	1.61	0.777E 00	0.145E 01
1.32	0.493E 00	0.722E 00	1.62	0.788E 00	0.149E 01
1.33	0.502E 00	0.740E 00	1.63	0.799E 00	0.153E 01
1.34	0.511E 00	0.759E 00	1.64	0.810E 00	0.157E 01
1.35	0.520E 00	0.778E 00	1.65	0.822E 00	0.161E 01
1.36	0.529E 00	0.797E 00	1.66	0.833E 00	0.165E 01
1.37	0.538E 00	0.817E 00	1.67	0.845E 00	0.169E 01
1.38	0.548E 00	0.837E 00	1.68	0.856E 00	0.173E 01
1.39	0.557E 00	0.857E 00	1.69	0.867E 00	0.177E 01
1.40	0.566E 00	0.878E 00	1.70	0.879E 00	0.182E 01
1.41	0.576E 00	0.900E 00	1.71	0.890E 00	0.186E 01
1.42	0.585E 00	0.921E 00	1.72	0.901E 00	0.191E 01
1.43	0.594E 00	0.944E 00	1.73	0.912E 00	0.196E 01
1.44	0.604E 00	0.966E 00	1.74	0.924E 00	0.201E 01
1.45	0.614E 00	0.990E 00	1.75	0.934E 00	0.206E 01
1.46	0.623E 00	0.101E 01	1.76	0.945E 00	0.211E 01
1.47	0.633E 00	0.104E 01	1.77	0.956E 00	0.216E 01
1.48	0.643E 00	0.106E 01	1.78	0.967E 00	0.221E 01
1.49	0.653E 00	0.109E 01	1.79	0.977E 00	0.227E 01
1.50	0.663E 00	0.112E 01	1.80	0.987E 00	0.232E 01

Tab. VII/4

δ	$\bar{A}_1(\delta)$	$\tilde{A}_1(\delta)$
----------	---------------------	-----------------------

1.81	0.997E 00	0.238E C1
1.82	0.1011E 01	0.244E C1
1.83	0.102E 01	0.250E C1
1.84	0.103E 01	0.256E C1
1.85	0.103E 01	0.262E C1
1.86	0.104E 01	0.269E C1
1.87	0.105E 01	0.276E C1
1.88	0.106E 01	0.283E C1
1.89	0.107E 01	0.290E C1
1.90	0.108E 01	0.297E C1
1.91	0.109E 01	0.305E C1
1.92	0.110E 01	0.313E C1
1.93	0.111E 01	0.322E C1
1.94	0.112E 01	0.330E C1
1.95	0.112E 01	0.339E C1
1.96	0.113E 01	0.349E 01
1.97	0.114E 01	0.359E C1
1.98	0.115E 01	0.369E C1
1.99	0.116E 01	0.380E C1
2.00	0.117E 01	0.392E C1

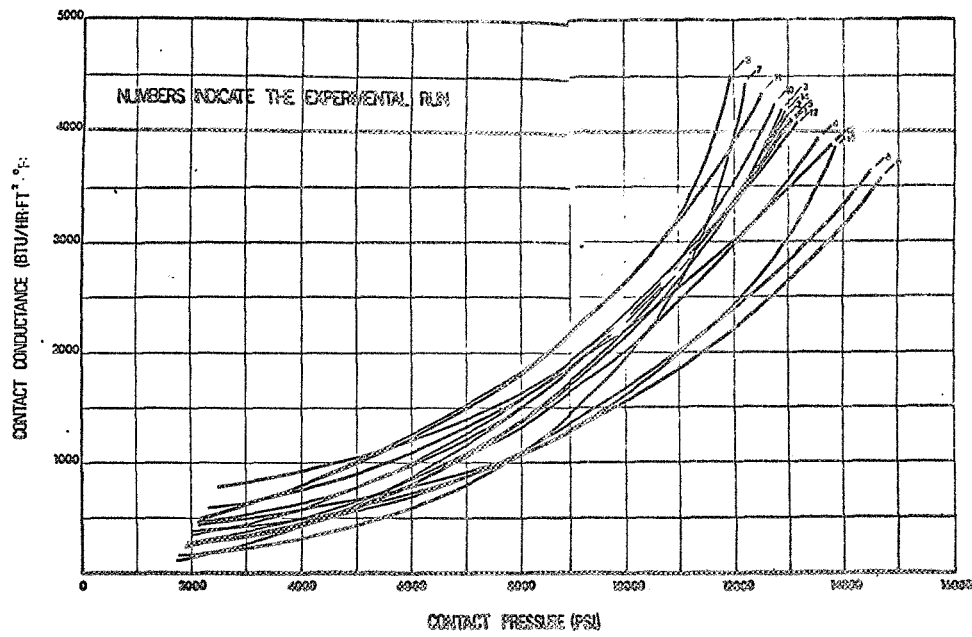


Fig. 1

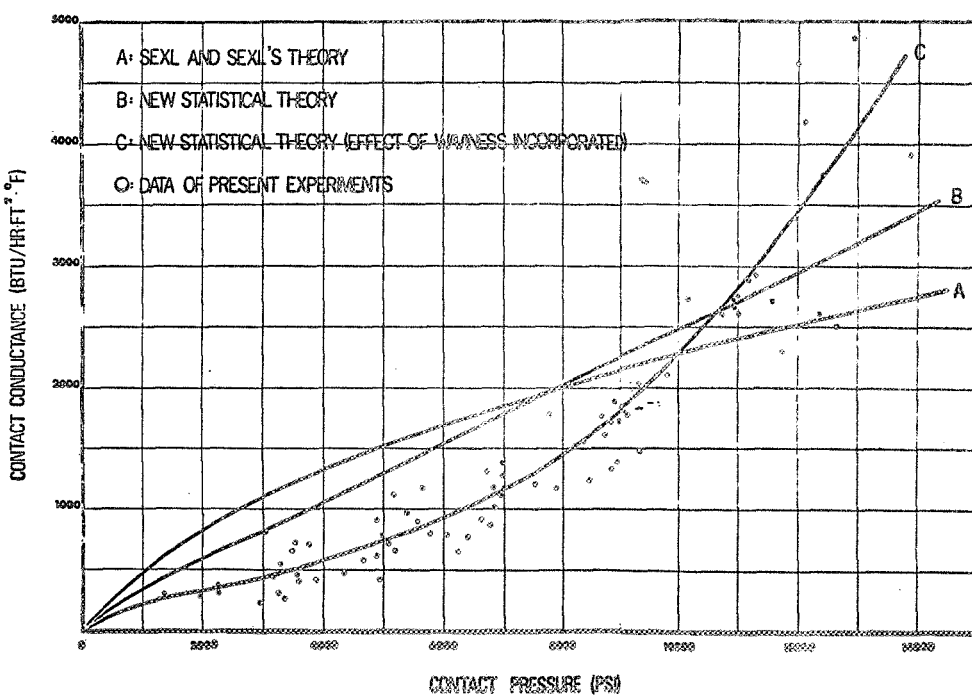
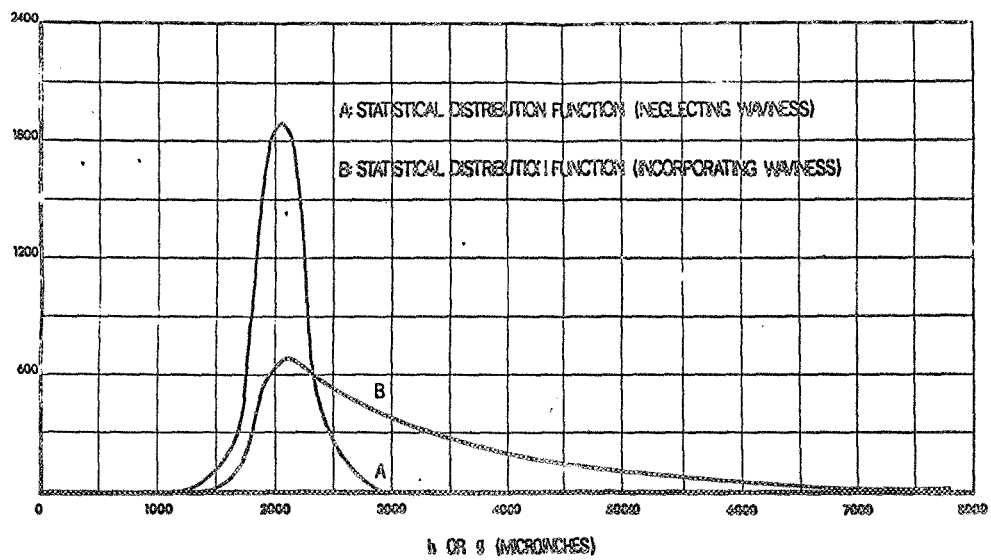


Fig. 2.



STATISTICAL DISTRIBUTION FUNCTION ϕ FOR ASPERITY HEIGHTS

Fig. 3

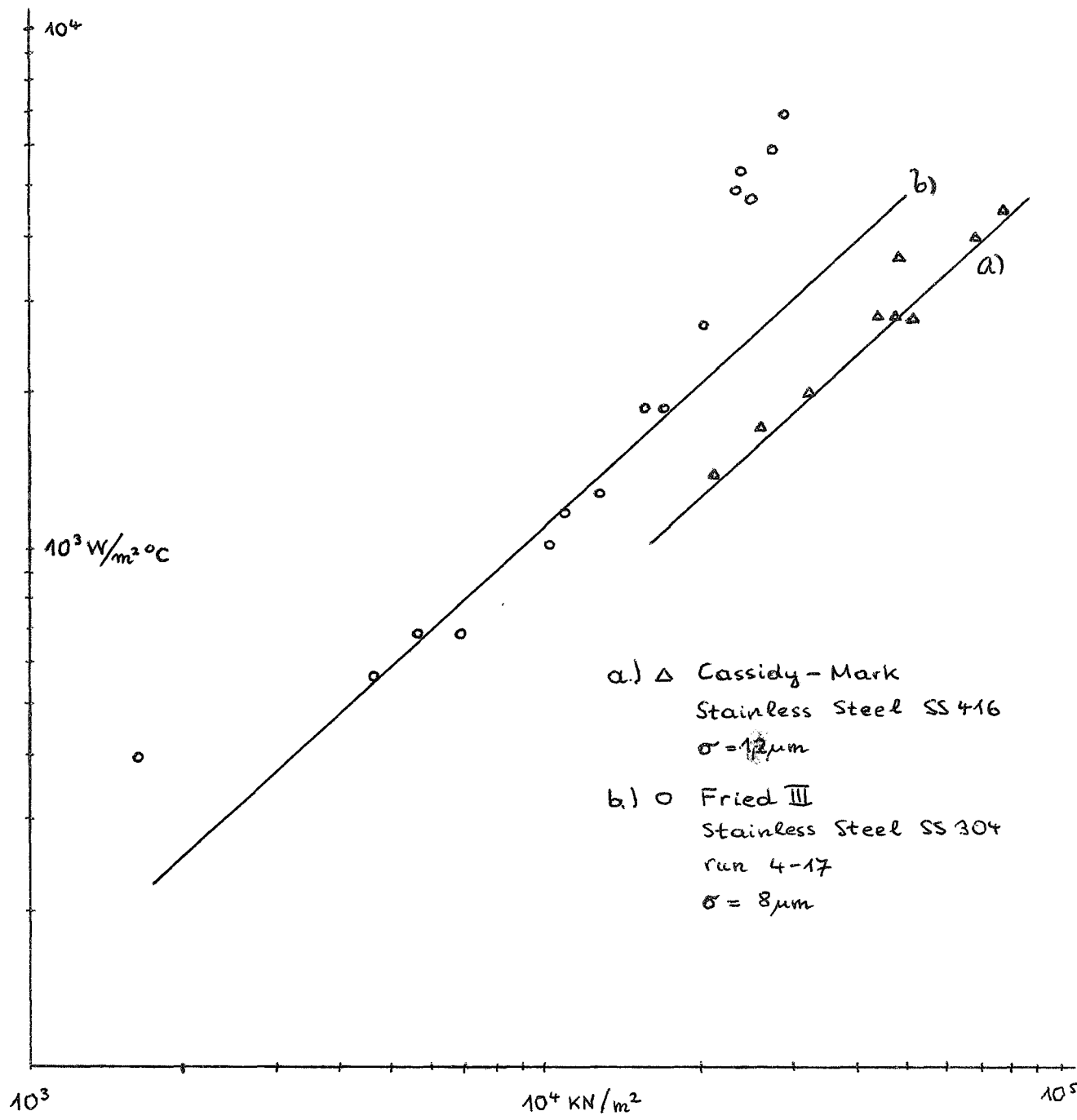


Fig. 4

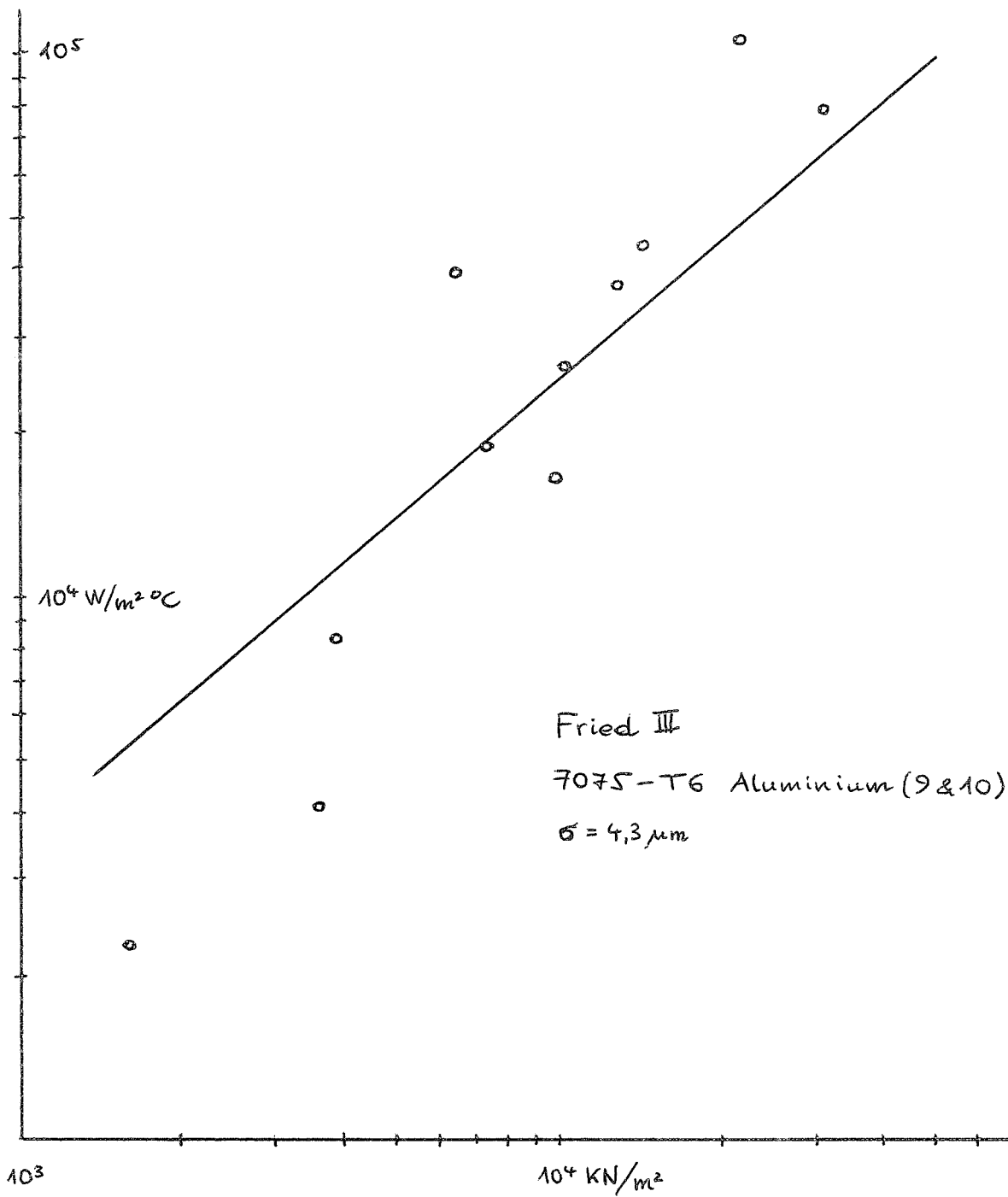


Fig. 5

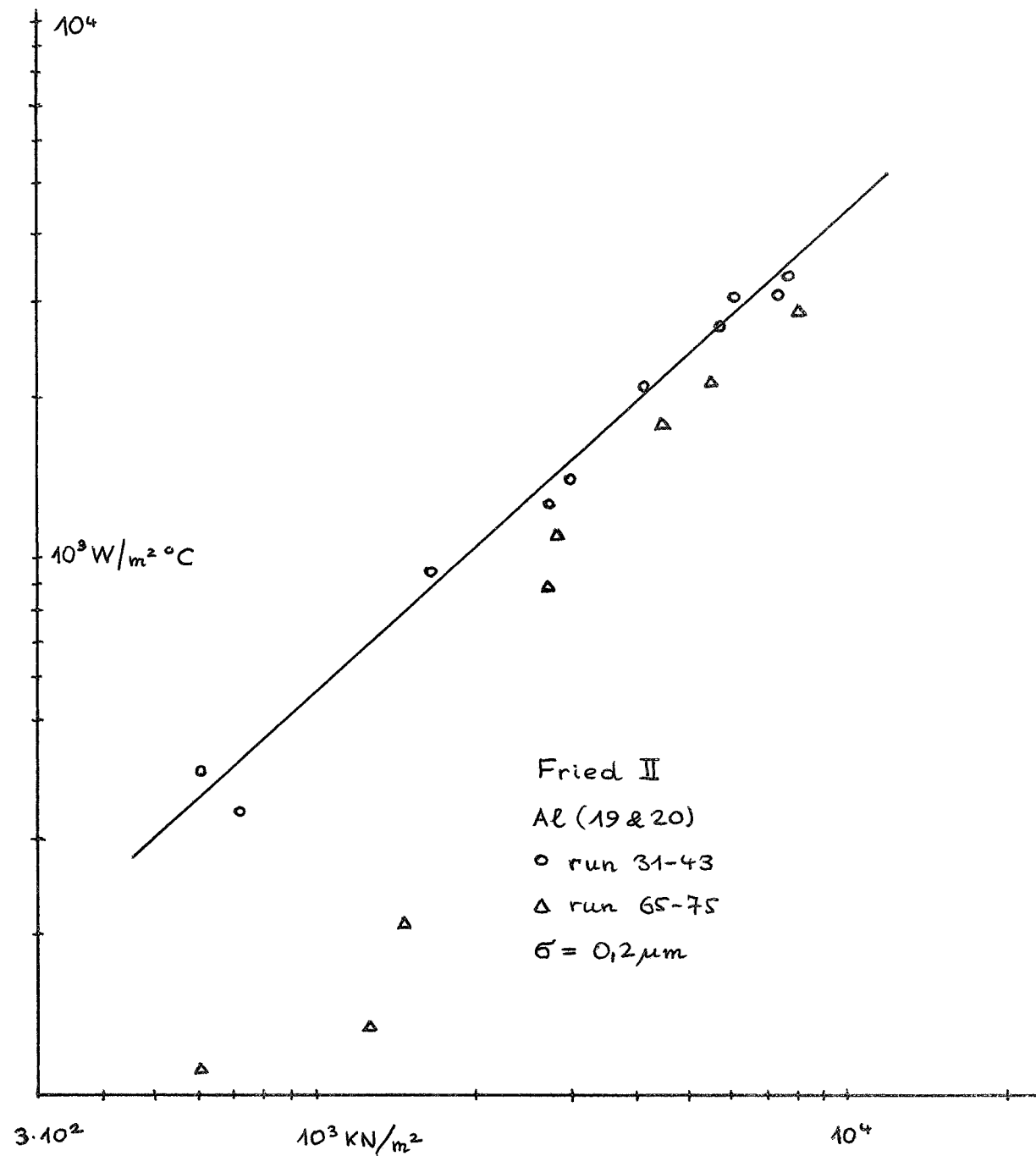


Fig. 6

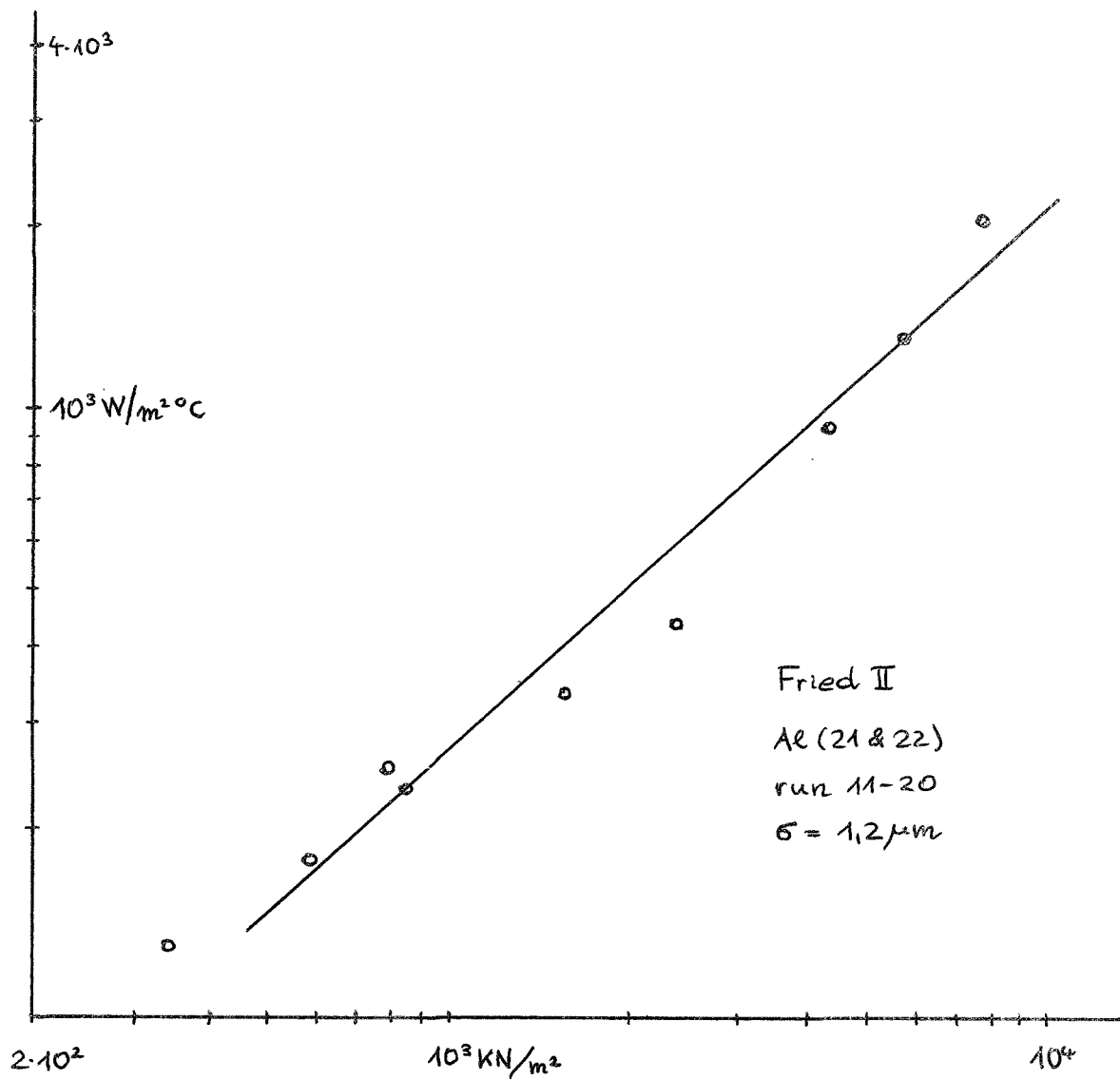


Fig. 7

III. LARGE SCALE ELASTIC DEFORMATIONS OF INTERFACES

1. Introduction

In the theories described in the previous chapters large scale deformations of the interfaces have been neglected. This is probably a good approximation, as long as thick cylinders of small cross section are considered, which are used in present experiments. In most applications one deals, however, with very large and relatively thin surfaces. These surfaces will undergo large scale elastic deformations, which can not easily be described by the theories discussed before. A possible method of incorporating these effects would be the choice of a pressure dependent height distribution. Due to such effects one expects significant differences between the result obtained in standard measurements of thermal joint conductance and actual applications.

2) Phenomenological Theory of Large Scale Deformations

When two large and thin plates are pressed together (pressure p) a situation results as shown in Fig. 1.



Fig. 1

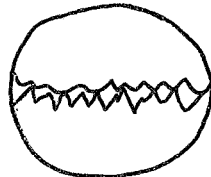


Fig. 2

In A and C there will be two macro-contact points, each consisting of many (inelastically) deformed asperities. These asperities are the ones which are measured with the help of profile readers and the theory of contact conductance deals mainly with the microscopic situation shown in Fig. 2. At low pressures there will generally be three such macro-contact

points for any given interface.

If the pressure is increased, however, a further macroscopic contact point will suddenly develop at B (Fig. 1), due to an elastic deformation of the interface. This large scale deformation has not been taken into account in any existing theory of interfacial thermal conductivity. Only the (mostly inelastic) deformations of the microscopic asperities shown in Fig. 2 have been considered hitherto.

To estimate the influence of these effects we shall develop several simple models of the macroscopic features of the contact. These models will alternatively describe the deformations of thin plates or of elastically deformed infinitely thick bodies. All the models used here are derived from examples contained in Landau-Lifschitz, Theory of Elasticity, Vol. 7.

Consider first a thin plate (thickness d) which is supported at the points A and B (Fig. 1). When the pressure p is applied uniformly the plate will bend as shown in Fig. 3.

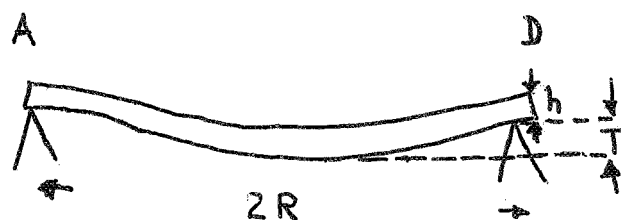


Fig. 3

Approximating the two supporting macro-contacts by a circle of radius R - where we assume the plate to be supported - we obtain for the amplitude T of the deformation

$$T = \frac{3p(1-\sigma^2)}{16h^3E} R^4 4\pi \quad (1)$$

where σ is the Poisson constant and E the Young modul of the material. Thus

$$\frac{R}{h} = \sqrt[4]{\frac{4\pi}{3} \frac{T}{h} \frac{1}{1-\sigma^2} \frac{E}{p}} \quad (2)$$

We can consider this to be an equation for the average distance (R) of macro-contact points as a function of pressure. T is a measure of the surface waviness. Since the number of contact points N is proportional to R^{-2} we have

$$N \propto p^{+1/2} \quad (3)$$

The fluctuations of the heat flow are

$$\frac{\Delta Q}{Q} \propto \frac{1}{\sqrt{N}} \propto p^{-1/4} \quad (4)$$

A 10.000 fold increase in the pressure will therefore increase the "thermal reliability" of the interface only by a factor 10.

In the limit of an infinitely thick plate the analysis proceeds similarly. The final result is

$$R = T \frac{1}{2} \sqrt{\frac{1}{1-\sigma^2} \frac{E}{p}} \quad (5)$$

Thus the fluctuations become

$$\frac{\Delta Q}{Q} \propto R \propto p^{-1/2} \quad (6)$$

Depending on the thickness of the plate we obtain therefore different power laws (4) or (6) resp. For samples which are of about equal diameter and thickness (as is the case in Bhandari's experiment [1]) an intermediate power law

$$\frac{\Delta Q}{Q} \propto p^{-1/3} \quad (7)$$

can be used, which agrees well with Bhandari's experiment.

The heat flow Q can be calculated in a similar manner. Since the considerations given here are only qualitative ideas we shall not attempt to determine numerical constants accurately, but concentrate only on the pressure dependence of the heat flow.

We have seen that the average distance between macroscopic asperities is

$$R \propto p^{-1/n} T^{1/m} \quad (8)$$

$n = 2, m = 1$ for infinitely thick, $n = 3, m = 2$ for average, $n = 4, m = 4$ for thin plates. The force F on one macro-contact point is

$$F = pf/N \quad (9)$$

(f is the total interface area, N the number of macro-contact points). This force F will be proportional to the area of the macro-contact point (radius r)

$$F = pf/N \propto r^2 \quad (10)$$

The total heat flow Q through the interface is then

$$Q = N r \propto \sqrt{pfN} \quad (11)$$

The number N of contact points is in turn given by

$$N = f/R^2 \quad (12)$$

or

$$Q \propto f \sqrt{p/R^2} \quad (13)$$

Therefore we obtain finally, inserting (8)

$$q = Q/f \propto p^{1/2 + 1/n} T^{-1/m} \quad (14)$$

For plates of average thickness ($n = 3$, $m = 2$) this becomes

$$q \propto p^{0.83} T^{-1/2} \quad (15)$$

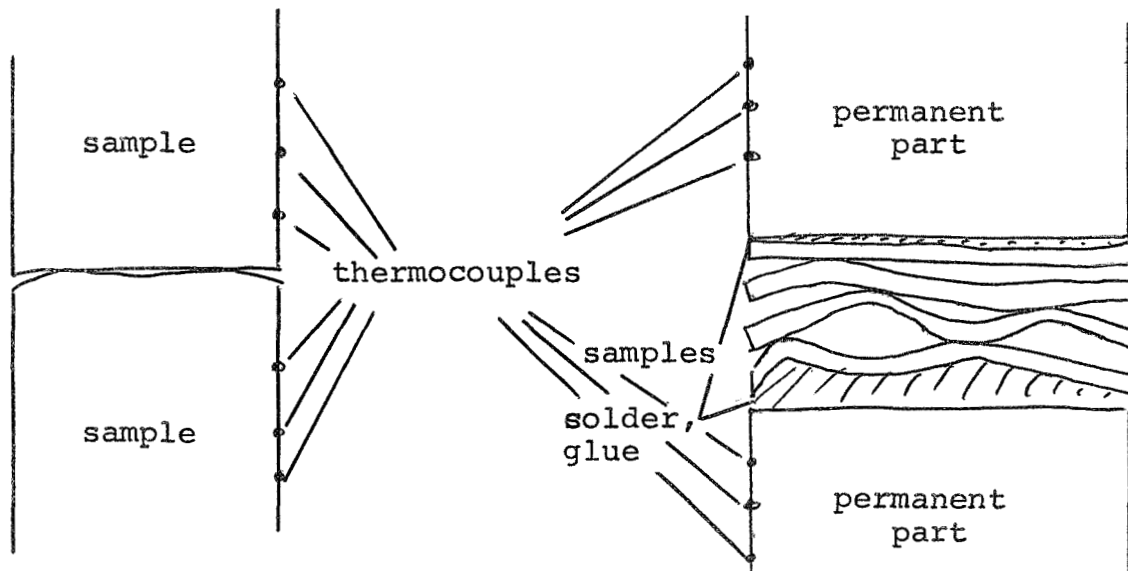
This is very similar to the law suggested by Tien [2]. For thin plates ($m = 4$, $n = 4$) we obtain, however,

$$q \propto p^{0.75} T^{-0.25} \quad (16)$$

Only a very weak dependence on the waviness of the surface described by T results in this case.

3. Conclusion

The approach suggested here promises to be a successful tool for the predictions of the thermal joint conductance in actual engineering applications. To supplement it we should like to suggest the (commercial) development of a measuring device for thermal joint conductance along the following lines (Fig. 4).



a) Standard device

b) New device

for the measurement of
interfacial thermal conductivity.

Fig. 4

In a standard apparatus (Fig. 4a) for the measurement of the thermal joint conductance thick samples are used. The thermo-couples for the determination of the temperature gradient are applied to these samples. This is a very tedious task, which has to be repeated for each individual measurement.

The new device suggested here should be constructed as shown in Fig. 4b. The thermo-couples should be attached to two cylinders, which are a permanent part of the apparatus. This task can, therefore, be performed with high accuracy by the manufacturers.

The surfaces which are of interest are the glued or soldered in such a manner to the cylinders that (almost) no resistance arises at these interfaces. (The best method for this will have to be determined experimentally). Then a number of samples - 3 to 5 - is inserted between the two surfaces obtained in this way, so that the total number of interfaces rises to 4 - 6. This increases the interface resistance and makes it more easily measurable and, at the same time, reduces the fluctuations greatly. Thus one measurement is sufficient to determine the average thermal conductance of a small surface sample and no repeated measurements are necessary.

Then the theory outlined above is applied in order to arrive at values for the resistance of the large surfaces used in the actual application.

We consider the combined experimental-theoretical method described above to be the most promising new development as far as actual engineering applications involving interfacial thermal conductivity are concerned.

References

- [1] Bhandari, N., M. Sc. Thesis, University of Miami 1969
- [2] Tien, C.L., Proc. 7th Conference on Thermal Conductivity,
755 - 760, 1967

CRYSTAL GROWTH AT ZERO GRAVITY CONDITIONS

R. Folk, R. Sexl

This report contains a survey of the theoretical literature on crystal growth with special emphasis on the changes which are to be expected when the crystal is grown under zero gravity conditions.

I. Nucleation

Before a crystal can grow from vapour, solution or melt nucleation must have taken place. Homogeneous nucleation occurs without the aid of catalysis by other particles, e.g. gaseous ions, impurities, suspended solids, etc., which are said to produce heterogeneous nucleation. We will consider here only homogeneous nucleation, following Gerlach [1]. The process of nucleation is described by addition or loss of single atoms to a cluster of atoms. Collision between clusters are highly improbable so that bimolecular reactions are an adequate description of the kinetics. To find the distribution of clusters of various size we have to solve the following differential difference equations:

$$\frac{dN_1}{dt} = Q(t) - \alpha_1 N_1 + \beta_2 N_2 - \sum_{m=1}^{\infty} \alpha_m N_m + \sum_{m=2}^{\infty} \beta_m N_m \quad (1)$$

$$\frac{dN_m}{dt} = \alpha_{m-1} N_{m-1} - (\alpha_m + \beta_m) N_m + \beta_{m+1} N_{m+1} \quad \text{for } m \geq 2$$

where t = time,

T = temperature,

$N_1(T, t)$ = concentration of single atoms of the nucleating component,

$N_m(N_1, T, t)$ = concentration of clusters containing m atoms,

$\alpha_m(N_1 T)$ = reaction rate constant for growth of a cluster
from size m to $m+1$,

$\beta_m(T)$ = reaction rate constant for decay of a cluster
from size m to $m-1$

$Q(t)$ = rate of addition of single atoms to the system.

It may be shown that the α_m are proportional to N_1 if the nucleating phase is a dilute solution or is a gas. On the other hand the growth rate constants are independent of N_1 for nucleation of a phase from a pure liquid. We are interested in the rate of nucleation, which is defined as the net rate at which critical nuclei grow to the next larger size. The critical nucleus is defined as the cluster of such a size that the Gibbs free energy of formation, ΔG , has a maximum.

From [2]

$$\Delta G = 4\pi r^2 + \frac{4\pi r^3}{3} \Delta G_v ,$$

where $r = \sqrt[3]{\frac{3\Omega m}{4}}$ radius of cluster with m atoms,

Ω = volume of atom,

ΔG_v = Gibbs free energy difference per unit volume,

γ = specific interfacial free energy,

we get, upon maximizing with respect to r or m , the free energy of formation of a critical nucleus at rest.

$$\Delta G_c = \frac{16\pi\gamma^3}{3\Delta G_v^2} \quad (2)$$

To find the rate of nucleation we assume steady state conditions (after sufficient time) in which the net rate of growth of clusters of one size to the next larger size is the same for clusters of all sizes up to and including the critical cluster size. The net rate of growth of clusters of size m to $m+1$ may be denoted by I_m so that

$$I_m = \alpha_m N_m - \beta_{m+1} N_{m+1} = I \quad (3)$$

for all $m \leq c$ at steady state conditions.

At dynamical equilibrium ($I_m = 0$) we have

$$\frac{N_m^e}{N_{m-1}^e} = \frac{\alpha_{m-1}}{\beta_m}$$

We assume that small deviations of the α_m 's and β_m 's from their equilibrium values may be neglected such that we may write

$$\frac{N_m^e}{N_{m-1}^e} = \frac{\alpha_{m-1}}{\beta_{m-1}} \quad (4)$$

and, inserting (4) in (3), we get

$$I_m = \alpha_m [N_m - \frac{N_m^e}{N_{m+1}^e} N_{m+1}] \quad (5)$$

Solving this equation (5) gives the exact steady state solution of our problem, which is

$$I = \alpha_c N_c^e Z_c , \quad (6)$$

where Z_c is called the nonequilibrium factor.

Z_c can only be evaluated in some special cases. First we consider the case $\beta_m \gg \beta_{m+1}$ for $m \approx c$, which is called the case of rapidly increasing stability nucleation. Then we get from (6)

$$I = \alpha_c N_c^e \quad (7)$$

Equation (7) states that the steady state nucleation rate for the case of rapidly increasing stability equals the rate of growth of the pseudoequilibrium concentration of critical nuclei. Inserting in (7) for α_c and N_c^e we will see that we get the nucleation rate derived by Volmer and Weber. When we set

$$N_c^e = N_1 e^{-\Delta G_c/kT} \quad (8)$$

$$\alpha_c = A_c \omega \quad (9)$$

where A_c = cross section of the critical nucleus,

ω = frequency factor of impingement,

(7) becomes [2]

$$I_{vw} = A_C \omega N_1 e^{-\Delta G_C/kT} = \omega 4\pi r_C^2 N_1 e^{-\frac{16\pi\gamma^3}{3\Delta G^2 kT}}$$

From this it follows that in the case of rapidly increasing stability nucleation there exists dynamical equilibrium between the critical nuclei and the smaller nuclei. It is seen that Z_C describes the deviation from dynamical equilibrium.

In the second case we assume $\beta_m \approx \beta_{m+1}$ for $m \sim c$ which is called slowly increasing stability nucleation. By evaluating Z_C under these assumptions, we get an approximate equation for the nucleation rate

$$I = \alpha_C N_C^e \left(\frac{w}{\pi kT} \right)^{1/2}, \quad (11)$$

$$\text{where } w = -\frac{1}{2} \left(\frac{d^2 \Delta G_m}{dm^2} \right)_{m=c}.$$

Inserting for ΔG_m gives

$$w = -\frac{\Delta G_C}{3c^2}$$

and

$$\left(\frac{w}{\pi kT} \right)^{1/2} = \frac{\Omega \Delta G_v}{8\pi\gamma(\gamma kT)^{1/2}},$$

which is the nonequilibrium factor derived by Becker and Döring. The nucleation rate becomes [2]

$$I_{BD} = \frac{\Omega \Delta G_v^2}{8\pi\gamma(\gamma kT)^{1/2}} I_{vw} . \quad (12)$$

The physical significance of rapidly or slowly increasing stability nucleation is seen by combining (4) with

$$N_m^e = N_1 e^{-\frac{\Delta G_m}{kT}} , \quad (13)$$

where ΔG_m is the Gibbs free energy of formation of a cluster of m atoms.

It is found that rapidly increasing stability nucleation occurs in the nucleation of small critical nuclei at low temperatures, whereas the slowly increasing stability nucleation will involve larger critical nuclei at higher temperatures. The process of clustering itself is described by the phenomenological constants α_m . Several physical situations may be described by formulae (6), (7) or (11). For instance let

$$N_c^e = N_1^c e^{-\frac{\Delta G_c}{kT}} ,$$

and

$$\alpha_c = N_1 e^{-\frac{\Delta G_d}{kT}} ,$$

where ΔG_d is the free energy of activation for a surface diffusion jump.

We get an expression of the form that has been derived

by Walton [3] for the heterogeneous nucleation of atoms on a surface:

$$I_w = N_1^{c+1} e^{-(\Delta G_d + \Delta G_c)/kT} \quad (14)$$

II. Molecular Kinetic Theories of Crystal Growth

We will briefly sketch the models of crystal growth considered here. The simplest situation is given by an ideal rough surface where atoms are added singly. A perfect singular surface, which has no preferred growth sites, needs two dimensional nucleation for growing. On an imperfect singular interface growth takes place at screwdislocations. We will treat here crystal growth from solution and only give short hints where there are differences from growth of crystals from vapour or melt [5].

1) Growth of a rough surface [4]

The driving force of solidification is the difference of the free energy ΔG between the two phases. It is a function of supersaturation in the case of growing from vapour or solution and temperature difference to the melting temperature in the case of growing from melt.

$$\Delta G = i k T \ln \sigma ,$$

where i = number of ions formed from one molecule of solute,
 σ = supersaturation; actual concentration (or vapour pressure) deviated by the equilibrium concentration (pressure)

In the case of melt growth

$$\Delta G = L - T\Delta S ,$$

which becomes

$$\Delta G = \frac{\Delta T}{T_m} L ,$$

where L = latent heat,

T_m = melting temperature,

ΔS = change of entropy.

The free energy of a particle can be represented by a distribution like Fig. 1

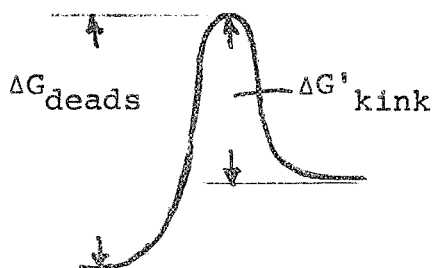


Fig. 1

ΔG_{dead} is the activation free energy for leaving the surface, and $\Delta G'_{\text{kink}}$ is the activation free energy for entering the kink directly from solution.

It is now assumed that the process determining the growth rate is the integration of a growth unit into the kink and not diffusion in the solution. This can be obtained by growth in a perfectly stirred solution. Diffusion controlled growth will be discussed lateron.

The velocity R of the growing interface is determined in this case by the net exchange Q from solution to crystal and the intermolecular spacing a .

$$R = Q a \quad (15)$$

The exchange rate (the flux per second through an area λ^2) may be written

$$Q = \frac{kT}{h} \exp\left\{-\frac{\Delta G^*_{\text{kink}}}{kT}\right\} - \exp\left\{-\frac{\Delta G_{\text{dead}}}{kT}\right\} \quad (16)$$

If we insert the relation

$$\Delta G = \Delta G_{\text{dead}} - \Delta G^*_{\text{kink}} \quad (17)$$

we get

$$R = a \frac{kT}{h} e^{-\frac{\Delta G^*_{\text{kink}}}{kT}} \{1 - e^{-\frac{\Delta G}{kT}}\}$$

In crystal growth from melt, it is assumed that the free energy for entering a growth site $\Delta G'_{\text{kink}}$ is not much different from the free energy for making a diffusion jump in the melt, and that the exponential factor may be expressed by the diffusion constant. In the solidification process from solution this assumption is certainly not valid because desolvation processes may be required before the integration can take place.

2) Two dimensional nucleation growth [4,2,6]

On a perfectly singular surface growth units coming out of the solution (vapour or melt) do not find any place of sufficient attraction. If there are two dimensional nuclei on the surface their ledges act as growth sites for molecules which are absorbed on the surface and diffuse in the absorption layer or which enter the ledge directly from the solution. As the considerations of Bennema [7], which are discussed later, show, surface diffusion can play an essential role in crystal growth from solution.

The rate of growth is deduced from the nucleation rate I and the growth of these two dimensional nuclei. We have to distinguish between two cases. In the first case the nucleation rate is growth limiting. That means the time between two consecutive nucleations on the crystal surface is much larger than the time required to cover all the surface. Then the growth velocity is given by

$$R = \ell I , \quad (19)$$

where ℓ is the height of the nucleus.

In the other case the growth rate of the nuclei is the growth velocity determining part. The growth rate can be evaluated by considering the area which is covered by the nuclei as function of time. This area is proportional to the third power of time. An approximation neglecting overlapping and the fact that new nuclei start in the time the new layer is covered gives the formula

$$R = \ell \{ \pi R_N^2 t \}^{1/3} , \quad (20)$$

where R_N is the growth rate of a nucleus.

The problem left now is to calculate the nucleation rate, but we have considered this problem in the first part. We take the formula of Volmer Weber (10) because it is assumed that there are only small nuclei on the surface required and the temperatures are not too high.

$$J = A_C \omega N_C^e \quad (21)$$

$$N_C^e = N_S e^{-\frac{\Delta G_C}{kT}} , \quad (22)$$

where N_S are the number of sites for nuclei.

$$\omega = \frac{\Omega}{\lambda^2} ; \quad A_C = 2\pi r_C \ell , \quad (23)$$

so that

$$I = N_S \frac{2\pi r_C \ell Q}{\lambda^2} e^{-\frac{\Delta G_C}{kT}} . \quad (21a)$$

The same considerations as in part I give

$$r_C = \gamma/\Delta G \quad (24)$$

$$\Delta G_C = \pi \ell \gamma^2 / \Delta G \quad (25)$$

With this we get the two growth rates

$$R = \ell I = \frac{2\pi N_S \gamma \ell^2}{4\lambda^2} kT e^{-\frac{\Delta G_{\text{kink}}}{kT}} \left\{ \frac{1 - e^{-\frac{\Delta G}{kT}}}{\Delta G} \right\} e^{-\frac{\pi \ell \gamma^2}{\Delta G kT}} \quad (26)$$

and

$$R = \ell \{ \pi R_N^2 I \}^{1/3} \sim \left\{ T^2 \left(\frac{1 - e^{-\frac{\Delta G}{kT}}}{\Delta G} \right)^2 e^{-\frac{\pi \ell \gamma^2}{\Delta G kT}} \right\}^{1/3} ,$$

where we have inserted for R_N the formula (18).

Because of the smallness of the nuclei involved (they may not be larger than 3 atoms) it is troublesome to use the macroscopic surface energy to compute the free energy of formation. Therefore it is desirable to obtain an expression for the nucleation rate which avoids those macroscopic quantities. This has been done by Walton [3]. He calculated the

equilibrium cluster concentration by minimizing the partition function. The size of the critical cluster must be evaluated by a trial and error analysis which is possible because of the small number of atoms involved. Using formula (7) with

$$\alpha_c = A_c \frac{Q' s}{\lambda} e^{(\Delta G_{deads} - \Delta G_{sdiff})/kT}, \quad (28)$$

where A_c = cross section of critical nucleus,

$\frac{Q'}{\lambda}$ = rate of absorption of molecules at the surface,

ΔG_{deads} = energy of absorption on the surface,

ΔG_{sdiff} = energy of surface diffusion,

s = mean spacing between two sites for nucleation

gives the nucleation rate.

$$N_c = \frac{1}{s^2} \left(\frac{Q' s^2}{\lambda v} \right)^c e^{(c \Delta G_{deads} + \Delta E_c)/kT}, \quad (29)$$

where v is the vibration frequency kT/h ,

ΔE_c = energy of formation of a critical cluster.

Q' can be calculated in the same way as Q , giving

$$Q' = \frac{kT}{h} e^{-\frac{\Delta G_{deads}}{kT}} [1 - e^{-\frac{\Delta G}{kT}}] \quad (30)$$

Inserting all these quantities into formulae (19) or (20) gives the two linear growth rates.

In the first case

$$R \sim [1 - e^{-\frac{\Delta G}{kT}}]^{c+1}, \quad (31)$$

and in the second case

$$R \sim [1 - e^{-\frac{\Delta G}{kT}}]^{c/3+1} \quad (32)$$

3) Surface diffusion model of Burton et al [8], [7]

At low supersaturations the probability for two dimensional nucleation is very low. Therefore there must be other sources for crystal growth observed at this low supersaturations. Thermal fluctuations produce in a low index plane no steps unless its temperature is close to the melting point. Steps therefore cannot account for crystal growth from solution in the case considered. Burton et al. proposed that screw dislocations act as sinks for growth units and the growth proceeds by rotation of these screw dislocations.

The theory of this mechanism was originally developed by Burton et al. [8] for crystal growth from vapour. Bennema [7] showed that the spiral growth by surface diffusion is important also in solidification from solution. This can be seen by the following arguments.

In principle the growth unit can enter directly from the bulk of the solution into the kinks of the steps of the spirals (this is assumed in the volume diffusion model discussed in the next section) or it can first enter the surface phase or absorption layer and then diffuse along the surface and possibly along the step to the kinks. Fig. 2 shows the free energies of all the processes mentioned.

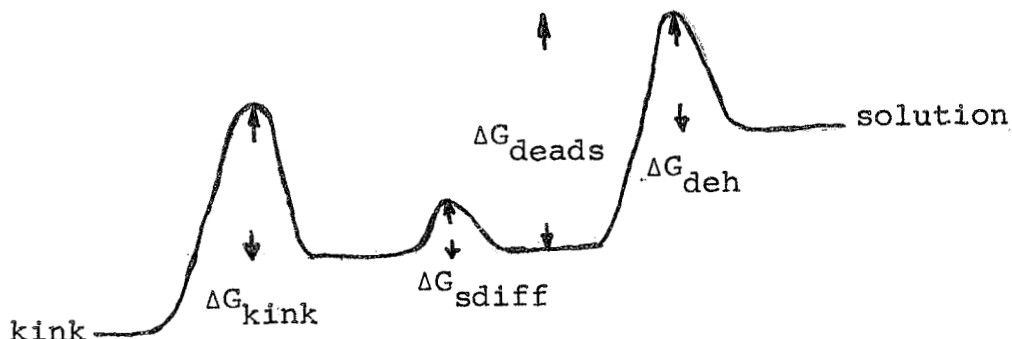


Fig. 2

- $\Delta G_{\text{dead}} =$ activation energy for leaving the surface layer,
- $\Delta G_{\text{deh}} =$ dehydration energy for entering the surface layer,
- $\Delta G_{\text{diff}} =$ activation energy for making a diffusion jump,
- $\Delta G_{\text{kink}} =$ activation energy for entering the kink.

Fig. 1 shows the case of the volume diffusion model.

It is now highly probable that the integration process of growth units directly from solution into the kinks is a more complicated process than entering the absorption layer,

because the growth unit must be desolvated more completely in the first case and the growth unit must be in a highly ordered state for the integration process. From this it can be seen, by comparing the growth rate predicted by the volume diffusion model with the surface diffusion model, that, for the range of supersaturation considered, the surface diffusion model gives the faster growth rate. Because of the assumption that $\Delta G_{\text{dead}} > \Delta G_{\text{sdiff}}$, which seems a reasonable quality of the absorption layer, it may be possible that, although the diffusion in the surface layer is much slower than in the bulk solution, the surface diffusion mechanism gives the fastest growth rate. The growth rate is found in the following way. First the growth of a step in which a thermal fluctuation produces kinks is considered. This is done by solving a diffusion equation which connects the surface current with a current from vapour. It is assumed that the movement of the step can be neglected. Then a parallel sequence of steps with distance y_0 is considered. From this the growth of the steps of the spiral can be evaluated by calculating y_0 for a spiral. This spiral winds itself up until the curvature at the centre reaches the value of the critical radius (the radius of the critical nucleus at the given supersaturation). From all this ω , the angular velocity of the spiral, is evaluated. The growth rate then becomes

$$R = \frac{\omega a}{2\pi} , \quad (33)$$

where a is the height of the step of the spiral.

By inserting for ω , we finally get the growth rate

$$R = C \frac{\sigma^2}{\sigma_1} - \tanh \frac{\sigma_1}{\sigma} , \quad (34)$$

where

$$C = \beta c_0 D_s n_{s0} \Omega / x_s^2 ,$$

$$\sigma_1 = \frac{9.5}{\epsilon} \frac{\gamma}{kT} \frac{a}{x_s} ,$$

and where β is a factor which takes into account that there is no equilibrium surface concentration near the kink so that

$$\sigma_s = (1-\beta) \sigma ,$$

where σ_s is the concentration near the kink. c_0 is a factor which takes into account that the mean diffusion distance x_s is not much greater than the distance x_0 between two kinks.

D_s = diffusion constant of growth in absorption layer of a crystal face,

n_{s0} = number of growth units in the surface layer per unit area,

Ω = volume of a growth unit in the crystal,

γ = edge free energy of a growth unit in a step,

ε = a measure for the number of interacting growth spirals
of a domination group of spirals,

β , D_s , c_0 , x_s , n_{so} can be expressed in terms of the energies
 ΔG_{kink} , ΔG_{sdiff} , ΔG_{deads} , ΔG_{deh} [9] by using Eyring's one
particle kinetical formalism.

4) Volume diffusion model of Burton et al. [8] and Chernov [10]

If we assume that the flux of absorbed growth units on
the surface layer can be neglected, the direct flux of growth
units from solution to kink is growth determining. As was
done in the surface diffusion model, a parallel sequence of
equidistant steps is considered. The distance then is taken
from a spiral. The task is to solve a diffusion equation in
the domain shown in Fig. 3

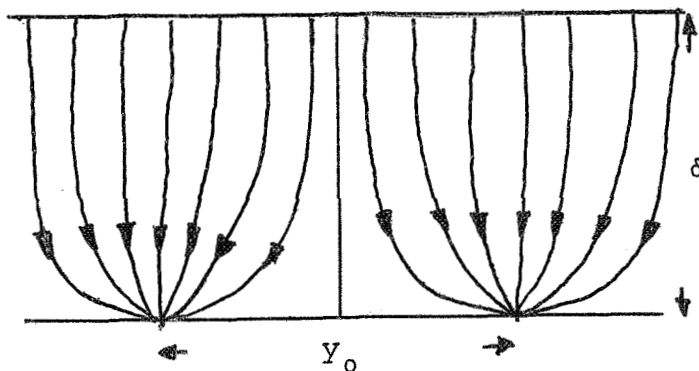


Fig. 3

y_0 is the distance between two steps. δ is the thickness of
the unstirred layer. It is assumed that in this layer no

convection takes place.

The difference between the models of Burton et al. and Chernov lies in the assumption of Chernov that the steps are linear continuous sinks whereas Burton et al. take into account that the kinks are separated.

Chernov obtains the following expression for R

$$R = \epsilon a \left(\frac{kT}{\gamma} \right) \beta c_e \sigma^2 \left[1 + \frac{\beta a}{D} \ln \left(\frac{\sigma c}{\sigma a} \sinh \frac{\sigma}{\sigma_c} \right) \right]^{-1} \quad (35)$$

Burton et al. obtain

$$R = \epsilon \frac{2\pi\lambda}{19ax_0} \beta D N_0 \Omega \left(\frac{kT}{\gamma} \right) \sigma^2 \left[1 + \frac{2\beta\lambda\pi(\delta-y_0)}{x_0 y_0} + 2 \frac{\beta\lambda}{x_0} \ln \frac{y_0}{x_0} \right]^{-1} \quad (36)$$

$$\text{where } G_c = \frac{4\gamma a}{\epsilon k T \delta} , \quad y_0 = \frac{19\gamma a}{\epsilon k T \sigma} ,$$

N_0 = number of growth units in solution per unit volume,

c_e = concentration at the saturation point,

and all other quantities have the same meaning as in (34).

It is seen that in the volume diffusion model the growth rate depends on the thickness of the diffusion layer δ , which has to be calculated from hydrodynamics. Convection may alter the growth velocity. All other models discussed above are insensitive to convection. It should be mentioned that the spiral growth mechanism applies to crystal growth from melt also.

The only difference is that we have to calculate a heat conducting problem instead of a diffusion problem. Chernov [10] has derived a similar expression to (35) for this case.

5) Dislocationless growth of crystals [11]

The kinetic growth mechanism in sections 3 and 4 was based on the assumption that there are screw dislocations as continuous sources of steps and thus as sinks for growth sites. Distler and Zvyagin questioned the general validity of spiral growth at low supersaturation (or supercooling). They suppose that there exist active local centers with a long range effect on the solid surface. These active centers should be surface defects (vacancies interstitial and impurity atoms possessing more free energy than the neighboring perfect areas of the surface). The screw dislocations are not in thermodynamical equilibrium, while pointdefects are in equilibrium and are invariably present in all crystals.

III. Diffusion Controlled Growth

In Part II we have considered crystal growth from solution, where the attachment kinetic is the rate determining process. It is not sufficient in any case, however, to consider only the molecular process and not the transport of solute in the solution. In general the concentration and temperature fields in the solution will determine the uniformity of the growth process. That means the shape of the interface of the crystal depends on concentration and temperature fields. Instabilities, such as dentritic growth, cell formation, segregation and inclusion of mother liquid can occur when certain conditions are fulfilled.

1) Growth rate [12]

A simple solute balance, neglecting solute capture by the advancing surface, gives the linear growth rate on a plane interface

$$R = \frac{1}{\rho} D \left(\frac{\partial C}{\partial x} \right)_{x=0} , \quad (37)$$

where ρ = density of the solid,

D = diffusion constant,

$\left(\frac{\partial C}{\partial x} \right)_{x=0}$ = concentration gradient normal to the interface evaluated at the interface.

In crystal growth from a supercooled melt instead of a solute balance we have to make an heat balance which leads to

$$R = \frac{1}{L} \left\{ K_s \left(\frac{\partial T_s}{\partial x} \right)_{x=0} - K_L \left(\frac{\partial T_L}{\partial x} \right)_{x=0} \right\} \quad (38)$$

where s , L = indices for solid resp. liquid,

K = thermal conductivities,

L = latent heat,

$\left(\frac{\partial T}{\partial x} \right)$ = temperature gradient.

The concentration gradient can now be expressed by

$$\left(\frac{\partial C}{\partial x} \right)_{x=0} = \frac{C_s - C_I}{l}$$

where C_s = concentration at the source,

C_I = concentration at interface,

l = distance from source.

If there is now stirring or convection the concentration gradient in the solution is reduced and the driving force is only the concentration gradient in the stagnant layer of thickness δ before the interface. Then

$$\left(\frac{\partial C}{\partial x} \right)_{x=0} = \frac{C_s - C_I}{\delta}$$

and

$$R = \frac{D}{\rho \delta} (C_s - C_I) \quad (39)$$

In general C_I equals not the equilibrium concentration at the given temperature but is something higher so that the molecular kinetic process is driven.

We express the linear growth rate, after Brice [4], by

$$R = A (C_I - C_e)^n , \quad (40)$$

where C_e is the equilibrium concentration, and the constants A and n depend on the growth mechanism. They can be obtained from part II by inserting for ΔG and evaluating the expressions, neglecting terms of the order $\frac{1}{2}\sigma$. Only in the case of the surface nucleation mechanism is A also a function of $C_I - C_e$.

2) The stability of a planar interface

The velocity of the crystal interface depends on the diffusion field in solution growth or the temperature field in melt growth. Till now we have studied only the growth of planar interfaces, but there may be perturbations like bumps or depressions. These bumps are thought to be the origin of dentrites. The theory of the stability of a planar interface (or spherical particle, cylinder, parabola etc.) investigates the growth or dissolution of such perturbations.

A first criterium for stability was given by Mullins and Sekerka [13]. They analyzed the growth of a particle from solution or melt. By solving the Laplace equation under the growth determining boundary values they found that only

particles up to a critical size grow with stable shapes. But too many simplifying assumptions have been made. Only the effect of the surface free energy on the boundary condition, which is a stabilizing effect, has been introduced. In this case the interface concentration becomes

$$C_I = C_0 + C_0 \Gamma K , \quad (41)$$

where $\Gamma = \frac{\gamma \Omega}{kT}$ is the capillary constant,

γ = surface free energy,

Ω = molar volume,

K = curvature of the perturbated surface,

C_0 = equilibrium concentration.

If there is surface diffusion, as considered by Coriell and Parker [14] the same stabilizing effect as before (curvature) drives the surface flow from a bump to a flat region on the surface. This makes the original shape more stable. The surface flux is related to the curvature by

$$I = -\Omega^{1/3} \frac{D_s \gamma}{kT} \nabla_s K = - \frac{D_s}{\Omega^{2/3}} \Gamma \nabla_s K , \quad (42)$$

where D_s = surface diffusion constant.

Another effective shape stabilizer is interface kinetics. For a long time it was assumed that at the interface we have

local equilibrium (41). As mentioned in part III 1) the deviation from the equilibrium value drives the molecular kinetic process. Interface kinetics becomes important if the kinetic coefficient A is very low. This is clear because then the integration process is the slowest part in the whole crystal growth process. Connecting (37) and (40) with the boundary condition shows that sluggish kinetics can enhance stability [15, 16].

Recently Brice [17] has discussed another criterion for stability of a crystal interface during growth. He uses the criterion that the gradient of the growth rate at the interface shall be negative so that a bump grows more slowly and a depression more rapidly than the rest of the interface. That means

$$\frac{dR}{dx} < 0 \quad (43)$$

From this a stability criterion can easily be derived for solution, melt and vapour growth by inserting for R. In all these stability criteria many uncertain material parameter are involved and only insufficient data are available to test the relations thoroughly. Another important factor influencing stability has been neglected till now. This is the influence of convective flow.

3) Convection in crystal growth

In crystal growth from an aqueous solution, convection increases the rate of solute transported to the growing crystal and so increases the growth velocity. Moreover, in stagnant solutions imperfect face development may be caused by the effect of exhaustion of supersaturation and development of starvation conditions. Depressions overgrowth and so inclusion of mother liquor may occur. But also in stirred solutions occlusion of mother liquor occurs [18]. This is explained by the formation of instabilities of the flat crystal face. If the supersaturation exceeds a critical limit appropriate to the particular face, agitation (convection) and temperature, it is thought that variations in concentrations cause the flat interface to break down. By overgrowth of such instabilities mother liquor is included in the crystal.

In crystal growth from melt, impurity (dopant) inhomogeneities can be observed [19, 20]. These inhomogeneities in the form of striations perpendicular to the growth direction are caused by changes in the growth rate, which in turn are caused by temperature fluctuations in the melt [21 - 23]. Instability of the liquid due to natural convection is thought to be cause of these fluctuations. Theory has to predict the onset of this instability in systems which are appropriate to the growth system. Systems for which attention must be paid to convective instability arise, for instance, in the Czochralski

or in the floating zone techniques.

a) Natural convection induced by gravity

A well known phenomenon is the onset of natural convection in liquid layers heated from below. Such a configuration is unstable against little disturbances in the fluid velocity. After a critical value of the temperature gradient is exceeded the hotter liquid begins to rise and the colder begins to sink. A cellular pattern can be observed in the fluid. Consider a horizontal infinitely extended system between two boundaries [24]. The critical Rayleigh parameter for this system is calculated in the following way:

The continuity, impulse and energy equations are linearized in the velocity and temperature disturbance. Buoyancy effects are taken into account in the force term only by setting $\rho = \rho_0(1 - \beta Gz)$, where β = volume expansion coefficient, G = temperature gradient in the undisturbed system.

Separation of variables lead to a system of differential equations whose solutions must be specified by boundary conditions. There may be two free, two rigid or one rigid and one free boundaries. They may have zero, finite or infinite conductivity. A system of algebraic equations for the coefficients of the linear independent solution is then obtained. The determinant of the system has to be zero and so the Rayleigh parameter is obtained as a function of the wavelength of disturbance and the thermal boundary condition.

The Rayleigh parameter is defined as

$$R_a = \frac{g\beta\Delta TL^3}{\alpha\nu} \quad (44)$$

where g = gravity acceleration,

ΔT = temperature difference,

L = characteristic length of the system,

α = thermal diffusivity,

ν = viscosity.

The critical Rayleigh parameter is the minimum of all parameters for the various wavelengths. Table 1 gives the critical parameters for some cases

Both free [20]		657.5
Both rigid [20]	isothermal	1707.8
One rigid, one free [20]		1100.7
Both rigid [25]	finite conductivity	720

Table 1

We see that finite conductivity enhances instability. Another important effect on stability is produced by rotation of the system (in the Czochralski method for instance). The same

procedure as above gives the critical Rayleigh parameter as a function of the Taylor number T

$$T = \frac{4\Omega^2}{v^2} L^4 \quad (45)$$

where Ω = angular velocity.

A new and very important feature of the problem arises because of the possibility of the onset of natural convection as overstability. That means the fluid motion sets in as periodic oscillations. These oscillations produce the striations in the crystal [26].

It can be seen that the critical parameter for the onset of overstability is always less than that for stationary convection. But the minimum value of the Rayleigh number for the onset of either of the two forms of convection is a function of the Prandtl number and the Taylor number. For very low Prandtl numbers (as it is the case for metal melts) it can be said that there exists a Taylor number above which convection sets in in the overstable mode.

The onset of convection may not only be induced by thermal but also by concentration gradients [27]. In such a case, overstability results because the diffusivity of heat is usually much greater than the diffusivity of solute. For instability produced by concentration gradients alone the responsible parameter is:

$$Ra_s = \frac{g\phi \Delta CL^3}{Dv} , \quad (46)$$

where ΔC = concentration difference,

ϕ = change of volume with content of solute,

D = diffusion coefficient.

If we have both gradients the condition for stability is

$$\frac{Ra}{Ra_c} + \frac{Ra_s}{Ra_{sc}} < 1 . \quad (47)$$

In liquid metals very low concentration gradients may lead to overstability. These very low gradients may be produced by the Soret effect [28], as Hurle et al. have recently shown.

b) Natural convection induced by surface tension

Investigations of flow instabilities in liquid films have shown that there is onset of convection even when the system should be thermally stable. This was explained by Pearson [29], who analyzed the stability of a liquid system as mentioned in part a) with temperature dependent surface tension. Temperature differences lead to different surface tensions and fluid flow from parts of low to higher surface tension. As before, convection sets in when a critical parameter, the Maragoni number, is exceeded. The Maragoni number is defined by

$$M = \frac{S\Delta TL}{\alpha v} , \quad (48)$$

where S = change of surface tension with temperature.

The same analysis can be done for variation of surface tension with concentration. Then the parameter is

$$M_S = \frac{S' \Delta CL}{Dv} , \quad (49)$$

where S' = change of surface tension with temperature.

Contrary to the results in the case of gravity driven instability, in this case rotation does not lead to overstable modes of convection [30].

Conclusion

In the preceding chapters we have studied the various aspects of crystal growth. First there is the molecular kinetic process itself. The driving force is the supersaturation or temperature difference from the melting point immediately at the crystal surface. The law is found by consideration of statistical mechanics which gives rates or densities that are related to the energies involved in the atomic process. This shows that there should be no effect of zero gravity on the molecular kinetic process of crystal growth.

The second phase of crystal growth is the transport of growth units to the growing surface through the solution, melt or vapour. Various processes contribute to the transport: diffusion, convection and thermodiffusion. It was shown before that natural convection plays an important role in crystal growth. Homogeneity of a crystal, say doped semiconductors or laser materials, can only be reached by control of convection in the melt. In zero gravity crystal growth, no buoyancy force can induce convection, but surface tension can.

References

- [1] R.L. Gerlach, J. Chem. Phys. 51, 2186 (1969)
- [2] Hirth, Pound, Condensation and Evaporation (Pergamon Press 1963)
- [3] W. Walton, J. Chem. Phys. 37, 2182 (1962)
- [4] Brice, J. Crystal Growth 1, 218 (1967)
- [5] Brice, The Growth of Crystals from the Melt (Noth Holland 1965)
- [6] Nielsen, Kinetics of Precipitation (Pergamon Press 1964)
- [7] Bennema, J. Crystal Growth 5, 29 (1969)
- [8] Burton et al., Phil. Trans. Roy. Soc. London A 243, 299 (1951)
- [9] Bennema, J. Crystal Growth 1, 278 (1967)
- [10] Chernov, Sov. Phys. Usp. 4, 116 (1961)
- [11] Distler, Zvyagin, Sov. Phys. Dokl. 12, 535 (1967)
- [12] Brice, J. Crystal Growth 1, 161 (1967)
- [13] Mullins, Sekerka, J. Appl. Phys. 34, 323 (1963)
- [14] Coriell, Parker, J. Appl. Phys. 37, 1548 (1966)
- [15] Coriell, Parker, Crystal Growth ed. Steffen Peiser p. 703 (1967)
- [16] Cahn, Crystal Growth ed. Steffen Peiser p. 681 (1967)
- [17] Brice, J. Crystal Growth 6, 9 (1969)
- [18] Brocks, Horton, Torgesen, J. Crystal Growth 2, 279 (1968)
- [19] Utech, Flemings, Crystal Growth ed. Steffen Peiser p. 651 (1967)

- [20] Barthel, Scharfenberg, Crystal Growth ed. Steffen Peiser,
Pergamon 1967 p. 133
- [21] Utech, Brower, Early, Crystal Growth ed. Steffen Peiser,
Pergamon 1967 p. 201
- [22] Hurle, Crystal Growth ed. Steffen Peiser, (Pergamon 1967)
p. 659
- [23] Weinberg, Trans. Met. Soc. ASME 227, 231 (1963)
- [24] Chandrasekhar, Hydrodynamics and Hydrodynamic Stability,
Clarendon Press (1961)
- [25] Hurle, Jakeman, Pike, Proc. Roy. Soc. 296A, 469 (1967)
- [26] Hurle, Jakeman, Pike, J. Crystal Growth 3,4, 633 (1968)
- [27] Nield, J. Fluid Mech. 29, 545 (1967)
- [28] Hurle, Jakeman, Pike, Phys. Fluids 12, 2704 (1969)
- [29] Pearson, J. Fluid Mech. 4, 489 (1958)
- [30] Vidal, Acrivos, J. Fluid Mech. 26, 807 (1966)